Université du Québec
Institut National de la Recherche Scientifique
(Énergie-Matériaux-Télécommunications)

Design, Fabrication and Characterization of MultifunctionalField-Effect Transistors (FETs) based on novel π-conjugated organic semiconductors

Afshin Dadvand

Thèse présentée pour l'obtention du grade de Philosophiae Doctor (Ph.D.) en
Sciences de l'énergie et des matériaux

Membres Du Jury :

Directeur de recherche	Prof. Federico Rosei, EMT-INRS
Codirecteur de recherche	Prof. Dmitrii F. Perepichka, Université de McGill
Examinateur interne et président du jury	Prof. Andreas Ruediger, EMT-INRS
Examinateur interne	Prof. Fiorenzo Vetrone, EMT-INRS
Examinateur externe	Prof. Christine Luscombe, Université de Washington
Examinateur externe	Prof. Jean-Michel Nunzi, Université de Queens

Remerciements

J'aimerais tout d'abord remercier mon directeur de recherche, le Professeur Federico Rosei, et mon codirecteur de recherche, le Professeur Dmitrii Perepichka, pour m`avoir accepté en tant qu'étudiant de doctorat au sein de leurs équipes de recherche ainsi que pour superviser ce projet et m'avoir conseillé et guidé tout au long de mes études.

Je remercie sincèrement le Dr. Andrey Moiseev, Dr. Chenglin Yan, Prof. Jacklyn Brusso, Dr. Ori Gidron, et Prof. Fabio Cicoira pour ses contribution scientifique au développement et l'avancement de ce projet.

Mes remerciements vont également au personnel technique et administratif de l'INRS et de McGill surtout Hélène Sabourin, Petr Fiurasek, Christoph Chabanier, Sébastien Delprat, Richard Rossi, et Weihua Wang pour leur aide et leurs précieux conseils.

J'aimerais remercier tous mes collègues et mes amis de l'INRS et de McGill pour les moments agréables passés ensemble. Un merci spécial à et à Oleksandr Ivasenko pour son amitié et son ouverture d'esprit.

J'exprime ma plus profonde reconnaissance à ma famille, et surtout mon père Hossein pour m'avoir toujours encouragé.

Abstract

For over 50 years the mainstream electronics industry has been dominated by thin film transistors based on inorganic semiconductors such as silicon and gallium arsenide. The fabrication of these devices requires high temperature and high vacuum deposition techniques that result in high production costs, which are particularly prohibitive for large-area electronics.

Organic semiconductors (OSCs) offer an attractive alternative since their fabrication processes are much less complex compared to conventional inorganic technology. In particular, low temperature deposition and solution processing techniques provide a simple, low cost alternative. π-Conjugated organic semiconductors are therefore attracting considerable attention for applications such as organic light-emitting diodes (OLEDs), field-effect transistors (OFETs) and photovoltaic cells. Furthermore, the mechanical properties (flexibility) of organic compounds coupled with their low temperature solution-based processing provides the potential for new applications including flexible displays, pliable electronic paper and smart cards. While molecular and polymer OLEDs have already been commercialized in a number of consumer products, OLED displays still employ an inorganic (amorphous silicon, a-Si) thin-film transistor (TFT) matrix to control the emissive pixels. Organic TFTs (OTFTs) are nevertheless extensively investigated by numerous, both industrial and academic, research groups. The mobility of the best OSCs have already approached and even surpassed that of a-Si (~1 cm^2 V/s). However, the limited stability of OSCs and the "difficult to control" molecular packing, particularly in solution-processed devices, are among the major limitations hampering industrial development, and the design of new OSCs continues to be an important area of materials research.

This project involves elaboration of the thin film technology of new organic semiconducting materials, including small molecules (fused polyaromatic systems and heterocyclic oligomers, mainly fused thiophene and selenophene derivatives) and polymers, and characterization of their electronic properties for applications in optoelectronic devices. A large emphasis of this project is the study of new organic materials as an active semiconducting layer in transistors. Along the typical switching function of OTFTs, the

research is directed to the design, fabrication and characterization of multifunctional transistors that can have electroluminescence and possible lasing properties.

Contributions to the Research

In this PhD thesis, Prof Federico Rosei (supervisor) and Prof. Dmitrii F. Perepichka (co-supervisor) provided funding, research objectives and intellectual guidance. The majority of this thesis was carried out in INRS-EMT and chemistry department of McGill University.

Chapter 3: The synthesis and XRD characterization of oligofuran derivatives were done by Dr. Ori Gidron. The fabrication and characterization of TFTs based on oligofuran derivatives film growth of oligofuran derivatives were carried out by me and Ori. I studied the temperature dependence of the mobility of transistors based on DH6F and electroluminescence property of DH6F. Oligothiophene and oligoselenophenes were synthesized in Prof. Michael Bendikov's laboratory. I performed the fabrication and characterization of TFTs based on these compounds.

Chapter 4: (a) Jaclyn L. Brusso and Oliver D. Hirst synthesised TTA and its derivatives. Jaclyn studied the optical properties of the materials. I performed the XRD film, TGA, and the fabrication and optoelectronic characterization of the thin film transistors. (b) Octathio [-8-] circulene (sulflower) and its selenium analogue (selenosulflower) were synthesized by Konstantin Yu. Chernichenko from Moscow State University. Solid-state cyclic voltammetry as well as DFT calculations were performed by Reyes M. Osuna from Malaga University (Spain). I performed studies on optical properties of materials, the growth mechanism using AFM and XRD, fabrication and optoelectronic characterization of the thin film transistors.

Chapter 5: 2,6- and 9,10-DPSAnt synthesized by Dr. Andrey G. Moiseev and Wei-Hsin Sun. I performed material purification, studying optoelectronic properties, TGA, DFT calculations, fabrication and characterization of OLETs.

Chapter 6: I designed the compound (HPVAnt) and it was synthesized by Dr. Andrey G. Moiseev and Wei-Hsin Sun. I fabricated and measured all TF-FETs and also studied optical characteristics of the compound. Andrey performed the photophysical studies on this compound including lifetime measurements. The growth of the single crystals and measuring their absolute quantum yield value and the fabrication and characterization of SC-FET were realized in Prof. Takenobu's lab (Waseda University) by me and Kosuke Sawabe. Dr. Brandon Djukic performed electrochemical measurements and X-ray analysis.

List of symbols and abbreviation

Symbol	Description
AFM	Atomic Force Microscopy
DFT	Density Functional Theory
EIL	Electron Injection Layer
EL	Electroluminescence
EML	Emissive Layer
ETL	Electron Transport Layer
FET	Field Effect Transistor
HIL	Hole Injection Layer
HMDS	Hexamethyldisilazane
HOMO	Highest Occupied Molecular Orbital
HTL	Hole Transport Layer
ITO	Indium Tin Oxide
LUMO	Lowest Unoccupied Molecular Orbital
MOSFET	Metal Oxide Semiconductor Field Effect Transistor
OFET	Organic Field-Effect Transistors
OLEDs	Organic Light Emitting Diodes
OLETs	Organic Light Emitting Transistors
OSCs	Organic Semiconductors
OTFTs	Organic Thin-Film Transistors
OTS	Octadecyltrichlorosilane
PLQY	Photoluminescence Quantum Efficiency
PV	Photovoltaic
RFID	Radio Frequency Identification Tags
SAM	Self-Assembled Monolayers
SC-FET	Single Crystal Field-Effect Transistors
TF-FET	Thin Film Field-Effect Transistors
TGA	Thermal Gravimetric Analysis
XRD	X-Ray Diffraction

Table of Contents

Table of Contents

Table of Contents

Introduction

Organic materials have been an integral part of the semiconductor industry since 1960 when Kahng and Attalla demonstrated the first metal-oxide-silicon field effect transistor (MOSFET). Photo-sensitive polymers have been the defining factor in achieving feature sizes below 45 nm, while other non-conductive polymers have been an important component for packaging chips or improving the performance of low-K dielectric material.[1] However, organic materials had not been seriously considered as active semiconducting layer until 1987.[2] Since the initial breakthrough remarkable progress has been made in organic field effect transistors (OFETs), due to the design of high performance active-layer materials. Organic materials as an active semiconducting layer are attractive for many components of electronic devices due to many fundamental advantages over their inorganic counterparts.[3] Solution processing techniques allows for simple deposition methods such as inkjet,[4,5,6] screen,[7,8] and micro contact printing.[9,10] The discovery of electrical conduction in organic polymers in 1977 by Heeger, MacDiarmid and Shirakawa[11,12] had a great impact in micro-electronics by offering new prospects for fabrication of low cost plastic components. Since then, the field of research commonly called "**organic electronics**" has made considerable progress and it is beginning to make significant inroads into the commercial world, and by continuous progress is becoming a mainstay of our technological existence.[13] "**Disposable electronics**" is also an emerging field of electronics based on organic materials, including chemical sensors[14,15] and radio frequency identification tags (RFIDs).[16] Today, the performance of some OSCs, such as pentacene[17] and rubrene[18] has already surpassed that of amorphous silicon. While organic materials are not currently suitable for applications requiring high switching speeds, their low cost material and fabrication process as well as some unique properties makes them ideal for large area applications, such as displays[19,20] and solar cells[21,22] or in certain applications coexisting with inorganic electronics.

Outline

In this research work, Organic Field-Effect Transistors (OFETs) were fabricated in different configurations incorporating an active semiconducting layer based on highly conjugated small molecules to provide efficient molecular packing and desirable optoelectronic properties. ***The first chapter*** of this thesis presents an introduction to the basic principles and materials of

organic optoelectronics, which is useful for the design and understanding of the optoelectronic devices and material combinations presented in this thesis. It starts with a description of the general properties of OSCs including the transport mechanisms. Then the basic operational principle of OFETs and the effect of the organic thin film growth on the performance of OFETs is discussed. The last section of this chapter focuses on the different possible radiative and nonradiative transitions in organic materials and attention is given to the working principle and different structure of light-emitting devices. The ***second chapter*** describes the materials and experimental techniques used in fabrication, characterization and optimization of OFETs. ***In chapter three,*** the contribution of different chalcogen atoms into the optoelectronic properties of conjugated oligomers having similar structure is investigated. The focus of this section is on *linear oligomers*. It presents the first study of semiconducting properties of α-oligofurans and provides experimental evidence that the effect of the type of the chalcogen atom on the charge mobility of heteroaromatic semiconductors is weak. The focus of ***chapter four*** is directed to the *fused oligothiophene*. In this chapter, the effects of the 2D conjugation extension as well as the effect of different heteroatoms and their position on the properties of molecular semiconductors are investigated through studies of *isomers of tetrathienoanthracene and heterocirculenes*. In ***chapter five,*** bis(styryl)anthracenes are studied as active semiconducting and emissive layer for OLETs. In c***hapter six,*** we investigate the design, fabrication and optoelectronic characterization of alkylated mono-styrylanthracene which combines necessary properties for OLET applications.

CHAPTER 1

Introduction to organic electronics: organic semiconductors, their properties and applications

1.1 Motivation for organic electronics

Although the performance of organic-based electronic devices has tremendously increased during the last decade, it is unlikely that organic semiconducting materials will reach the performance of their single crystal inorganic semiconductors such as Si, Ge, GaN, GaAs or InP. The poor thermal and environmental stability of OSCs is an issue that should be addressed. So, why there is a growing interest in "organic electronics" research? Is this field only considered to answer some fundamental physical and chemical questions or shall we expect certain practical applications when the technology has been mastered? There are indeed some important motivations for organic electronics that can be summarized as follows:

Low temperatures processing. In contrast to modern Si CMOS technology, which involves temperature (>1000 ^{o}C), most OSCs can be processed at room or slightly elevated temperature. This can minimize the *mismatches* due to thermal expansion and allows processing on larger area substrates. Moreover, the **mechanical properties** of OSCs makes them compatible with *flexible substrates, such as (polymer) foils* for lightweight and foldable products such as RFID tags, portable sensors, electronic paper, and flat panel displays. In general, the fabrication processes of organic based devices are potentially much less complex and do not require high-vacuum deposition processes or sophisticated photolithographic patterning methods. This makes organic electronics a potentially *low cost technology*.

Easily tunable molecular structure to fulfill specific requirement. A large variety of OSCs can be synthesized and tailored with different functional groups to *chemically tune* their optoelectronic properties to meet the requirements of specific applications. The unlimited choice of variation in organic materials provides unique possibilities to develop integrated circuit technologies for various large area, low-cost applications. This has already opened up the exciting field of organic electronics and the interest in optical and electrical properties of OSCs has tremendously grown in the recent years. However, new types of OSCs require addressing new concepts and models that allow the modification of chemical, physical and structural properties and as a result, device performance. Currently we are capable of controlling material properties at the molecular level and also impose different molecular packing during growth, add side groups that enhance particular properties.

1.2 Charge transport mechanism in organic materials

OSCs are considered wide-band-gap and small bandwidth semiconductors having the HOMO-LUMO gap in the range of 1-4 eV.[23] Possessing such a large band-gap at room temperature, it might be expected that the organic materials are insulators (an electron would have to acquire a large thermal energy to jump from the valence band to the conduction band). However, there are different methods to generate charge carriers in the OSCs; including injection of carriers from metallic electrodes, optical excitation (create an electron-hole pair), and electrostatic/chemical doping.

Different mechanisms of transport have been suggested for organic material in *single-crystal, polycrystalline* or *amorphous.* The band theory developed for inorganic semiconductors can also be applied for OSCs. In this case the charge transport mechanism is considered to be the same as in the extended states of the valence and conduction bands of single crystal inorganic semiconductors. It should be noted that in OSC, there are weak bonds between molecules, which consist of van der Waals and dipole-dipole attractions. This can result in lesser intermolecular orbital overlap that causes a narrower band width and a short mean free path compared to inorganic semiconductors. According to band theory, the scattering of electrons or phonons and impurities as well as temperature affect the mobility. The mobility is described[24] according to the following equation :

$$\mu \sim T^{-n} \quad (1.1)$$

Where T is the absolute temperature and n depends on the scattering mechanism. The largest hole FET mobility at ambient temperature, about 20-35 cm^2/Vs,[25,26] was observed in naphthalene single crystals, while a mobility of about 10^2 cm^2/Vs was measured employing Time-Of-Flight (TOF) experiments at cryo-temperatures of several Kelvins.[27] In the case of polycrystalline and amorphous materials, the mobility is often thermally activated, showing a phonon-assisted hopping mechanism of charge transport. In this mechanism of transport, the hopping between localized sites is thermally activated and mobility increases with the temperature. For a hopping charge transport, the mobility varies with temperature T, the activation energy E, and can be described with the following equation:[28]

$$\mu \sim V_P \exp\left(\frac{-E}{KT}\right) \exp(2\alpha R) \qquad (1.2)$$

Where V_P is the lattice vibration frequency, E is the energy difference between two hopping sites, k is Boltzmann's constant, and T is the absolute temperature. V_P exp (-E/kT) shows the probability of the localized hopping electron transferring to the next site at an energy E above the initial one. The last term, $\exp(-2\alpha R)$, describes the overlap of the wave-functions between adjacent hopping sites; R is the separation between sites and α is determined by the decay rate of the wave-function with distance.

It is known that packed molecular films with tight inter-molecular π-stacking leads to pronounced charge carrier mobilities. In this regard, the transfer integral and reorganization energy are parameters that are highly important for the charge transport in OSCs. Generally, the larger the transfer integral and the smaller the reorganization energy leads to higher charge mobility in OSCs.[29,30] Both the transfer integral and reorganization energy are highly dependent on the packing (arrangement) of the OSCs. Information regarding π-stacking motifs, such as cofacial vs. herringbone vs. tilted π-stacks provides valuable information to predict the charge carrier mobility.

Cofacial or coplanar arrangements (in oligoheterocycles for example) exhibit large repulsive interactions while a considerable stabilization exists for tilted π-stacking or slipped (herringbone) π-stacking, due primarily to electrostatic interactions. Tilted packing usually demonstrates nearly an order of magnitude higher orbital overlap than the corresponding cofacial arrangements at identical center-to center intermolecular spacing.[30]

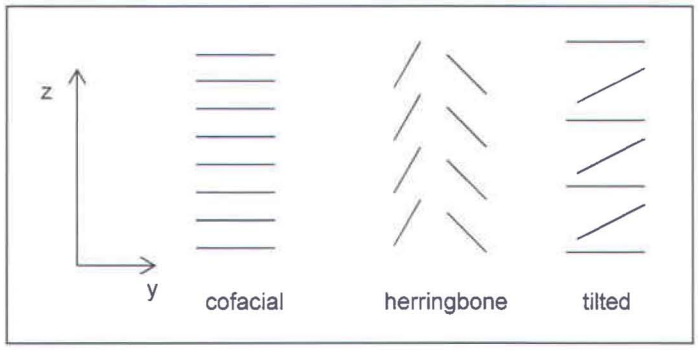

1.3 Organic field-effect transistors

Taking into account the advantages and possibilities that the OSCs offer, it is important to study the structure of the OFETs and their components. In spite of two decades of research, the fundamental comprehension of charge transport in these devices is still not satisfactory. OFETs are three-terminal devices, similar to Si MOSFETs but without a bulk contact. The three termini are the usual source (normally grounded), drain and gate electrodes, held at desired potentials. OFETs are mainly prepared in one of four configurations. The first two configurations, presented in Figure 1.1 have the gate dielectric deposited first on the substrate: **Bottom gate/top-contact configuration** (source and drain contacts are deposited on the OSC) and **bottom gate/bottom-contact geometry** (source and drain electrodes are contacting directly the gate dielectric and OSC covering the whole device).[31]

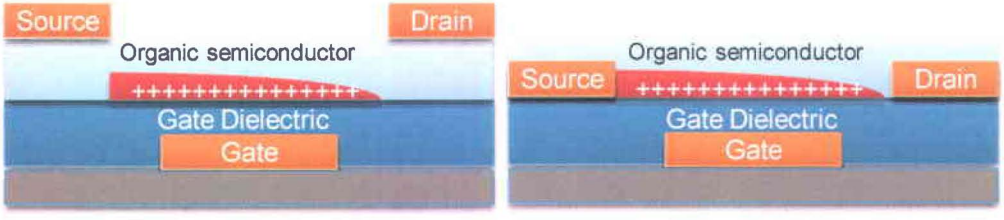

Figure 1.1: Schematic drawings of bottom-gate OFETs: top-contact (left) and bottom-contact (right) [32]

The top-contact transistors often result in better performance (higher field effect mobility) due to various factors but probably the main reason for higher mobility is that the OSC*s* grows on a smooth surface provided by a dielectric. In *bottom-contact devices*, charge transport can be influenced by the crystalline structure of the deposited OSC in the vicinity of metal electrodes. In fact, the microcrystalline structure of the OSC in the middle of the channel is rather different from the channel edges, although functionalizing the metal electrodes can limit this disturbance

of the OSC growth by modifying the surface energy of the electrodes. On the other hand, a drawback of top-contact devices is that manufacturing and particularly downsizing is hindered because lithographic processes cannot be carried out on the OSC surface; the electrodes are usually deposited by thermal evaporation through the shadow mask.

The other two OFET configurations have the gate of the transistor on top, as shown in Figure 1.2. In the **top-gate/bottom-contact** structure first source and drain are patterned on top of a (flexible or rigid) substrate, followed by OSC deposition, and then the gate dielectric and finally the gate electrode are deposited. In the **top-gate/top-contact** configuration the OSC is first deposited on the substrate followed by the deposition of the electrodes, the gate dielectric and the gate electrode. When using a polymeric dielectric, this configuration can prevent the degradation of the underlying OSCs by the ambient atmosphere.[31]

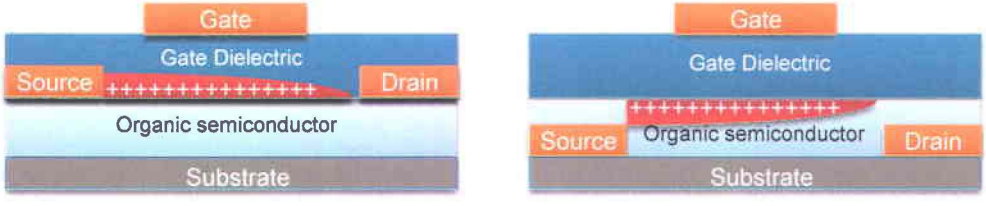

Figure 1.2: Schematic structure of top-gate OTFTs: top-gate/top-contact (left) and top-gate/bottom-contact (right)[32]

1.3.1 Factors limiting the mobility in OFETs

In thin films of OSCs, it is not possible to reach the same structural order as in a single crystal. Often, there is a remarkable difference in the performance of FETs incorporating organic thin film that made with a single crystal of OSCs. The polycrystalline thin film includes different types of defects including grain boundaries. Very often these structural imperfections create an electronic defect, a trap. Traps are the result of structural defects (grain boundary) in OSCs and/or nature of dielectric surface. Grain boundaries also act as electronic defects that limit the charge transport in an organic film.[33]

1.3.2 Operation of the organic transistors

In FETs, a gate electrode should be electrically isolated from the rest of the device. OFETs function in accumulation mode rather than depletion mode because of the low density of carriers in OSC, the charge transport takes place only in a thin layer of the semiconductor, close to the interface with the dielectric, i.e. the bulk semiconductor is not affected by the gate field. By

applying a negative bias to the gate and drain of a p-type OFET, a linear current regime is observed for $V_{DS}<V_G$. As V_{DS} becomes increasingly negative, the density of accumulated charges decreases from the source to the drain, and the current I_{DS} increases linearly (Figure 1.3). When the potential of the drain becomes more negative than that of the gate, a zone of depletion appears close to the drain (pinching of the channel) and the current tends to saturate.

The output characteristic of a FET is the series of I_{DS} versus V_{DS} curves with a fixed V_G. The transfer characteristic is the series of I_{DS} versus V_G curves with a fixed V_{DS}. These measurements can give the same information, as long as a sufficient number of gate voltages (drain voltages) are scanned as output (transfer) characteristics. Transfer characteristics are typically taken at two fixed V_{DS}: one is set as small as possible; much smaller than the maximum scanning gate voltage and the second V_{DS} is set larger than the maximum scanning V_G. These two regimes are known as the linear and saturation regime, respectively. From the transfer characteristics of the OFET, we can extract various parameters such as the field effect mobility (μ_{FET}) of the linear field and saturation field, the threshold voltage, and the on/off ratio. μ_{FET} has received by far the greatest attention and it is considered a common performance metric to compare OFETs materials and fabrication techniques. To characterize the OFET, we use the characterization model developed for Metal Oxide Semiconductor Field Effect Transistor (MOSFET) in which the mobility of the charge carrier is assumed constant and the transverse field in the conducting channel is much higher than the longitudinal field.

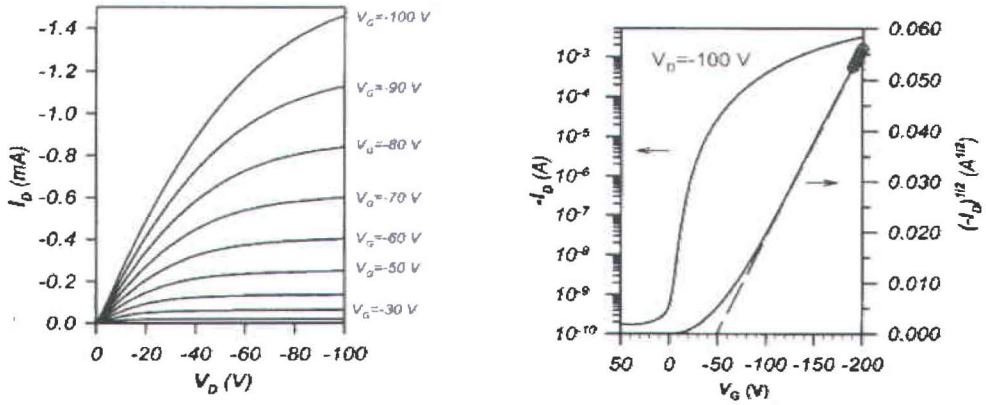

Figure 1.3 : Output and transfer characteristics of a top-contact pentacene-TFT[32]

In the standard MOSFET drain-current equation, μ_{FET} is a proportional factor that relates the I_{DS} to the V_G and V_{DS}, threshold voltage V_{th}, the channel width W and length L, and the gate

dielectric capacitance per unit area C_{ox}. The standard I_D current equation for an n-channel device:[32]

- in the linear region of operation ($V_{DS} < V_{GS}-V_t$): $I_{DS} = \frac{WC_i\mu}{L}\left(V_G - V_{th} - \frac{V_{DS}}{2}\right)V_{DS}$ (1.3)
- in the saturation region of operation ($V_{DS} \geq V_{DS}-V_t$): $I_{DS} = \frac{WC_i\mu}{2L}(V_G - V_{th})^2$ (1.4)

The values of the μ_{FET} measured in the two regions of operation are somewhat different, so often they are referred to as $\mu_{FET,lin}$ and $\mu_{FET,sat}$. Throughout this work, μ_{FET} is referred to the value that is measured in the saturation region.

In OFETs, mobility can be field-dependent due to the existing traps and also due to the limited injection through Schottky barrier at metal/OSC contacts. Thus, it is very important that the contact effects (see 1.3.5) do not affect mobility calculation. OFETs are operated away from the injection-limited regime as the bias magnitude is increased. For this reason, I_{DS} increases slightly superlinearly with V_{DS} as is expected in the linear regime of operation of an OFET.[34]

1.3.3 Threshold voltage

The threshold voltage can be defined as the gate voltage at which the conduction channel starts to form. OFETs operate in accumulation region where there is no depletion layer to isolate the conducting channel from the substrate[35] thus in these devices the charge transport mechanisms differ from silicon-based Metal Insulator Semiconductor Field Effect Transistors (MISFETs). Ideally, for an organic transistor operating in accumulation mode, V_{th} should be zero. However, the real V_{th} is non-zero due to various factors.[36] When there is misalignment of the energy levels of the metal contacts with the HOMO of p-type materials or with the LUMO of n-type materials, a non-ohmic injection barrier is formed at the metal–semiconductor interface.

V_{th} can be extracted either by extrapolating the linear region of the $I_{DS}(V_{GS})$ curve to $I_{DS}=0$ or from measurements in the saturation region by plotting $\sqrt{I}_{DS}$ versus V_G and extrapolating to $I_{DS}=0$. For many applications such as active matrix displays, low V_{th} are required to keep the drive voltage low.

1.3.4 On/Off ratio

The "on/off ratio" is the ratio between the currents in the transistor in on and off states. Since in organic transistors the channel is not isolated from the rest of the semiconductor, an ohmic current $I_{DS,bulk}$ is in parallel with the conduction current I_{DS} in the channel. The total current is:

$$I_{DS,total} = I_{DS,bulk} + I_{DS,channel} \qquad \text{and the ratio is} \qquad \frac{I_{DS,channel}}{I_{DS,bulk}} = \frac{I_{on}}{I_{off}} \qquad (1.5)$$

The on/off ratio shows the ability of a transistor to work as a switch from the on state to the off state. For applications in logic circuits this ratio has to be higher than 10^6.[37] To improve the on/off ratio I_{on} can be increased by modifying the transistor geometry. As was already mentioned, the drain-source current I_{DS} in the saturation region is proportional to the ratio W/L. Thus, the on/off ratio can be improved by increasing the width of the channel and/or by decreasing its length.[38] However, top-contact devices with channel lengths smaller than 10 μm may have short circuits due to resolution limit achieved with shadow mask.[39] The most effective way to improve the on/off ratio is reducing the off-current by purification of OSCs prior to deposition[40] and/or patterning active organic layer to eliminate leaks and reduce noise interferences.[41]

1.3.5 Contact resistances

The contact resistance in organic transistors, as well as channel resistance, has a significant effect on device performance. The total resistance of the device (R_{on}) is the sum of R_C the contact resistance and R_{ch}, the resistance of the channel.[42]

$$R_{on}=R_{c}+R_{ch} \qquad \text{while} \qquad R_{c}=R_{source}+R_{drain} \qquad (1.6)$$

The contact resistance depends on the structure of the transistor and the nature of the electrodes, e.g., its work function. It also decreases with increasing gate voltage. This can be explained by the increased density of charge carriers in the channel and close to the contacts that would have a similar effect as doping the contacts.[43,44] Contact resistance are often higher in the bottom-contact structure and depend on the drain voltage. [48] The differences existing in bottom-contact and top-contact devices can have various origins. One reason can be the larger injection surface in a top-contact structure[45] or non-uniform and disturbed growth of organic material by triple interfaces in bottom-contact structures. In addition, the interface dipoles between the organics

and the metal are sometimes different according to the deposition order (organic semiconductor on metal or metal on organic semiconductor).[46]

In general, by decreasing L and also increasing μ, a faster response time for OFETs can be achieved. Decreasing the channel length allows larger output currents. However, although R_c is independent of the channel length, R_{ch} is proportional to L. Thus, when the channel length decreases, the relative influence of R_c increases and for very small L, R_c can dominate and limit the performance. The dependence of the output characteristics on L can be used to extract R_s. Thus, in the linear regime, the overall device resistance R_{on} can be calculated from equation:[47]

$$R_{on}(L) = \frac{\partial V_{DS}}{\partial I_{DS}} :_{V_{DS}\to 0} = R_{ch}(L) + R_c = \frac{L}{W\mu C_i(V_G - V_{th})} + R_c \qquad (1.7)$$

R_c can be decreased by optimizing the metal contacts, the film morphology of the OSC or the procedure of metal deposition on the organics. For example, it can be up to 100 times lower when the metal electrodes are deposited by lamination rather than by evaporation.[48] This could be due to the thermal and morphological degradation of OSCs during evaporation. The degradation of OSCs can be caused by heat or the diffusion of the metal atoms into organics, etc. , R_c can be reduced by modifying the interface between the contacts that inject the current and the OSC, either by using Self-Assembled Monolayer (SAM) or by doping the OSC. There can be, however, a risk of amplifying the I_{off} because of the doping effect of this layer.[37]

1.4 OSCs: structure and transport properties

The active layer in organic electronic devices may consist of different types of semiconducting **small molecules** or **polymeric** OSCs[49] which similar to their inorganic counterparts can be **n- or p-type**. The majority of the OTFTs studied to date were made using p-type OSCs in which electrical conduction is mainly due to the movement of positive holes. A **p-type semiconductor** is a *hole-transport material*, having a low ionization potential, while an **n-type semiconductor** is an *electron-transporting material*, possessing a high electron affinity. Majority of known π-conjugated molecules have high HOMO levels and exhibit electron-donating properties which makes them good candidates for p-type semiconductors.

High performance n-type semiconductors are important components of p–n junction diodes, bipolar transistors, and complementary circuits. However, n-type devices usually show lower charge carrier mobility and a much strong sensitivity to the oxygen and moisture in air.[50] Moreover, certain dielectrics such as SiO_2, or polymeric dielectrics containing hydroxyls such as

PVP (polyvinyl phenol) can be the source of electron trapping.[51] For this reason, surface treatment of gate dielectrics or using certain polymer-based dielectrics such as parylene and PMMA are necessary. Another reason for lower performance of n-type OFET compared to p-type OFET is that the metals used for making contact to OSCs have work functions better suited for hole injection into the HOMO than of electrons into the LUMO, which associates with the band levels of the organic materials. For most p-type OSCs, the ionization potential is about 5 eV, which is near the Au work function. Low-work function metals such as Al, Ca, and Mg possess workfunction close to LUMO of organics however they usually oxidize easily and in some cases form reactive complexes with the OSCs.[52] The hole and electron injection in OTFTs require the Fermi levels of the metal electrodes to be close to the HOMO and LUMO, respectively. In general, for n-channel OFET operation, OSCs should posses an electron affinity approximately 4 eV below vacuum for facile electron injection through metal electrodes.[53] The LUMO level of the organic material can be tuned to facilitate the electron transport by adding strong electron-withdrawing groups such as -F, -CN, and -Cl to the outer rings of molecules.

1.4.1 Small molecules

Small molecules employed for OTFTs are low molecular weight conjugated, usually polycyclic compounds that can pack into well-organized polycrystalline films and generally have a higher mobility compared to polymeric semiconductors. Small-molecule OSCs may further be classified[49] as **linear fused ring**[54,55] (e.g. pentacene and rubrene), **heterocyclic oligomers**[56] (e.g. oligothiophenes) and **two-dimensional fused ring compounds** e.g. naphthalenetetracarboxylic dianhydride (NTCDA)[57,58,59] and phthalocyanine derivatives.[60,61,62] Small molecules can be deposited by vacuum evaporation giving crystalline thin films, thus facilitating intermolecular charge transfer. Vacuum evaporation of low molecular weight OSCs allows for depositing highly pure material. Also, it facilitates the fabrication of multilayer heterostructures with a high degree of structural order.

Linear fused ring poly-aromatics, in particular *oligoacenes* (Scheme 1.1), are among the most studied π-conjugated OSCs. The HOMO level of linear acenes significantly increases with the number of fused benzene ring which in turn facilitates hole injection into the active conducting layer of an organic device. Moreover, their planar structure promotes the crystal packing thus

enhancing intermolecular interaction. They also possess a low reorganization energy, which helps efficient charge transport.

Anthracene (**1.1a**) is the smallest member of oligoacenes with reported FET characteristics. FETs based on anthracene single crystal show mobility of 0.02 cm^2/Vs, only at very low temperatures.[63] However, no thin film FET mobility of anthracene has been reported for anthracene. Higher mobilities have been reported using substituted anthracene derivatives. Substitution at 2,6-position on anthracene can extend the π-conjugations thus the charge mobility. OTFTs based on the 2,6-Bis[2-(4-pentylphenyl)vinyl]anthracene (**1.1b**) show mobility of 0.1-1.28 cm^2/Vs.[64] The enhancement in charge mobilities has been also observed in different anthracene oligomers (**1.1c**, **1.1d**)[65,66].

Tetracene is the smaller homologue of pentacene which has a shorter π-conjugated system. Single crystal-tetracene FETs show mobility of ~1.3 (cm^2/Vs)[67] and thin films yield a mobility of 0.1 cm^2/Vs.[68] Some halogen substituted tetracene derivatives (**1.1g**, **1.1h**) are shown capable to pack slipped face-to-face stacks which enhances π-orbital overlap and therefore increase the charge mobility. For example, single crystal FETs based on tetrachlorotetracene crystals show p-type behavior with a field-effect mobility of 1.7 cm^2/Vs.[69] Tetraphenyl-substituted tetracene, rubrene (**1.1f**), is one of the best materials for SC-OFETs. Rubrene is an example of OSC with a slip-stack arrangement within each stack and strong preference for growing in (ab) plan ($l_b > l_a > l_c$, where l is the length of each dimension). Rubrene SC-FETs show one of the highest OFET mobility of up to 10-20 (cm^2/Vs).[70,71]

Pentacene (**1.1i**) is a popular molecule for OTFT fabrication due to its excellent field effect mobility and good film-forming properties.[72] OTFT characteristics of pentacene have been extensively studied since the 1970s. The highest field-effect mobilities reported for polycrystalline thin film of pentacene are 0.3–0.7 cm^2/Vs on SiO_2/Si substrates,[73] 1.5 cm^2/Vs on chemically modified SiO_2/Si substrates,[74] and 3 cm^2/Vs on polymer gate dielectrics.[75] The remarkably high electronic transport properties of pentacene thin films are due to their relatively high structural order. Even higher mobilities were achieved in single crystals (e.g. μ=35 cm^2/Vs at room temperature and μ=58 cm^2/Vs at 225 K) using space-charge-limited current (SCLC) methods.[17] There are not many OFETs reported on higher oligoacene. The highest mobility

obtained for (**1.1k**)[76] and (**1.1m**)[77] are 10^{-5} cm^2/Vs and 0.05 cm^2/Vs, respectively. Despite the strong electron withdrawing effect of quinone, these molecules only show hole mobility.

Scheme 1.1. Chemical structure and mobility of some *heteroacene* OSCs[78]

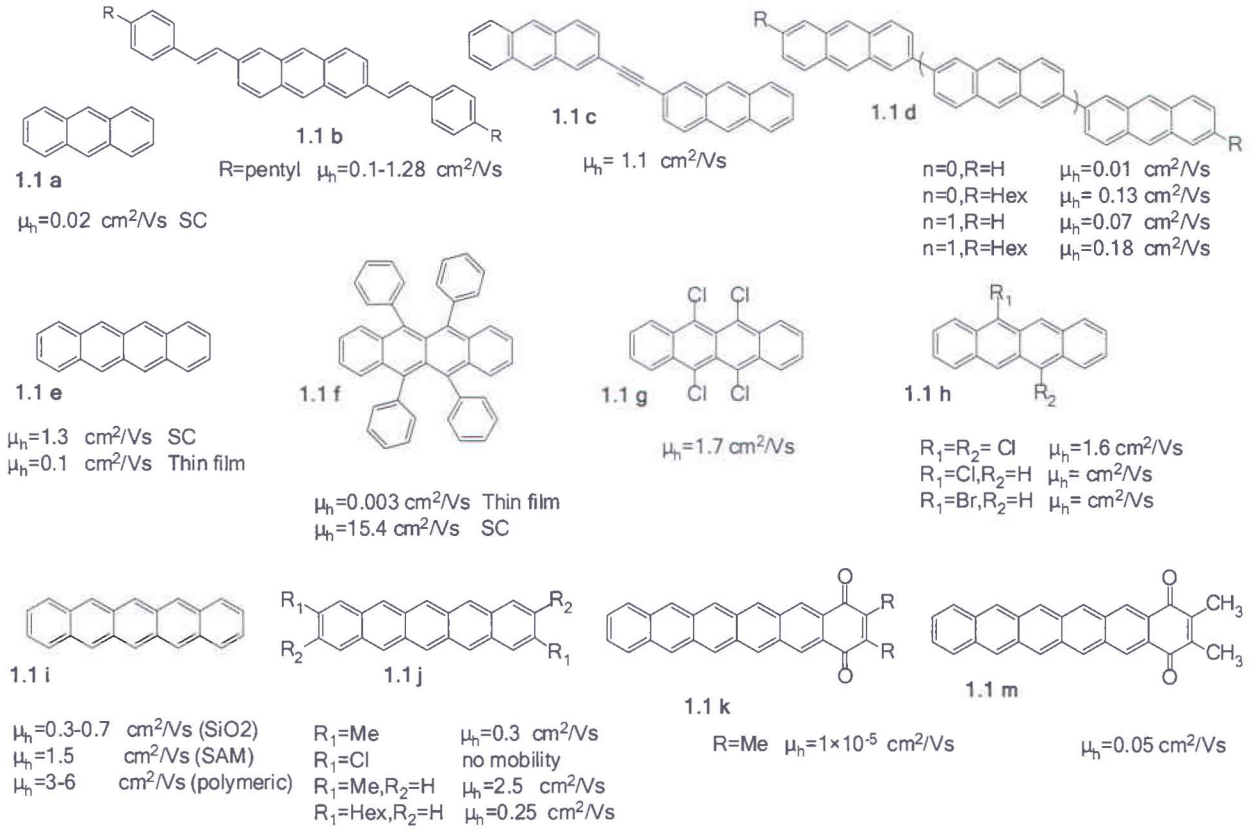

Conjugated oligothiophenes and their derivatives (scheme 1.2) have also been the most intensely studied as OSCs due to the synthetic versatility of thiophene heterocycle and ease of functionalization.[79] With except to terthiopenes all unsubstituted oligothiophenes are planar in the crystalline form (inter-ring torsion is less than 1 degree).[80] They pack in a herringbone arrangement however substitution may force the molecules to adopt a face-to-face π-stacking arrangement.[81]

In general, increasing conjugation length of oligothiophenes yields an increase in mobility but lowers their solubility. This makes purification and deposition more difficult. Molecular engineering of oligothiophenes can not only improve their solubility but also in some cases enhance mobility. It has been shown that introducing alkyl substituents at β-position of thiophene ring results in improvement of solubility however induces the loss of planarity and

consequently affects transport properties.[80] Linear alkyl groups at terminal α-position can induce preferred molecular orientation thereby enhance mobility up to one order of magnitude (**1.2 a**, **1.2b**, **1.2d**, and **1.2f**).[82] This is been demonstrated in an increase of mobility from 0.01 cm^2/Vs for un-substituted 6T[81] to 0.13 cm^2/Vs for alkylated α-6T (**1.2b**).[83] However in the case of β-substitution alkyl groups significantly reduce the charge mobility (**1.2c**).[84]

Oligothiophenes that are substituted at the central position of the backbone with phenyl units have been shown to have a broader band gap and relatively higher thermal stability compared to thiophene homo-oligomers with same length.[85] A systematic study on a series of dibenzothiophenes (**1.2d**) showed a lower HOMO level compared to corresponding oligothiophene with same length and mobility in the order of 0.1 cm^2/Vs.[86] Fused benzothiophene end-groups of 4T (**1.2e**)[87] also showed the improvement of the mobility compared to unsubstituted 4T. Obviously, the family of conjugated oligothiophene based OSCs that are used as active materials in OFETs includes many substituted and fused ring compounds which is out of the scope of this short review.

Scheme 1.2. Chemical structure and mobility of some oligothiophene derivatives[78]

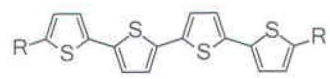

1.2 a

R= H μ_h=0.014 cm^2/Vs
R= C_6H_{13} μ_h=0.02-0.23 cm^2/Vs
R= $C_{10}H_{21}$ μ_h=0.2 cm^2/Vs
R= cyclohexyl μ_h=0.038 cm^2/Vs
R= $C_{12}H_{25}$ μ_h=3E-5 cm^2/Vs

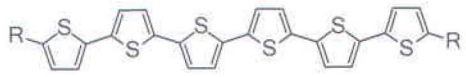

1.2 b

R= H μ_h=0.07 cm^2/Vs
R= C_2H_5 μ_h=1.1 cm^2/Vs
R= C_6H_{13} μ_h=1 cm^2/Vs
R= $C_{10}H_{21}$ μ_h=0.5 cm^2/Vs
R= $C_{12}H_{25}$ μ_h=0.016 cm^2/Vs
R= $C_{18}H_{37}$ μ_h=0.013 cm^2/Vs

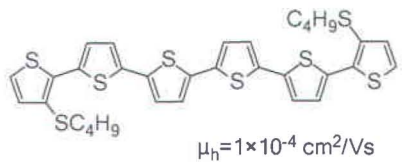

1.2 c

μ_h=1×10^{-4} cm^2/Vs

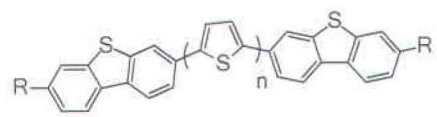

1.2 d

n=1 R= C_6H_{13} μ_h=0.012 cm^2/Vs
n=2 R= C_6H_{13} μ_h=0.14 cm^2/Vs
n=2 R= H μ_h=0.08 cm^2/Vs
n=2 R=cyclohexyl μ_h=0.17 cm^2/Vs
n=3 R= C_6H_{13} μ_h=0.025 cm^2/Vs
n=4 R= C_6H_{13} μ_h=0.023 cm^2/Vs

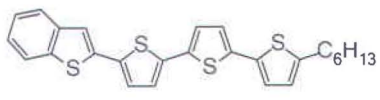

1.2 e μ_h=0.011 cm^2/Vs

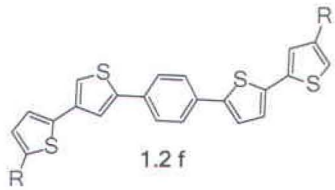

1.2 f

R= H μ_h=5×10^{-4} cm^2/Vs
R= C_6H_{13} μ_h=0.042 cm^2/Vs
R= $C_{10}H_{21}$ μ_h=0.3 cm^2/Vs

Replacement of the benzene rings of *oligoacenes* by thiophene rings (Scheme 1.3) has been shown to enhance the air stability to *oligoacenes*. For example alkylated anthradithiophenes (**1.3c**) demonstrate mobility of up to 0.15 cm^2/Vs with great oxidative stability.[88] Perhaps the

best example is triethylsilyl anthradithiophene (**1.3a**), substituted in central aromatic ring, which demonstrated mobility of 1 cm^2/Vs in solution-processed FET configuration.[89] Substitution of the carbon atoms in *oligoacenes* with different heteroatoms such as nitrogen or sulphur can also modify their optoelectronic properties and increase oxidative stability.

Scheme 1.3. Chemical structure and mobility of some thioacenes-based oligomers[78]

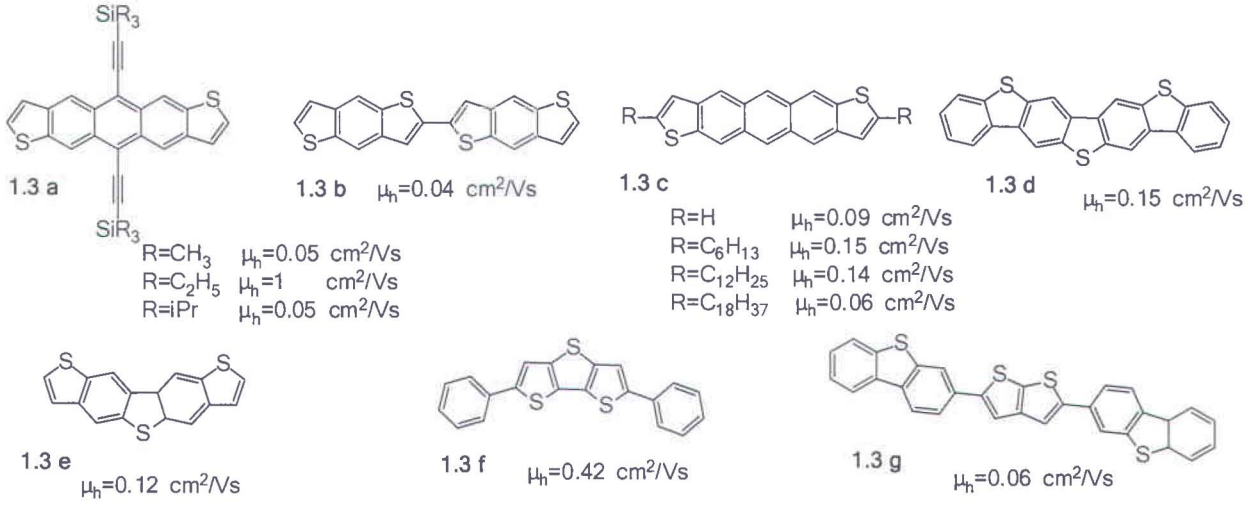

Different molecular structures of small molecules have been studied as n-type semiconductors, such as naphthalenetetracarboxylic dianhydride (NTCDA) (**1.4a**),[57,58,59] and phthalocyanine derivatives[60] (**1.4f**). Bao et al. studied the use of this technique to design a novel air-stable n-type semiconductor based on $F_{16}CuPc$ (**1.4f**) with a maximum electron mobility of 0.03 cm^2/Vs.[60] Fullerenes (C_{60} and C_{70}) and their derivatives (**1.4e**) are also an important class of n-type OSCs. Fullerenes have almost spherical shape which provides an isotropic charge transport in solid state. The electron mobility of up to 0.56 cm^2/Vs was evaluated for OFETs fabricated by molecular beam deposition of C_{60}.[90] Naphthalene- (Scheme **1.4a**) and perylene-diimide (**1.4b**) derivatives are other representatives of n-type OSCs with the electron mobility of about 0.16 cm^2/Vs[91] and 1.3 cm^2/Vs[92], respectively. Recently synthesized electron transport materials such as thiazole oligomers with trifluoromethylphenyl groups[93,94] can reach electron mobilities up to 1.83 cm^2V/s (**1.4 i**).

Scheme 1.4. Chemical structure of and mobility of some n-type small molecule OSCs[78]

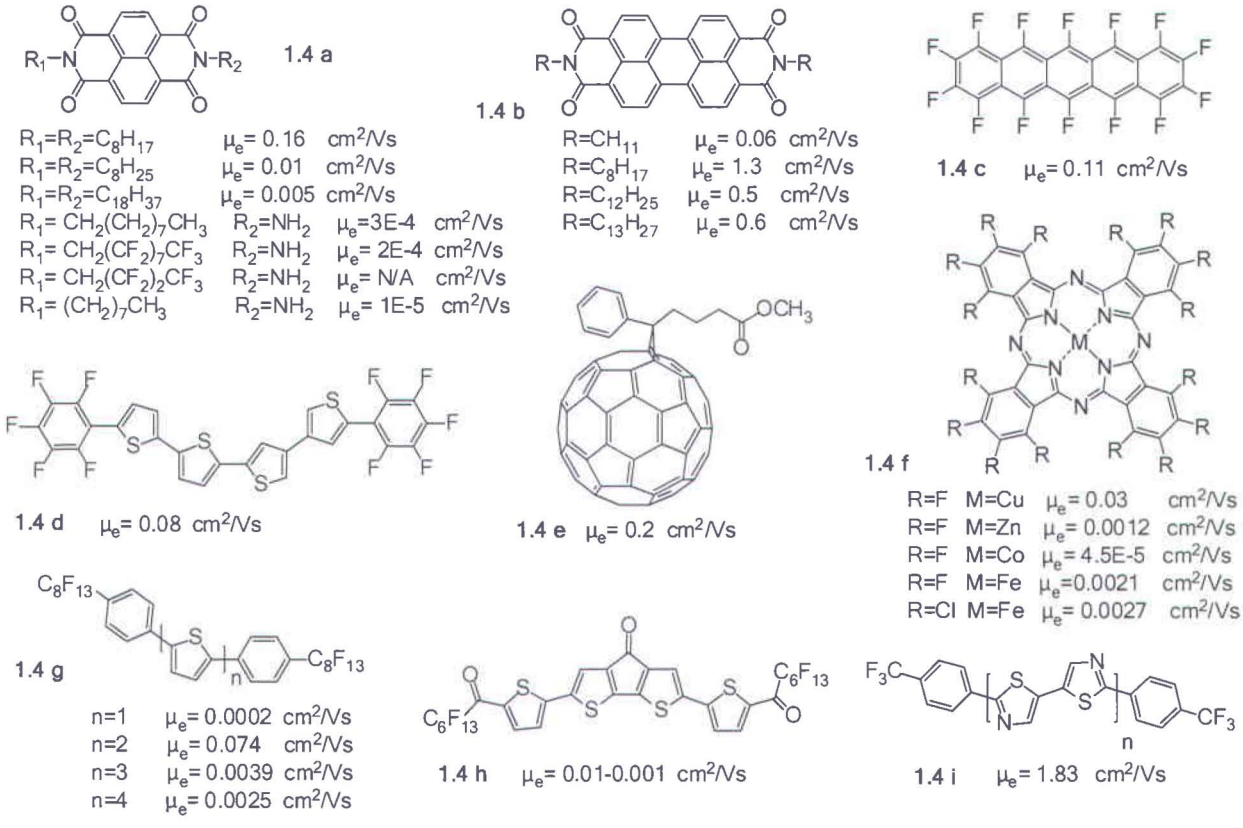

1.4.2 Conjugated polymers

Conjugated polymers are well studied materials to be used as semiconductors because they can easily form thin films on large surface areas by inexpensive solution processing. Polymers can be deposited with different solution processing techniques such as spin-coating,[95] dip-coating,[96] spray-coating,[97,98,99] ink jet printing,[100] stamping,[101] and screen printing.[102] The simplicity of these manufacturing techniques has a great impact in increasing interest in polymers. However, the structure of polymer films is less ordered than that of small molecules and is more difficult to purify. For these reasons, small molecules usually have a higher mobility which can reach few cm^2/Vs compared to polymers. Polythiophene is one of the very first solution-processed OSCs used as active layer in OTFTs. Various substituents have been incorporated on the polymer backbone to impart functionality, enhance solubility, or induce self-assembly. Among them, poly(3-hexylthiophene), P3HT (**1.5a**) is the most studied one.[103] It has been demonstrated that highly regioregular, head-to-tail arrangement, P3HT self-orients to a well ordered lamellar structure with an *edge-on orientation* of the thiophene rings relative to the substrate.[104] Such an

orientation gives the field-effect mobility ranging 0.05-0.2 cm^2/Vs.[105,103] On the other hand, some polymers having low degree of regioregularity prefers lamellae structure with a *face-on orientation* and shows mobility in the order of 10^{-4} cm^2/Vs.[105]

It has been shown that oxygen can act as dopant in P3HT and decrease the overall OFET performance. The ionization potential of P3HT can be improved by introducing electron-deficient units.[106] The nature of the side chain in poly(3-alkyllthiophene) also influences the morphology of the thin film and resulting OFETs performance.[107] This was demonstrated in polythiphenes containing electron withdrawing alkyl carboxylates[108] (**1.5m**) and tetraflurobenzene[109] (**1.5n**) showed mobility up to 0.07 cm^2/Vs and 0.002 cm^2/Vs, respectively. Polymers containing an electron-accepting silole unit also showed high air stability and mobility of about 0.06 cm^2/Vs.[110] Thiophene-thiazolothiazole copolymers (**1.5d**) demonstrated excellent air stability as well as high mobility of 0.14 cm^2/Vs.[111] Introduction of condensed heterocyclic units can also increase intermolecular interactions thus improving OFETs performance. In this respect, thienothiophene polymers showed higher environmental stability along with high mobilities in the range of 0.2-0.6 cm^2/Vs.[112] In the later case, the high value for mobility was attributed to the relatively large crystalline domain sizes.

Scheme 1.5. Chemical structure and mobility of some p-type polymer semiconductors[78]

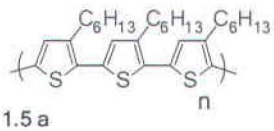

1.5 a

μ_h=0.05-0.2 cm^2/Vs

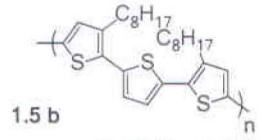

1.5 b

μ_h=0.03 cm^2/Vs

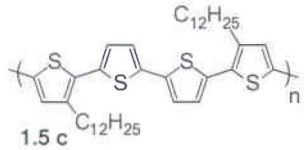

1.5 c

μ_h=0.14 cm^2/Vs

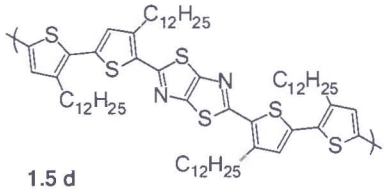

1.5 d

μ_h=0.14 cm^2/Vs

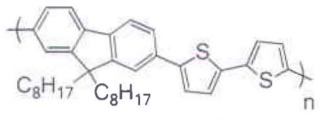

1.5 e μ_h=0.02 cm^2/Vs

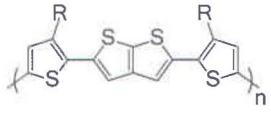

1.5 f

R= C_8H_{17} μ_h=N/A
R= $C_{10}H_{21}$ μ_h=0.15 cm^2/Vs
R= $C_{12}H_{25}$ μ_h=0.12 cm^2/Vs

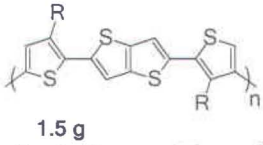

1.5 g

R= $C_{10}H_{21}$ μ_h=0.3 cm^2/Vs
R= $C_{12}H_{25}$ μ_h=0.3 cm^2/Vs
R= $C_{14}H_{29}$ μ_h=0.63 cm^2/Vs

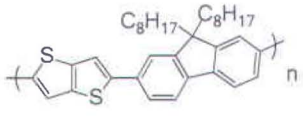

1.5 i

μ_h=0.001 cm^2/Vs

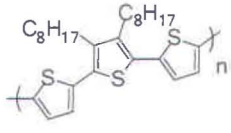

1.5 j μ_h=0.01 cm^2/Vs

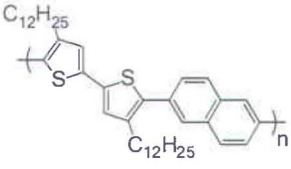

1.5 p μ_h=6×10^{-4} cm^2/Vs

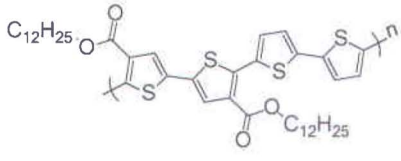

1.5 m μ_h=0.07 cm^2/Vs

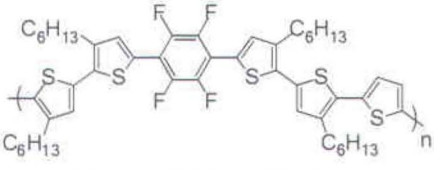

1.5 n μ_h=0.002 cm^2/Vs

Scheme 1.6. Chemical structure and mobility of some n-type polymer semiconductors [78]

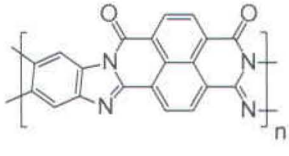

1.6 a μ_e=0.1 cm^2/Vs

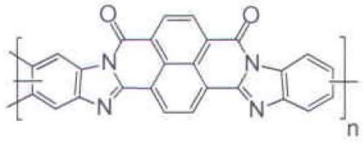

1.6 b μ_e=1×10^{-6} cm^2/Vs

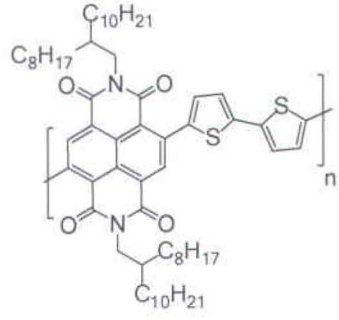

1.6 e μ_e=0.45-0.85 cm^2/Vs

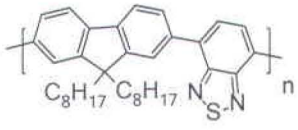

1.6 c μ_e=4.8E-3 cm^2/Vs

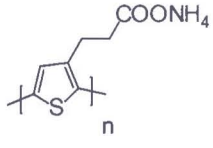

1.6 d μ_e=0.5-0.7 cm^2/Vs

However, despite the impressive performance of a few n-channel OSCs and recent progress in developing new electron-deficient π-conjugated cores[113,114] only few high-performance and air-stable n-type polymers have been reported. Maybe the best example is the recent report of the electron mobility of 0.45–0.85 cm^2/Vs for naphthalene-bis(dicarboximide) (NDI) polymer (scheme 1.6 e) under ambient conditions in combination with Au contacts and various polymeric dielectrics.[113]

In summary, it is important to know that the chemical structure of compound plays an important role in determining the physical properties of π-conjugated systems. By molecular engineering, we can control the magnitude of π-overlap along the molecular backbone and minimize structural defects. Planarization of the backbone and its packing in the form of π-stacks lead to better materials and device performance and stability.

1.5 Organic thin film growth

In general, achieving high charge-carrier mobility (μ>1 cm^2/Vs) in OSCs requires dense crystalline molecular films with strong π-π interactions. Moreover, proper control of the orientation of the organic molecules on the substrate is also necessary to obtain optimal charge carrier transport in the desired direction. In an OFET, vertical orientation of molecules on substrate can maximize the charge-carrier mobility in the direction of π-stacking.[115,116] Such a vertical orientation can be promoted by substitution of alkyl chains at the ends of the π-conjugated molecules and by precise control of the deposition condition. However, such an orientation can limit the absorption of the incident light by molecular film and charge transport in devices such as photovoltaics.[117] In general, the optimization of the deposition conditions, post-processing treatment, the nature of substrate surface and its interface with organic material play major parts in device performance.[118]

➢ Important parameters controlling the growth of thin film of "small molecule" OSCs are *evaporation rate* and *substrate temperature.* During vacuum deposition of small molecules, kinetic parameters such as the rate of deposition and also substrate temperature can profoundly affect the growth of the deposited film. A low rate of deposition (0.1-10 Å/s) is generally employed to achieve highly uniform film. AFM micrographs of 50 nm pentacene thin films deposited on silicon dioxide at different deposition rates are shown in Figure 1.5 (a,b,c). It can be easily observed that decreasing the deposition rate leads to bigger grain size and changes the

morphology of the deposited thin film. The deposition rate depends on pressure, molecular weight and source temperature and can be calculated by: $R = P(2\pi mkT)^{-1/2}$, where P and T are the pressure and temperature respectively; k is Boltzmann's constant, and m the molecular weight. [119]

By increasing the substrate temperature during thin film deposition the average grain size can be increased due to the increased mobility of the deposited molecules on the substrate, resulting in lower nucleation density and better alignment of the molecules. The optimal temperature of the substrate during deposition will thus depend largely on the evaporated molecules. The influence of the substrate temperature on the deposition of pentacene thin films on silicon dioxide is shown on Figure 1.4 (d,e,f).

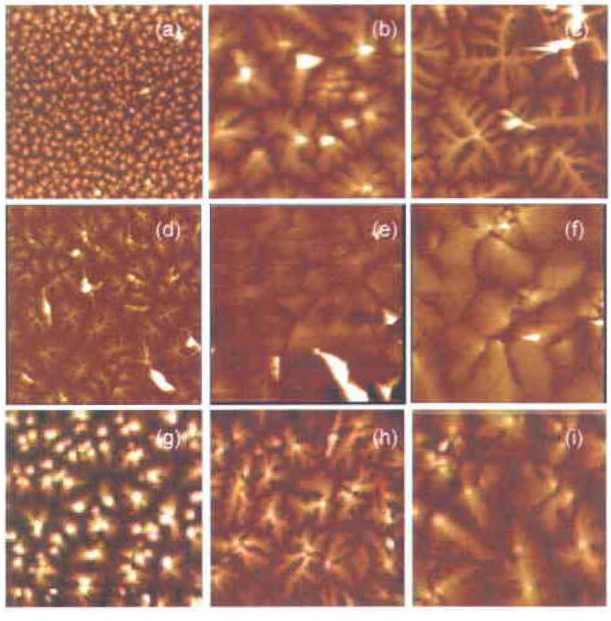

Figure 1.4: AFM micrographs of a 50 nm **pentacene** thin film deposited on silicon dioxide at different deposition rates at room temperature: (a) 0.6ML/s, (b) 0.1 ML/s, (c) 0.04 ML/s; AFM micrographs of pentacene on SiO_2 at different substrate temperatures: (d) 25°C, (e) 60°C, (f) 65°C; Influence of substrate material on pentacene thin film morphology: (g) SiO_2, (h) Poly methyl methacrylate (PMMA), (i) Polyvinyl Phenol (PVP).[119]

➢ For semiconducting polymers, the methods of deposition (spin-coating, drop-casting, etc.), the solvent[95] and the post annealing conditions, are important parameters defining the film growth and thus the performance of the OFET. For each material it is essential to find the deposition conditions that allow a favorable molecular ordering.

1.6 Organic single crystals

As discussed above, the morphology of OSC films and performance of OTFTs strongly depends on fabrication conditions. OTFTs that are fabricated from the same material can exhibit very different electrical properties. In other words, the intrinsic properties of the organic materials in OTFTs are generally altered by the structure of their films. [120]

In this regard, devices based on the single-crystals offer a better possibility of revealing the relation of molecular structure to its optoelectronic properties.[121] The carrier mobility in single crystal FETs can be an order of magnitude higher than that in the best OTFTs.[122]Crystals can be grown from solution or vapour-phase. The solution growth processing is probably simpler and widely used growth method.[123] In this method, crystals are grown from saturated solution by allowing the solvent to slowly evaporate. The choice of solvent can affect the quality of the grown crystal.[124] In this method, some solvents may remain inside the crystal or at the surface and act as an impurity. Moreover, many small molecules studied for OFETs, such as pentacene, are highly insoluble. For these reasons crystals for OFETs are more commonly grown from the vapor phase. In a general experimental setup, the starting material is loaded into the high temperature zone of a furnace and maintained slightly above the sublimation temperature of the organic material. Vapour of the material then is carried by the gas stream (argon, helium, nitrogen…) to the region with a lower temperature where re-crystallization takes place at the wall of the reactor or directly on the substrate. In this method, the important factors influencing the morphology and the quality of the crystals are the purity of the starting material, carrier gas, gas flow velocity, and the temperature.[125] Vapour grown single crystals could be easily nucleated and grown at the regions of microcontact-printed SAMs such as HMDS and OTS, which can be widely used in OSCs, including p-type materials, such as anthracene, tetracene, pentacene, and rubrene and also n-type materials, such as $F_{16}CuPc$, C_{60}, and TCNQ.[126]

1.7 Dielectric

The gate dielectric has a strong effect on device properties. An important parameter in gate dielectrics is the capacitance per area: $C_i = \varepsilon_0(\frac{\varepsilon}{d})$ where, ε is dielectric constant, d the dielectric thickness, and ε_0 dielectric permittivity. Thus, to achieve large capacitance it is necessary to reduce the thickness and/or increase the permittivity of the dielectric. In general, interface between the OSC and the gate dielectric surface plays an important role in intermolecular charge

transport. Surface treatment (in the case of silicon dioxide or silicon nitride) and use of polymeric insulators can improve the interface quality. The influence of the substrate on the pentacene thin film morphology is depicted in Figure 1.4 (g,h,i). The images show a 50 nm pentacene film deposited all at 65 °C with the same deposition rate on different substrates. It can be seen that the substrate material strongly affects the morphology of the film.[119]

1.7.1 Inorganic dielectric materials

This type of insulators can not be deposited from solution and also their mechanical properties are not compatible with flexible substrate.[127] SiO_2 grown *in situ* on a highly doped Si gate having a dielectric constant of about 3.9, is the most widely used gate dielectric, providing a common platform to evaluate new OSC.[127,128] The field-effect mobility depends on the accumulated charge in the OFETs channel. Also, the density of this charge is proportional to the dielectric constant and gate bias.[129] A straightforward method to improve the gate capacitance is to replace SiO_2 with a gate dielectric material having a higher permittivity.[130] Dielectrics with higher permittivity might allow increasing device density on integrated logic circuits because of their lower thickness. Using this type of dielectric material will reduce the operation voltage of OFETs. For example, pentacene OFETs having amorphous barium strontium titanate (BST, k=16), barium zirconium titanate (BZT, k=17.3), and Si_3N_4 (k=6.2) as gate dielectric showed mobility in the range of 0.3-0.6 cm^2/Vs at a low bias of 5 V.[131] Moreover, the inorganic dielectric surfaces, except SiO_2, show a rather rough surface that leads to smaller grain size during film growth, affecting the charge transport in the device.[132] Adopting a bilayer of high-K material and SiO_2 could be one way to achieve a low-bias operation and high performance.[133]

1.7.2 Polymeric dielectric materials

Polymeric dielectric materials are attractive because they can be easily formed by spin-coating, printing, or drop-casting and other solution-based techniques, under ambient conditions, while common inorganic insulators require high temperatures for deposition. Various studies showed that the performance of OFET with polymeric gate dielectric could be of the same order, or even higher than that obtained with inorganic insulators. However, they have several drawbacks such as high leakage current and variation in dielectric constant leading to irreproducible properties.[129]

The OSCs deposited on polymers often present large dendritic grains similar to those formed on oxides with low roughness.[134] There have been some studies on OFETs with polymeric

dielectrics showing high mobility comparable with their inorganic counterpart due to the suppressed charge trapping at the dielectric/semiconductor interface.[135] Transistors based on pentacene made on PVP[136] or PMMA[137] showed the mobility of up to 0.7 cm^2/Vs and 0.75 cm^2/Vs, respectively. Despite the lower mobility compared to those of made on SiO_2, it seems interesting to use polymers instead of inorganic dielectrics to move towards plastic electronics. The rather low permittivity of most dielectric polymers reflects in high operating voltage of the resulted transistors.

Scheme 1.7: Chemical structure of some polymeric dielectrics: PVP (polyvinylphenol), PS (polystyrene), PMMA (polymethylmethacrylate), PVC (polyvinylchloride), BCB (benzocyclobutene), PVA (polyvinylalcohol), PVDF (polyvinylidenfluoride)

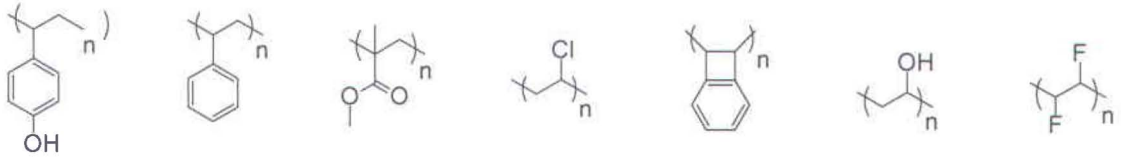

PVP (k=3) | PS (k=2.4) | PMMA (k=2.6) | PVC (k=3) | BCB (k=2.64) | PVA (k=7.8) | PVDF (k=6.8)

1.8 Tuning the interfaces

1.8.1 Surface functionalization of gate dielectric

The interface between the organic material and the gate dielectric defines the growth and morphology of OSC films. The control of this interface is important because the charge transport takes place in the first few layers close to the dielectric.[138] Chemical modifications of a dielectric surface with self-assembled monolayers (SAMs) can improve the charge carrier transport and yield higher device performance.[139] The SAM can be formed via the reaction of molecules and the surface either in solution or in the gas phase. After functionalizing, the surface is terminated with specific tail groups.

Scheme 1.8: Chemical structure of octadecyltrichlorosilane (OTS) and hexamethyldisilazane (HMDS)

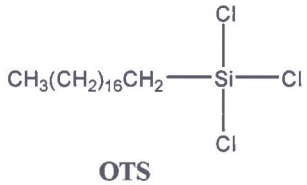

OTS

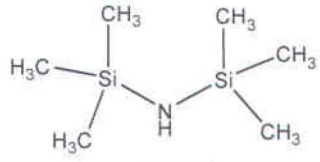

HMDS

The interaction of the tail group of SAM with the OSC can favour the organization of the deposited molecules. Alkylsiloxane SAMs on oxide surfaces have been typically used in fabrication of OFETs, especially to reduce the surface energy of the gate dielectric, determine the orientation and morphology of the organic semiconductor films, and to improve charge transport.[140,141,142] As for example, depending on the properties of the substrate surface that result from SAM treatment P3HT can adopt two different orientations parallel and perpendicular to the gate insulator leading to mobility differing by factor of four.[143,144]

Different studies on the performance of pentacene-based devices showed higher FET mobility for devices with surface treatment.[132,140] The enhancement of pentacene-FET mobility could be due to the increased grain size of the pentacene molecules and also a high molecular surface mobility and reduced interactions with the surface of a hydrophobic substrate. Figure 1.5 shows AFM micrographs of smaller pentacene grains on SiO_2 treated with OTS. Although SAM improves the growth of organic semiconductors and eventually the performance of the device, they do not reduce the operating voltage.[145]

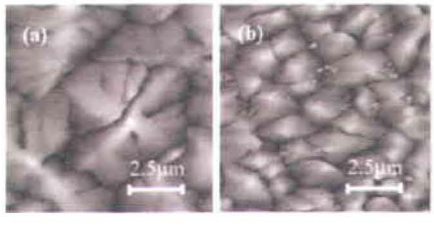

Figure 1.5: AFM micrographs of pentacene on: (a) SiO_2, and (b) SiO_2 with OTS.[146]

SAMs with thicknesses of a few nanometers can also be used as gate dielectrics in OFETs. The Vuillaume group reported the first oligothiophene FETs with SAM dielectric layers.[147] The leakage current through densely packed SAM with highly ordered aliphatic chains was remarkably low, even though the dielectric layer was only a few nanometers thick.

1.8.2 Surface functionalization of contacts

The electrode surface can also be functionalized to improve the device performance by reducing the contact resistance. This can be possible via introducing a SAM of thiol-based electron acceptor molecules on the source and drain electrodes.[148]

Scheme 1.9: chemical structures of molecules used to modify the metal electrodes: a) 3,4-dichlorobenzenethiol, b) pentafluorobenzenethiol, c) 4-nitrobenzenethiol, and d) 4-nitrobenzenethiol.

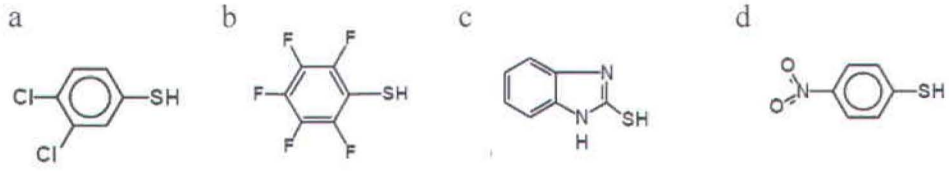

The crystalline structure of the thin film at the edge of the channel, at the vicinity of the electrodes and OSC, causes the limitation of the performance in bottom contact devices. The large grain, well ordered structure in the center of the channel changes into a microcrystalline structure as we move closer to the edge of the channel. At the edge of the channel between the interface with the bottom contact electrode is seen as an area with a large number of grain boundaries; that affects the performance of the device.[149] Another approach to improve charge carrier injection and the I-V characteristics in the linear region is to use doping to increase the carrier density near the device contacts. However, dopants cause instability in organic semiconductors and they can diffuse into the conducting channel and drastically increase the off current.[148]

1.9 Organic light-emitting devices

Since the first reports of electroluminescence (EL) in organic thin films,[150,151,152] organic light-emitting devices have attracted considerable attention. Due to the tremendous progress in the development of OLEDs using polymers as well as small molecule semiconductors,[153,154] these devices are considered to be one of most promising technologies for display and lighting applications. Another recently emerging class of organic light-emitting devices is the organic light-emitting transistor (OLETs). In this section, the principal aspects of both device configurations will be shortly reviewed.

1.9.1 Basics of light emission

Various energy level of a molecular system typically consist of electronic, vibrational, rotational and translational levels. Upon optical excitation of a molecule an electron can be promoted from the HOMO to the LUMO or to a higher empty orbital. Then an electric field is formed and surrounding molecules are polarized. The quasi-particle of an excited molecule that is formed in this way is called "exciton". Excitons can also be generated electrically by the injection of electrons to LUMO and holes to HOMO (essentially, electron-hole recombination). The different energy levels of a molecule and the transitions between them are described by a Jablonski diagram (Figure 1.6).[155]

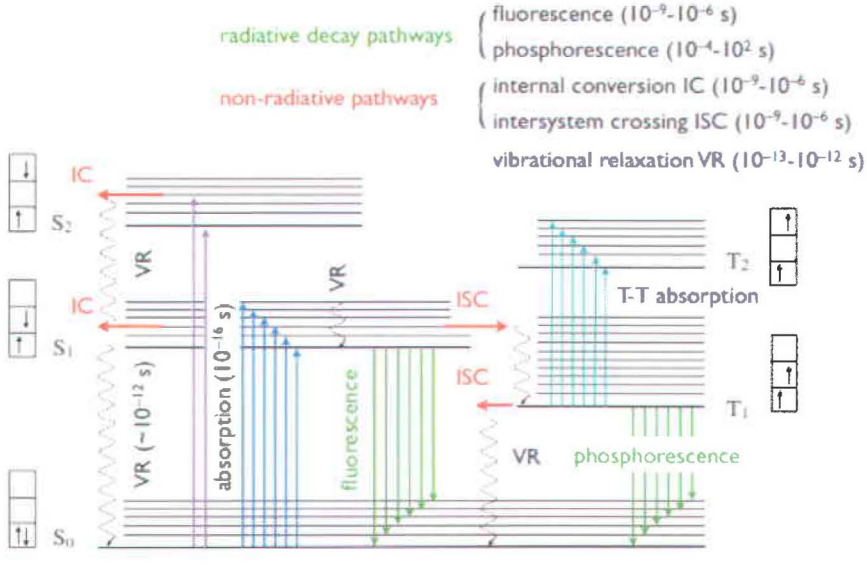

Figure 1.6: Diagram of the possible process following the absorption of a photon by a molecule.

The absorption of a photon by a chromophore generates an excited state. This phenomenon is then reversed and the excited state releases its excess energy via different mechanisms as follows:

➢ One way is by the emission of a photon, which is called **fluorescence or phosphorescence** depending on the multiplicity of the excited state. **Fluorescence** is a fast radiative process in which the spin multiplicities of the initial and the final states remain the same. In general, fluorescent organic molecules contain extended conjugated π-electron systems such as in polycyclic aromatic hydrocarbons. Non-fluorescent compounds which strongly absorb UV or visible light can sometimes be converted into fluorescent derivatives by chemically

attaching a fluorescent tag. **Phosphorescence** involves the transition from the T_1 excited state to the S_0 ground state which requires spin-orbit coupling to conserve total spin-momentum. In general, the intensity of phosphorescence is much smaller than the intensity of fluorescence from singlet excited states. However, the triplet state has a longer lifetime (from μsec to sec), compared to ns for fluorescence.

1.9.2 Organic light emitting diode OLED

Thin format, cheap manufacturing, light weight, color tunability, and wide viewing angle are some of the advantages of OLEDs compared to inorganic solid-state based LEDs.[156] The OLED technology is also believed to possess good chromaticity properties (color purity) that will enable correct and good visual presentation of data. Historically, one of the major drawbacks for OLEDs was their relatively short life-time which is the result of degradation of the emitting material that can be prevented by design of stable materials and encapsulation of the organic layers. Todate, OLEDs with operation life times exceeding 100,000 h have been demonstrated by several industrial players.[157,158]

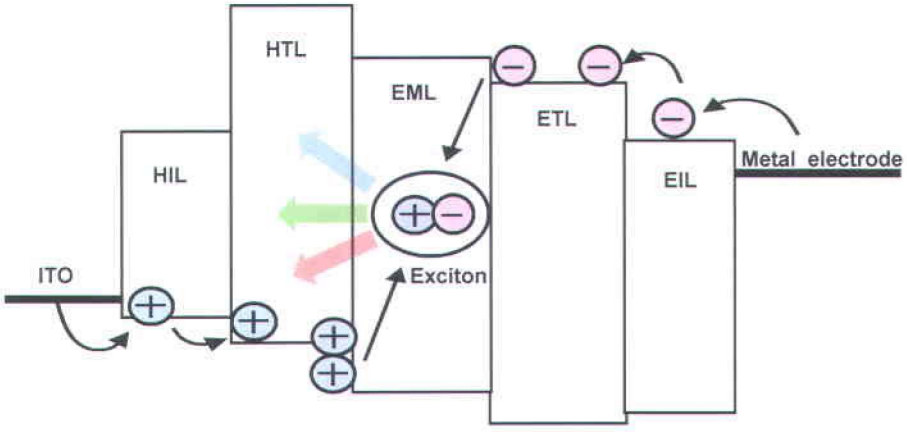

Figure 1.7: Energy diagram in multilayer OLEDs[158]

Any OLED structure consists of an anode, a cathode and of organic layer(s). The anode material is usually made of Indium Tin Oxide (ITO), which has been a material of choice due to its high transparency and conductivity. Popular materials for the cathode are metals such as Al, Ca, and Mg. The anode has a high work function while the cathode possesses a low work function to provide a low energy barrier for the injection of holes and electrons, respectively. One or more organic layers are sandwiched between the anode and the cathode

through processes such as evaporation or solution processing (spin coating, spray-coating, and screen printing). In this structure, conduction of the charge carriers to the emitting zone can be hindered by the usually disordered structure of employed OSC and also by the mismatch between molecular orbital of OSC and workfunction of electrodes. To minimize the energy barrier between the electrodes and the organic material and to enhance the injection of the charge carriers, this structure can be modified to a double layer in which the organic layer is commonly composed of a Hole Transport Layer (HTL) and Electron Transport Layer (ETL). For the same reason, the multi-layered structure can improve the performance of the OLED and also increase the range of the emitted colors. To control and enhance the hole injection from the anode to the HTL and electron injection from the cathode to the ETL, a Hole Injection Layer (HIL) and Electron Injection Layer (EIL), respectively, are introduced to the structure of the OLEDs. The excitons are formed and consequently the light is emitted from the Emissive Layer (EML). HIL is a p-type organic material which controls and enhances the injection of the holes from the anode. It posses a low LUMO resulting in a low energy barrier between anode and organic layer which in turn facilitates the hole injection to the organic layer. Porphyrinic metal complexs such as copper phthalocyanine (CuPc), self assembled silane compounds, conducting polmers such as polyethylenedioxythiophene) (PEDOT) are common organic materials used as HIL. The HTL, similar to the HIL, requires high hole mobility.[158] It transports holes from the HIL to the EML and in some cases hinders negative charges from the cathode. Carbazole[159] and fluorene[160] derivatives, as well as aromatic amines such as triphenylamine derivatives[161] are frequently used organic materials as HTL.[158] ETL is an n-type organic material, having high electron mobility, which transports the electrons from the EIL to the EML. Hydroxyquinoline aluminium (Alq_3), due to its robustness and high quantum yield, oxidiazol compounds, and cyano- and F-substituted compounds are often used as ETL.[158] Obviously, the enhancment of the electron injection is essential for high performance OLEDs and the proper insertion of a thin buffer layer between the electrode and the organic layer may serve this purpose.[162,163] Most of the buffer materials used are insulators, including PMMA, LiF, and Al_2O_3.[158]

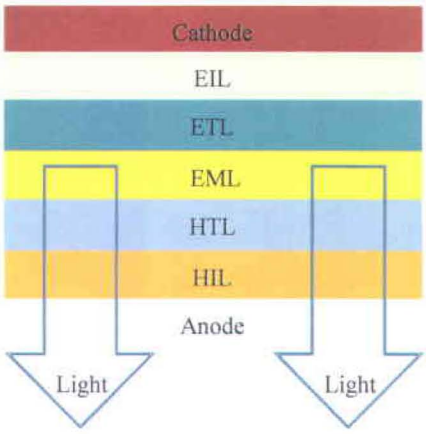

Figure 1.8: A multi-layered OLED structure[158]

The substrate should protect the organic layers from moisture and air to prevent degradation. The materials used as substrate can be rigid such as glass or have a flexible nature (plastics). A silicon backplane with an additional substrate is often employed for top-emitting displays.

The external EL quantum efficiency (η_{ext}) in OLEDs is limited by different parameters including the out-coupling efficiency $\eta_{out\text{-}coupling}$, the charge balance γ, the photoluminescent quantum efficiency of organic material Φ_{PL} and the ratio of the singlet to triplet excitons r_{st} formed by electrical injection[164]:

$$_{ext} = \gamma\, r_{st}\, \Phi_{PL\ out-coupling} = _{int\ out-coupling} \qquad (1.8)$$

Reducing the injection barriers at the interface between electrode and organic[165] and also matching the mobility of the holes and electrons[164] can improve γ. Whereas, using rough substrates with low refractive index and transparent contacts[166,167] can increase $\eta_{out\text{-}coupling}$ of OLEDs.

Based on simple spin statistics, each four electron-hole pairs injected in the active organic semiconductor layer of an OLED, one singlet and three triplets are created.[168] However, as already mentioned, only singlet excitons lead to efficient luminance in organic molecules. This will limit the maximum internal quantum efficiency (η_{int}) to 25% when fluorescent light-emitting molecules are used. Considering an $\eta_{out\text{-}coupling}$ of about 20%, the maximum η_{ext} of a fluorescent OLED is limited to about 5%. However, η_{int} can be increased by incorporating heavy atom organo-metallic compounds such as guest dopants in the light-

emitting layer (r_{st} will be enhanced).[168] OLEDs based on these phosphorescent dyes have demonstrated the best highest performance, to date, with η_{int} approaching 100%[169] and η_{ext} between 20% and 30%.[170,171]

1.9.3 Organic light emitting transistors

Organic light emitting transistors (OLETs) combine the electrical switching functionality of a field-effect transistor and the capability of light generation in a single device, paving the way to highly integrated optoelectronic systems.[172,173,174] OLETs have a similar architecture to OTFT with three contacts (source, drain, and gate), an organic thin film as an active layer and a gate dielectric. Recombination of in-plane moving electrons and holes produces excitons. The intensity of electroluminescence is controlled by the drain and gate voltage. The gate electrode not only defines the total charge injection, but allows balancing the electron and hole currents, controlling the ratio of the formed excitons as well as their position in the channel. OLETs have been demonstrated for both ambipolar and unipolar OSC. In unipolar OLETs, which are mostly p-type, injected electrons from the drain recombine at high bias voltage with holes close to the drain causing incomplete recombination of the charge-carriers as well as quench of excitons by metals.[175] On the other hand, in an ambipolar OLET, electrons and holes are easily injected from the drain and source, respectively, and light emission takes place in the middle of the channel. The emission position can be selected by varying the gate bias between zero and the drain voltage. The emission occurs where the local charge in the channel is zero and local potential is equal to the gate bias. Any changes to the potential or current in this spot will shift the emission place.[176]

Figure 1.9: Schematic structure of OLET[180]

Under certain conditions, the position of light emission can be estimated. The total channel length L_{total} can be considered as a sum of the channel-length traveled by the electrons (L_e) and the holes (L_h) from the electrodes.

$$L_{tot} = L_e + L_h \quad , \quad I_{DS,sat} = \frac{WC_i\mu_{e/h}}{2L_{e/h}}(V_G - V_{th}^{e/h})^2 \qquad (1.9)$$

where W is the width of the channel, C_i the capacitance of the dielectric and $\mu_{e/h}$ are the electron or hole mobilities. The effective gate voltage for the electron channel at negative V_g is given by $V_G - V_{DS}$. Taking these equations and $I_e = I_h = I_{DS}$ into account the following expression can be derived for the ratio of the length of electron to hole channel.[177]

$$\frac{L_h}{L_e} = \frac{\mu_h}{\mu_e} \cdot \frac{(V_G - V_{th}^h)^2}{(V_G - V_{DS} - V_{th}^e)^2} \qquad (1.10)$$

There are few reports on light emitting transistors (LETs) based on inorganic materials such as gallium arsenide (GaAs), indium phosphide (InP), and gallium nitride (GaN).[178,179] The epitaxial growth of the crystalline layer of inorganic materials is quite expensive and can be performed only on a specific class of crystalline substrates, which limits their compatibility with other technologies and consequently the range of potential applications. On the other hand, LETs based on organic materials have several advantages over their inorganic counterparts including the low-cost fabrication methods on a large scale, and the tunability of the optoelectronic properties of OSCs.[180,181,182,183]

Here, it is necessary to compare OLETs with OLEDs so as to better understand the advantages of this novel device. In a typical (vertical) configuration OLED, charge transport is perpendicular to the organic layers whereas in a planar configuration used in OLETs, the transfer of charge occurs at the interface of the dielectric and organic layers. Due to higher crystallinity of OSC used in OLETs, the charge mobility is about four orders of magnitude higher in OLETs compared to OLEDs resulting in direct effects on exciton emission and the lifetime of the materials.[180] In a typical OLED structure, the minority carriers move only a few tens of nanometers in order to reach carriers of the opposite sign and recombine.

In a typical OLET, the electrons and holes should travel longer distances that sets higher standards to the charge transport properties of materials for OLETs. Strong molecular packing in OSCs which have high field effect mobility increases the non-radiative decay of excitons resulting in poor emission efficiency. In other words, OLETs with good EL efficiency show poor mobility. This will result in a very poor power efficiency of the device, since they would require high driving voltage. The first demonstration of OLET was based on vacuum sublimed thin film

of tetracene (**1.9a**) using a device structure with interdigitated gold source and drain electrodes.[173] High energy barrier between drain (electron injecting electrode) and the LUMO of tetracene, leading to low electron current in tetracene, resulted in exciton formation in the vicinity of drain electrodes and quenching at the metals. Since then, few other tetracene-based LETs have been reported. Some of these works directed to optimizing the device characteristics and the possibility of achieving ambipolar transport in tetracene thin films.[184,185] Even in devices employing Au and Ca as the hole and electron injecting electrodes, EL is localized close to the drain electrode.[186] Besides tetracene, other OSCs have also been used as active materials in "*unipolar*" OLETs.[187,188,189,190] 2-(4-pentylstyryl)tetracene (**1.9b**) also showed hole mobility of 0.2 cm^2/Vs and green EL bottom-contact LET configuration.[191]

OLETs based on single crystal of phenylthiophene derivative (BP3T) showed "*unipolar*" p-type behavior with a mobility as high as 0.29 cm^2/Vs (**1.9c**).[192] In general, single crystals with high charge mobility and luminescence efficiency render the material requirement for high performance OLETs. However, the number of reported single-crystal ambipolar LETs is still very limited[193,194,195,196,197] Several other thiophene based oligomers such as (**1.9d**)[198] and (**1.9f**)[199] have also been used in OLETs with "*unipolar*" characteristics. Only few studies have been reported on the OLETs based on polymers. Among them, poly[9,9-di(ethylhexyl)fluorene] (**1.9g**),[188] and poly[2-methoxy,5-(2'-ethylhexoxy)-1,4-phenylenevinylene], MEH-PPV(**1.9h**),[187] both showed "*unipolar*" LET with similar hole mobility of 10^{-4} cm^2/Vs.

Despite the considerable progress in the performance of "*unipolar*" OLETs, η_{ext} is still very low and needs to be drastically enhanced before practical applications would be possible. OFET materials with mobility exceeding 1 cm^2/Vs result in poorly luminescent devices. In fact, the tight molecular packing that allows high charge mobility provides non-radiative decay paths for excitons that yields a low EL efficiency. Moreover, the majority of high performance OSCs are "*unipolar*" (mostly hole) transporting materials.

One approach to achieve a high charge mobility and efficient EL is the fabrication of "*ambipolar*" OLETs. This can be realized by incorporating the heterostructure of a p- and an n-type OSCs either by co-evaporation or by subsequent deposition of both materials (Figure 1.10).[200,201]

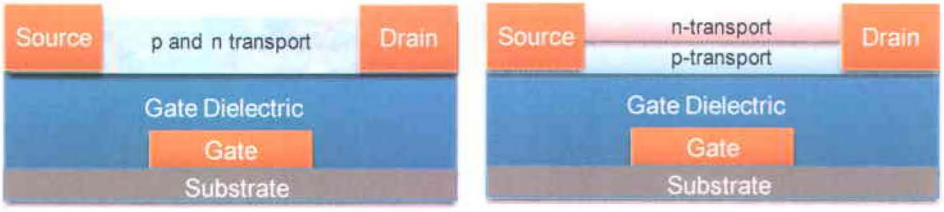

Figure 1.10: Schematic of heterostructure OLETs[180]

In this regard, the first "*ambipolar*" OLET was fabricated based on the bulk *hetero-junction of co-evaporated* films of n-type N,N'-ditridecylperylene-3,4,9,10-tetracarboxyldiimide (P13) and the oligothiophene α-T5 (p-type OSC). It showed an electron and hole mobility of 5×10^{-3} cm^2/Vs and 2.5×10^{-2} cm^2/Vs (**1.9i**).[202] In a similar approach replacing α-T5 with dihexyl-quaterthiophene (DHT4) showed a better balance of hole and electron mobility of 3×10^{-3} cm^2/Vs (**1.9j**) and 9×10^{-4} cm^2/Vs, respectively.[203]

Bilayer[204] and trilayer[205] semiconducting *heterostructure* OLETs have also been proposed aiming at reducing the exciton–charge annihilation and electrode photon losses. Such a device configurations are expected to balance electron and hole injection and increase EL efficiency of the OLET. However, the 'growth compatibility' between n- and p-type OSCs is an issue in forming a continuous interface and in controlling the resulting optoelectronic response of the OLET.[180]

Besides the heterostructure "*ambipolar*" OLETs, few "single layer" OLETs based on polymers (**1.9k**, **1.9m, 1.9n**)[206,207,208] and small molecules (**1.9p**)[209] showed ambipolar characteristics. For example, poly(9,9-di-*n*-octyl-fluorene-*alt*-benzothiadiazolo), F8BT (**1.9k**) exhibited a hole and electron mobility of 7.5×10^{-4} cm^2/Vs and 8.5×10^{-4} cm^2/Vs, respectively, with a green EL.[177,207] Detailed overview on recent progress in OLETs, several review papers that can be found in literature.[180,174]

Scheme 1.10: chemical structure of some OSCs employed in OLETs[174, 180]

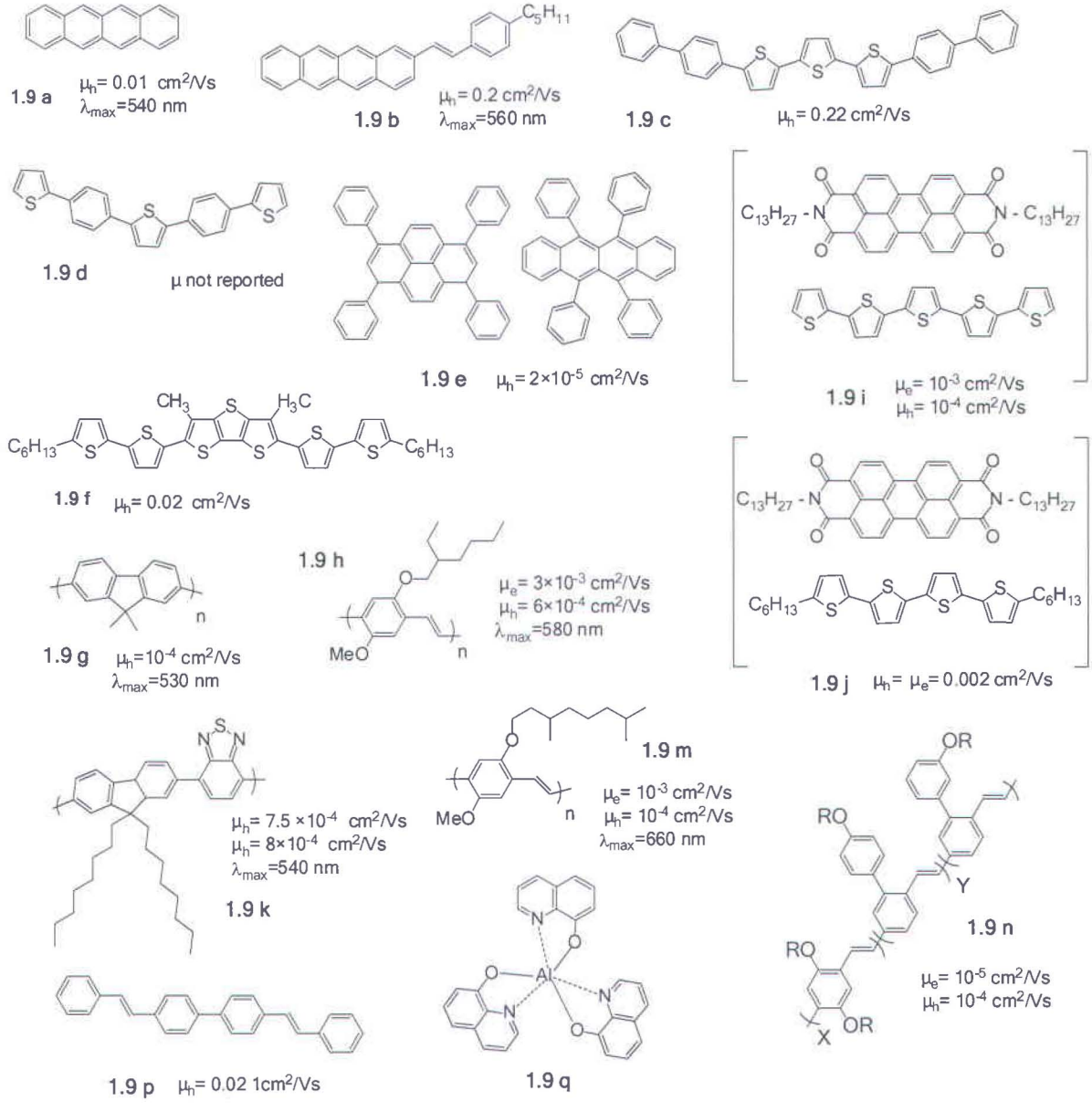

1.10 Concluding remarks and summary

OFETs can rival the performance of FETs based on amorphous silicon (a-Si :H). However, devices based on organic materials are promising for realizing low-cost and large scale flexible electronics. Nevertheless, for a large area organic complementary integrated circuit that can be applied to commercial devices, there are many unsolved questions. The structure–property relationship of OSCs is not still entirely clear and need to be addressed taking into account the complexity of OFETs including film morphology, traps, contact resistance, etc. Apart from the

issues concerning low charge mobility, the device lifetime and stability as well as the fabrication techniques are also considered important challenges. However, substantial improvements have taken place in organic device fabrication techniques, especially for solution-processed techniques, which make the fabrication process simple compared to vacuum evaporation techniques. Another important issue is related to device degradation. Despite of the great advancements achieved in recent years by organic materials science, there is a long way to go to fully realize the benefits of organic electronics.

This chapter provided a short review of various aspects of organic electronics field. It included a short introduction on OSC materials followed by a basic concept of charges carrier transport in them. OTFTs and different methods to improve their performance have been extensively highlighted.

References

[1] Shaw, J.M.; Seidler P.F., *IBM J. Res & Dev* **2001**, Vol. 45, No 1, 3-9.

[2] Koezuka, H.; Tsumura, A.; Ando, T., Field-Effect Transistor with Polythiophene Thin-Film. *Synth Met* **1987,** *18* (1-3), 699-704.

[3] Reese, C.; Bao, Z. N., Organic single-crystal field-effect transistors. *Mater Today* **2007,** *10* (3), 20-27.

[4] Kawase, T.; Shimoda, T.; Newsome, C.; Sirringhaus, H.; Friend, R. H., Inkjet printing of polymer thin film transistors. *Thin Solid Films* **2003,** *438*, 279-287

[5] Arias, A. C.; Ready, S. E.; Lujan, R.; Wong, W. S.; Paul, K. E.; Salleo, A.; Chabinyc, M. L.; Apte, R.; Street, R. A.; Wu, Y.; Liu, P.; Ong, B., All jet-printed polymer thin-film transistor active-matrix backplanes. *Appl Phys Lett* **2004,** *85* (15), 3304-3306.

[6] Chabinyc, M. L.; Salleo, A., Materials requirements and fabrication of active matrix arrays of organic thin-film transistors for displays. *Chem Mater* **2004,** *16* (23), 4509-4521.

[7] Bao, Z. N.; Lovinger, A. J.; Dodabalapur, A., Highly ordered vacuum-deposited thin films of metallophthalocyanines and their applications in field-effect transistors. *Adv Mater* **1997,** *9* (1), 42-44.

[8] Garnier, F.; Hajlaoui, R.; Yassar, A.; Srivastava, P., All-Polymer Field-Effect Transistor Realized by Printing Techniques. *Science* **1994,** *265* (5179), 1684-1686.

[9] Bao, Z. N.; Rogers, J. A.; Katz, H. E., Printable organic and polymeric semiconducting materials and devices. *J Mater Chem* **1999,** *9* (9), 1895-1904.

[10] Gates, B. D.; Xu, Q. B.; Stewart, M.; Ryan, D.; Willson, C. G.; Whitesides, G. M., New approaches to nanofabrication: Molding, printing, and other techniques. *Chem Rev* **2005,** *105* (4), 1171-1196.

[11] Chiang, C. K.; Fincher, C. R.; Park, Y. W.; Heeger, A. J.; Shirakawa, H.; Louis, E. J.; Gau, S. C.; Macdiarmid, A. G., Electrical-Conductivity in Doped Polyacetylene. *Phys Rev Lett* **1977,** *39* (17), 1098-1101.

[12] In 2000, A. J. Heeger, A. G. MacDiarmid, H. Shirakawa received the Nobel Prize in chemistry for the discovery and development of electrically conductive polymers.

[13] Forrest, S. R., The path to ubiquitous and low-cost organic electronic appliances on plastic. *Nature* **2004,** *428* (6986), 911-918.

[14] Crone, B. K.; Dodabalapur, A.; Sarpeshkar, R.; Gelperin, A.; Katz, H. E.; Bao, Z., Organic oscillator and adaptive amplifier circuits for chemical vapor sensing. *J Appl Phys* **2002,** *91* (12), 10140-10146.

[15] Li, D. W.; Borkent, E. J.; Nortrup, R.; Moon, H.; Katz, H.; Bao, Z. N., Humidity effect on electrical performance of organic thin-film transistors. *Appl Phys Lett* **2005,** *86* (4), 42105.

[16] Baude, P. F.; Ender, D. A.; Haase, M. A.; Kelley, T. W.; Muyres, D. V.; Theiss, S. D., Pentacene-based radio-frequency identification circuitry. *Appl Phys Lett* **2003,** *82* (22), 3964-3966.

[17] Jurchescu, O. D.; Baas, J.; Palstra, T. T. M., Effect of impurities on the mobility of single crystal pentacene. *Appl Phys Lett* **2004,** *84* (16), 3061-3063.

[18] Sundar, V. C.; Zaumseil, J.; Podzorov, V.; Menard, E.; Willett, R. L.; Someya, T.; Gershenson, M. E.; Rogers, J. A., Elastomeric transistor stamps: Reversible probing of charge transport in organic crystals. *Science* **2004,** *303* (5664), 1644-1646.

[19] Bernius, M. T.; Inbasekaran, M.; O'Brien, J.; Wu, W. S., Progress with light-emitting polymers. *Adv Mater* **2000,** *12* (23), 1737-1750.

[20] Friend, R. H.; Gymer, R. W.; Holmes, A. B.; Burroughes, J. H.; Marks, R. N.; Taliani, C.; Bradley, D. D. C.; Dos Santos, D. A.; Bredas, J. L.; Logdlund, M.; Salaneck, W. R., Electroluminescence in conjugated polymers. *Nature* **1999,** *397* (6715), 121-128.

[21] Brabec, C. J.; Sariciftci, N. S.; Hummelen, J. C., Plastic solar cells. *Adv Funct Mater* **2001,** *11* (1), 15-26.

[22] Kline, R. J.; McGehee, M. D.; Kadnikova, E. N.; Liu, J. S.; Frechet, J. M. J., Controlling the field-effect mobility of regioregular polythiophene by changing the molecular weight. *Adv Mater* **2003,** *15* (18), 1519-1522.

[23] Pope, M.; Swenberg, C. E., Electronic Processes in Organic Crystals and Polymers, 2nd ed. (Oxford University Press, New York, 1999)

[24] Laquindanum, J. G.; Katz, H. E.; Lovinger, A. J.; Dodabalapur, A., Benzodithiophene rings as semiconductor building blocks. *Adv Mater* **1997,** *9* (1), 36-39.

[25] Menard, E.; Podzorov, V.; Hur, S. H.; Gaur, A.; Gershenson, M. E. ;Rogers, J. A., High-performance n- and p-type single-crystal organic transistors with free-space gate dielectrics. *Adv Mater* **2004,** 16 (23-24), 2097-2101.

[26] Takeya, J.; Nishikawa, T.; Takenobu, T.; Kobayashi, S.; Iwasa, Y.; Mitani, T.; Goldmann, C.; Krellner, C.; Batlogg, B., Effects of polarized organosilane self-assembled monolayers on organic single-crystal field-effect transistors. *Appl Phys Lett* **2004,** *85* (21), 5078-5080.

[27] Warta, W.; Norbert, K., Hot holes in naphthalene: High, electric-field-dependent mobilities. *Phys. Rev. B* **1985**, 32, 1172–1182.

[28] Olivier, Y.; Lemaur, V.; Bredas, J. L.; Cornil, J., Charge hopping in organic semiconductors: Influence of molecular parameters on macroscopic mobilities in model one-dimensional stacks. *J. Phys. Chem. A* **2006**, 110 (19), 6356-6364.

[29] Hutchison, G. R.; Ratner, M. A.; Marks, T. J., Hopping transport in conductive heterocyclic oligomers: reorganization energies and substituent effects. *J Am Chem Soc* **2005,** 127, 2339-2350.

[30] Hutchison, G. R.; Ratner, M. A.; Marks, T. J., Intermolecular charge transfer between heterocyclic oligomers. Effects of heteroatom and molecular packing on hopping transport in organic semiconductors. *J Am Chem Soc* **2005,** *127* (48), 16866-16881.

[31] Lin, Y. Y.; Gundlach, D. J.; Jackson, T. N., Contact dependence of alpha-sexithienyl thin film transistor characteristics. *Electrical, Optical, and Magnetic Properties of Organic Solid State Materials III* **1996,** *413*, 413-418.

[32] Dimitrakopoulos, C. D.; Malenfant, P. R. L., Organic thin film transistors for large area electronics. *Adv Mater* **2002,** *14* (2), 99-117.

[33] Katz, H. E.; Bao, Z. N.; Gilat, S. L., Synthetic chemistry for ultrapure, processable, and high-mobility organic transistor semiconductors. *Accounts Chem Res* **2001,** *34* (5), 359-369.

[34] Dodabalapur, A.; Wang, L. A.; Fine, D.; Basu, D., Electric-field-dependent charge transport in organic thin-film transistors. *J Appl Phys* **2007,** *101* (5), 054515

[35] Horowitz, G.; Hajlaoui, R.; Bouchriha, H.; Bourguiga, R.; Hajlaoui, M., The concept of "threshold voltage" in organic field-effect transistors. *Adv Mater* **1998,** *10* (12), 923-927.

[36] Horowitz, G.; Lang, P.; Mottaghi, M.; Aubin, H., Extracting parameters from the current-voltage characteristics of field-effect transistors. *Adv Funct Mater* **2004,** *14* (11), 1069-1074.

[37] Wang, J.; Wang, H.; Zhang, J.; Yan, X.; Yan, D., Organic thin-film transistors with improved characteristics using lutetium bisphthalocyanine as a buffer layer. *J. Appl. Phys* **2005**, 97, 026106.

[38] Saragi, T. P. I.; Fuhrmann-Lieker, T.; Salbeck, J., High ON/OFF ratio and stability of amorphous organic field-effect transistors based on spiro-linked compounds. *Synthetic Met* **2005,** *148* (3), 267-270.

[39] Torsi, L.; Dodabalapur, A.; Katz, H. E., An Analytical Model for Short-Channel Organic Thin-Film Transistors. *J Appl Phys* **1995,** *78* (2), 1088-1093.

[40] Sirringhaus, H.; Friend, R. H.; Li, X. C.; Moratti, S. C.; Holmes, A. B.; Feeder, N., Bis(dithienothiophene) organic field-effect transistors with a high ON/OFF ratio. *Appl Phys Lett* **1997,** *71* (26), 3871-3873.

[41] Mattis, B. A.; Pei, Y. N.; Subramanian, V., Nanoscale device isolation of organic transistors via electron-beam lithography. *Appl Phys Lett* **2005,** *86* (3), 033113.

[42] Jin, S. H.; Jung, K. D.; Shin, H.; Park, B. G.; Lee, J. D., Grain size effects on contact resistance of top-contact pentacene TFTs. *Synthetic Met* **2006,** *156* (2-4), 196-201.

[43] Luan, S. W.; Neudeck, G. W., An Experimental-Study of the Source Drain Parasitic Resistance Effects in Amorphous-Silicon Thin-Film Transistors. *J Appl Phys* **1992,** *72* (2), 766-772.

[44] Klauk, H.; Schmid, G.; Radlik, W.; Weber, W.; Zhou, L. S.; Sheraw, C. D.; Nichols, J. A.; Jackson, T. N., Contact resistance in organic thin film transistors. *Solid State Electron* **2003,** *47* (2), 297-301.

[45] Street, R. A.; Salleo, A., Contact effects in polymer transistors. *Appl Phys Lett* **2002,** *81* (15), 2887-2889.

[46] Watkins, N. J.; Yan, L.; Gao, Y. L., Electronic structure symmetry of interfaces between pentacene and metals. *Appl Phys Lett* **2002,** *80* (23), 4384-4386.

[47] Zaumseil, J.; Baldwin, K. W.; Rogers, J. A., Contact resistance in organic transistors that use source and drain electrodes formed by soft contact lamination. *J Appl Phys* **2003,** *93* (10), 6117-6124.

[48] Necliudov, P. V.; Shur, M. S.; Gundlach, D. J.; Jackson, T. N., Modeling of organic thin film transistors of different designs. *J Appl Phys* **2000,** *88* (11), 6594-6597.

[49] Kagan, C. R.; Andry, P., *Thin-film transistors*. Marcel Dekker: New York, 2003; p xii, 528 p.

[50] Zhu, M.; Liang, G. R.; Cui, T. H.; Varahramyan, K., Depletion-mode n-channel organic field-effect transistors based on NTCDA. *Solid State Electron* **2003,** *47* (10), 1855-1858.

[51] Chua, L. L.; Zaumseil, J.; Chang, J. F.; Ou, E. C. W.; Ho, P. K. H.; Sirringhaus, H.; Friend, R. H., General observation of n-type field-effect behaviour in organic semiconductors. *Nature* **2005,** *434* (7030), 194-199.

[52] Hotta, S.; Waragai, K., Alkyl-Substituted Oligothiophenes - Crystallographic and Spectroscopic Studies of Neutral and Doped Forms. *J Mater Chem* **1991,** *1* (5), 835-842.

[53] Katz, H. E.; Bao, Z., The physical chemistry of organic field-effect transistors. *J Phys Chem B* **2000,** *104* (4), 671-678.

[54] Payne, M. M.; Parkin, S. R.; Anthony, J. E., Functionalized higher acenes: Hexacene and heptacene. *J Am Chem Soc* **2005,** *127* (22), 8028-8029.

[55] Katz, H. E.; Dodabalapur, A.; Torsi, L.; Elder, D., Precursor synthesis, coupling, and TFT evaluation of end-substituted thiophene hexamers. *Chem Mater* **1995,** *7* (12), 2238-2240.

[56] Servet, B.; Horowitz, G.; Ries, S.; Lagorsse, O.; Alnot, P.; Yassar, A.; Deloffre, F.; Srivastava, P.; Hajlaoui, R.; Lang, P.; Garnier, F., Polymorphism and Charge-Transport in Vacuum-Evaporated Sexithiophene Films. *Chem Mater* **1994,** *6* (10), 1809-1815.

[57] Chan, C. K.; Kim, E. G.; Bredas, J. L.; Kahn, A., Molecular n-type doping of 1,4,5,8-naphthalene tetracarboxylic dianhydride by pyronin B studied using direct and inverse photoelectron spectroscopies. *Adv Funct Mater* **2006,** *16* (6), 831-837

[58] Nakayama, K.; Umehara, M.; Yokoyama, M., Electron injection layers consisting of naphthalene tetracarboxylic dianhydride and indium in n-type organic field-effect transistors. *Jpn J Appl Phys 1* **2006,** *45* (2A), 974-976.

[59] Anthony, J. E.; Facchetti, A.; Heeney, M.; Marder, S. R.; Zhan, X. W., n-Type Organic Semiconductors in Organic Electronics. *Adv Mater* **2010,** *22* (34), 3876-3892.

[60] Bao, Z. A.; Lovinger, A. J.; Brown, J., New air-stable n-channel organic thin film transistors. *J Am Chem Soc* **1998,** *120* (1), 207-208.

[61] Davidson, K.; Jones, R.; McDonald, S., Controlled orientation of Langmuir-Blodgett films of substituted phthalocyanines. *Synthetic Met* **2001,** *121* (1-3), 1399-1400.

[62] Bao, Z.; Lovinger, A. J.; Dodabalapur, A., Organic field-effect transistors with high mobility based on copper phthalocyanine. *Appl Phys Lett* **1996,** *69* (20), 3066-3068.

[63] Aleshin, A. N.; Lee, J. Y.; Chu, S. W.; Kim, J. S.; Park, Y. W., Mobility studies of field-effect transistor structures based on anthracene single crystals. *Appl Phys Lett* **2004,** *84* (26), 5383-5385.

[64] Meng, H.; Sun, F. P.; Goldfinger, M. B.; Gao, F.; Londono, D. J.; Marshal, W. J.; Blackman, G. S.; Dobbs, K. D.; Keys, D. E., 2,6-bis[2-(4-pentylphenyl)vinyl]anthracene: A stable and high charge mobility organic semiconductor with densely packed crystal structure. *J Am Chem Soc* **2006,** *128* (29), 9304-9305.

[65] Ito, K.; Suzuki, T.; Sakamoto, Y.; Kubota, D.; Inoue, Y.; Sato, F.; Tokito, S., Oligo(2,6-anthrylene)s: Acene-oligomer approach for organic field-effect transistors. *Angew Chem Int Edit* **2003,** *42* (10), 1159-1162.

[66] Gerlach, C. P.; Kelley, T. W.; Muyres, D. V., New, high-performance acenyl semiconductors. *Abstr Pap Am Chem S* **2004,** *227*, U171-U171.

[67] Goldmann, C.; Haas, S.; Krellner, C.; Pernstich, K. P.; Gundlach, D. J.; Batlogg, B., Hole mobility in organic single crystals measured by a "flip-crystal" field-effect technique. *J Appl Phys* **2004,** *96* (4), 2080-2086.

[68] Gundlach, D. J.; Nichols, J. A.; Zhou, L.; Jackson, T. N., Thin-film transistors based on well-ordered thermally evaporated naphthacene films. *Appl Phys Lett* **2002,** *80* (16), 2925-2927.

[69] Chi, X. L.; Li, D. W.; Zhang, H. Q.; Chen, Y. S.; Garcia, V.; Garcia, C.; Siegrist, T., 5,6,11,12-Tetrachlorotetracene, a tetracene derivative with pi-stacking structure: The synthesis, crystal structure and transistor properties. *Org Electron* **2008,** *9* (2), 234-240.

[70] Podzorov, V.; Pudalov, V. M.; Gershenson, M. E., Field-effect transistors on rubrene single crystals with parylene gate insulator. *Appl Phys Lett* **2003,** *82* (11), 1739-1741.

[71] Rogers, J. A.; Menard, E.; Podzorov, V.; Hur, S. H.; Gaur, A.; Gershenson, M. E., High-performance n- and p-type single-crystal organic transistors with free-space gate dielectrics. *Adv Mater* **2004,** *16* , 2097-2101.

[72] Myny, K.; De Vusser, S.; Steudel, S.; Janssen, D.; Muller, R.; De Jonge, S.; Verlaak, S.; Genoe, J.; Heremans, P., Self-aligned surface treatment for thin-film organic transistors. *Appl Phys Lett* **2006,** *88,* 222103-1-3 (2006)

[73] Gundlach, D. J.; Lin, Y. Y.; Jackson, T. N.; Nelson, S. F.; Schlom, D. G., Pentacene organic thin-film transistors - Molecular ordering and mobility. *IEEE. Electr. Device L* **1997,** *18* (3), 87-89.

[74] Lin, Y. Y.; Gundlach, D. J.; Nelson, S. F.; Jackson, T. N., Stacked pentacene layer organic thin-film transistors with improved characteristics. *IEEE Electr Device L* **1997,** *18* (12), 606-608.

[75] Klauk, H.; Halik, M.; Zschieschang, U.; Schmid, G.; Radlik, W.; Weber, W., High-mobility polymer gate dielectric pentacene thin film transistors. *J Appl Phys* **2002,** *92* (9), 5259-5263.

[76] Miao, Q.; Lefenfeld, M.; Nguyen, T. Q.; Siegrist, T.; Kloc, C.; Nuckolls, C., Self-assembly and electronics of dipolar linear acenes. *Adv Mater* **2005,** *17* (4), 407-412.

[77] Rhee, S. S.; Hunter, E., Structural Role of the Matrix Protein of Type-D Retroviruses in Gag Polyprotein Stability and Capsid Assembly. *J Virol* **1990,** *64* (9), 4383-4389.

[78] "Organic Thin Film Transistors", Z. Bao and J.J. Locklin Eds, CRC Press, 2007.

[79] Barbarella, G.; Melucci, M.; Sotgiu, G., The versatile thiophene: An overview of recent research on thiophene-based materials. *Adv Mater* **2005,** *17* (13), 1581-1593.

[80] Fichou, D., Structural order in conjugated oligothiophenes and its implications on opto-electronic devices. *J Mater Chem* **2000,** *10* (3), 571-588.

[81] Katz, H. E.; Torsi, L.; Dodabalapur, A., Synthesis, material properties, and transistor performance of highly pure thiophene oligomers. *Chem Mater* **1995,** *7* (12), 2235 -2237.

[82] Garnier, F.; Yassar, A.; Hajlaoui, R.; Horowitz, G.; Deloffre, F.; Servet, B.; Ries, S.; Alnot, P. Molecular Engineering of Organic Semiconductors: Design of Self-assembly Properties in Conjugated Thiophene Oligomers. *J. Am. Chem. Soc.* **1993**, *115*, 8716–8721.

[83] Horowitz, G.; Hajlaoui, R.; Fichou, D.; El Kassmi, A., Gate voltage dependent mobility of oligothiophene field-effect transistors. *J Appl Phys* **1999,** *85* (6), 3202-3206.

[84] Katz, H. E.; Laquindanum, J. G.; Lovinger, A. J., Synthesis, solubility, and field-effect mobility of elongated and oxa-substituted alpha,omega-dialkyl thiophene oligomers. Extension of "polar intermediate" synthetic strategy and solution deposition on transistor substrates. *Chem Mater* **1998,** *10* (2), 633-638.

[85] Tian, H. Wang, J. Shi, J. Yan, D. Wang, L. Geng, Y. Wang, F. Novel thiophene-aryl co-oligomers for organic thin film transistors. *J. Mater. Chem* **200,** 15 (29), 3026-3033.

[86] Bao, Z. N.; Meng, H.; Zheng, J.; Lovinger, A. J.; Wang, B. C.; Van Patten, P. G., Oligofluorene-thiophene derivatives as high-performance semiconductors for organic thin film transistors. *Chem Mater* **2003,** *15* (9), 1778-1787.

[87] Deman, A. L.; Tardy, J.; Nicolas, Y.; Blanchard, P.; Roncali, J., Structural effects on the characteristics of organic field effect transistors based on new oligothiophene derivatives. *Synth Met* **2004,** *146* (3), 365-371.

[88] Katz, H. E.; Laquindanum, J. G.; Lovinger, A. J., Synthesis, morphology, and field-effect mobility of anthradithiophenes. *J Am Chem Soc* **1998,** *120* (4), 664-672.

[89] Anthony, J. E.; Payne, M. M.; Parkin, S. R.; Kuo, C. C.; Jackson, T. N., Organic field-effect transistors from solution-deposited functionalized acenes with mobilities as high as 1 cm^2/Vs. *J Am Chem Soc* **2005,** *127* (14), 4986-4987.

[90] Kobayashi, S.; Takenobu, T.; Mori, S.; Fujiwara, A.; Iwasa, Y., Fabrication and characterization of C-60 thin-film transistors with high field-effect mobility. *Appl Phys Lett* **2003,** *82* (25), 4581-4583.

[91] Katz, H. E.; Lovinger, A. J.; Johnson, J.; Kloc, C.; Siegrist, T.; Li, W.; Lin, Y. Y.; Dodabalapur, A., A soluble and air-stable organic semiconductor with high electron mobility. *Nature* **2000,** *404* (6777), 478-481.

[92] Frisbie, C. D.; Chesterfield, R. J.; McKeen, J. C.; Newman, C. R.; Ewbank, P. C.; da Silva, D. A.; Bredas, J. L.; Miller, L. L.; Mann, K. R., Organic thin film transistors based on N-alkyl perylene diimides: Charge transport kinetics as a function of gate voltage and temperature. *J Phys Chem B* **2004,** *108* (50), 19281-19292.

[93] Ando, S.; Murakami, R.; Nishida, J.; Tada, H.; Inoue, Y.; Tokito, S.; Yamashita, Y., n-Type organic field-effect transistors with very high electron mobility based on thiazole oligomers with trifluoromethylphenyl groups. *J Am Chem Soc* **2005,** *127* (43), 14996-14997.

[94] Newman, C. R.; Frisbie, C. D.; da Silva, D. A.; Bredas, J. L.; Ewbank, P. C.; Mann, K. R., Introduction to organic thin film transistors and design of n-channel organic semiconductors. *Chem Mater* **2004,** *16* (23), 4436-4451.

[95] Bao, Z.; Dodabalapur, A.; Lovinger, A. J., Soluble and processable regioregular poly(3-hexylthiophene) for thin film field-effect transistor applications with high mobility. *Appl Phys Lett* **1996,** *69* (26), 4108-4110.

[96] Callewaert, M.; Gohy, J. F.; Dupont-Gillain, C. C.; Boulange-Petermann, L.; Rouxhet, P. G., Surface morphology and wetting properties of surfaces coated with an amphiphilic diblock copolymer. *Surf Sci* **2005,** *575* (1-2), 125-135.

[97] Ju, D. Y.; Ji, V.; Gassot, H., Computer predictions of thermo-mechanical behavior and residual stresses in spray coating process. *J Phys IV* **2004,** *120*, 381-388.

[98] Ichiki, M.; Zhang, L.; Yang, Z.; Ikehara, T.; Maeda, R., Thin film formation on non-planar surface with use of spray coating fabrication. *Microsyst Technol* **2004,** *10* (5), 360-363.

[99] Beers, K. L.; Douglas, J. F.; Amis, E. J.; Karim, A., Combinatorial measurements of crystallization growth rate and morphology in thin films of isotactic polystyrene. *Langmuir* **2003,** *19* (9), 3935-3940.

[100] Kawase, T.; Sirringhaus, H.; Friend, R. H.; Shimoda, T., Inkjet printed via-hole interconnections and resistors for all-polymer transistor circuits. *Adv Mater* **2001,** *13* (21), 1601-1605.

[101] Loo, Y. L.; Willett, R. L.; Baldwin, K. W.; Rogers, J. A., Additive, nanoscale patterning of metal films with a stamp and a surface chemistry mediated transfer process: Applications in plastic electronics. *Appl Phys Lett* **2002,** *81* (3), 562-564.

[102] H. E. Katz, J. Johnson, A. J. Lovinger, W. J. Li, *Appl Phys Lett* **2001,** 79, 2996-2998.

[103] Chang, J. F.; Sun, B. Q.; Breiby, D. W.; Nielsen, M. M.; Solling, T. I.; Giles, M.; McCulloch, I.; Sirringhaus, H., Enhanced mobility of poly(3-hexylthiophene) transistors by spin-coating from high-boiling-point solvents. *Chem Mater* **2004,** 16 (23), 4772-4776.

[104] Wang, G. M.; Swensen, J.; Moses, D.; Heeger, A. J., Increased mobility from regioregular poly(3-hexylthiophene) field-effect transistors. *J Appl Phys* **2003,** *93* (10), 6137-6141.

[105] Sirringhaus, H.; Brown, P. J.; Friend, R. H.; Nielsen, M. M.; Bechgaard, K.; Langeveld-Voss, B. M. W.; Spiering, A. J. H.; Janssen, R. A. J.; Meijer, E. W.; Herwig, P.; de Leeuw, D. M., Two-dimensional charge transport in self-organized, high-mobility conjugated polymers. *Nature* **1999,** 401 (6754), 685-688.

[106] McCulloch, I.; Bailey, C.; Giles, M.; Heeney, M.; Love, I.; Shkunov, M.; Sparrowe, D.; Tierney, S., Influence of molecular design on the field-effect transistor characteristics of terthiophene polymers. *Chem Mater* **2005,** *17* (6), 1381-1385.

[107] Jenekhe, S. A.; Babel, A., Alkyl chain length dependence of the field-effect carrier mobility in regioregular poly(3-alkylthiophene)s. *Synth Met* **2005,** *148* (2), 169-173.

[108] Murphy, A. R.; Liu, J.; Luscombe C.; Kavulak, D.; Fréchet, J. M. J.; Kline, J. R.; McGehee, M. D. Synthesis, Characterization, and Field-Effect Transistor Performance of Carboxylate Functionalized Polythiophenes with Increased Air Stability. *Chem. Mater.***2005**, *17* (20) , 4892-4899.

[109] Crouch, D. J.; Skabara, P. J.; Heeney, M.; I, M.; Coles, S. J.; Hursthouse, M. B., Hexyl-substituted oligothiophenes with a central tetrafluorophenylene unit: crystal engineering of planar structures for p-type organic semiconductors. *Chem Commun* **2005,** (11), 1465-1467.

[110] Facchetti, A.; Usta, H.; Lu, G.; Marks, T. J., Dithienosilole- and dibenzosilole-thiophene copolymers as semiconductors for organic thin-film transistors. *J Am Chem Soc* **2006,** *128* (28), 9034-9035.

[111] McCullough, R. D.; Osaka, I.; Sauve, G.; Zhang, R.; Kowalewski, T., Novel thiophene-thiazolothiazole copolymers for organic field-effect transistors. *Adv Mater* **2007,** *19* (23), 4160-4165

[112] Heeney, I, M.; M.; Bailey, Genevicius, C.; Shkunov, I, M.; Sparrowe, M.; Tierney, D.; Wagner, S.; Zhang, R.; Chabinyc, W. M. ;Kline, R. J.; McGehee, M. D.; Toney, M. F. Liquid-crystalline semiconducting polymers with high charge-carrier mobility. *Nat Mater* **2006,** *5* (4), 328-333.

[113] Facchetti, A.; Yan, H.; Chen, Z. H.; Zheng, Y.; Newman, C.; Quinn, J. R.; Dotz, F.; Kastler, M., A high-mobility electron-transporting polymer for printed transistors. *Nature* **2009,** *457* (7230), 679-687.

[114] Waldauf, C.; Schilinsky, P.; Perisutti, M.; Hauch, J.; Brabec, C. J., Solution-processed organic n-type thin-film transistors. *Adv Mater* **2003,** *15* (24), 2084-2088.

[115] Garnier, F.; Yassar, A.; Hajlaoui, R.; Horowitz, G.; Deloffre, F.; Servet, B.; Ries, S.; Alnot, P., Molecular Engineering of Organic Semiconductors - Design of Self-Assembly Properties in Conjugated Thiophene Oligomers. *J Am Chem Soc* **1993,** *115* (19), 8716-8721.

[116] Videlot, C.; El Kassmi, A.; Fichou, D., Photovoltaic properties of octithiophene-based Schottky and p/n junction cells: Influence of molecular orientation. *Sol Energ Mat Sol C* **2000,** *63* (1), 69-82.

[117] Roncali, J.; Frere, P.; Blanchard, P.; de Bettignies, R.; Turbiez, M.; Roquet, S.; Leriche, P.; Nicolas, Y., Molecular and supramolecular engineering of pi-conjugated systems for photovoltaic conversion. *Thin Solid Films* **2006,** *511*, 567-575.

[118] Roncali, J.; Leriche, P.; Cravino, A., From one- to three-dimensional organic semiconductors: In search of the organic silicon? *Adv Mater* **2007,** *19* (16), 2045-2060.

[119] Haas, U.; Anja, H.; Hannes, M.; Barbara, L., Polytronic, Growth process control of pentacene thin films and its application in full organic thin film transistors, *IEEE International Conference on Polymers and Adhesives*, **2004**, 1-6.

[120] Nelson, S. F.; Lin, Y. Y.; Gundlach, D. J.; Jackson, T. N., Temperature-independent transport in high-mobility pentacene transistors. *Appl Phys Lett* **1998**, 72 (15), 1854-1856.

[121] Podzorov, V.; Menard, E.; Borissov, A.; Kiryukhin, V.; Rogers, J. A.; Gershenson, M. E., Intrinsic charge transport on the surface of organic semiconductors. *Phys Rev Lett* **2004**, 93 (8), 086602.

[122] De Boer, R. W. I.; Gershenson, M. E.; Morpurgo, A. F.; Podzorov, V., Organic single-crystal field-effect transistors. *Physica Status Solidi a-Applied Research* **2004,** *201* (6), 1302-1331

[123] Mas-Torrent, M.; Durkut, M.; Hadley, P.; Ribas, X.; Rovira, C., High mobility of dithiophene-tetrathiafulvalene single-crystal organic field effect transistors. *J Am Chem Soc* **2004,** *126* (4), 984-985.

[124]Arkhipov, V. I.; Emelianova, E. V.; Heremans, P.; Bassler, H., Analytic model of carrier mobility in doped disordered organic semiconductors. *Phys Rev B* **2005**, *72* (23), 235202.

[125] Panzer, M. J., Newman, C. R. & Frisbie, C. D. *Low-voltage operation of a pentacene field-effect transistor with a polymer electrolyte gate dielectric. Appl. Phys. Lett.* **2005**, 86, 103503.

[126] Jiang, L.; Dong, H. L.; Hu, W. P., Organic single crystal field-effect transistors: advances and perspectives. *J Mater Chem* **2010,** *20* (24), 4994-5007.

[127] Facchetti, A.; Yoon, M. H.; Marks, T. J., Gate dielectrics for organic field-effect transistors: New opportunities for organic electronics. *Adv Mater* **2005,** *17* (14), 1705-1725.

[128] Majewski, L. A.; Grell, M.; Ogier, S. D.; Veres, J., A novel gate insulator for flexible electronics. *Org Electron* **2003,** *4* (1), 27-32.

[129] Kim, C. S.; Jo, S. J.; Lee, S. W.; Kim, W. J.; Baik, H. K.; Lee, S. J.; Hwang, D. K.; Im, S., High-k and low-k nanocomposite gate dielectrics for low voltage organic thin film transistors. *Appl Phys Lett* **2006,** *88* (24), 243515-1-3.

[130] Bersuker, G.; Zeitzoff, P.; Brown, G.; Huff, H.R., Bersuker, P. Zeitzoff, G. Brown, and H. R. Huff, Novel Dielectric Materials For Future Transistor Generations. *Materials Today,* **2004,** 7, 26-33.

[131] Dimitrakopoulos, C. D.; Kymissis, I.; Purushothaman, S.; Neumayer, D. A.; Duncombe, P. R.; Laibowitz, R. B., Low-voltage, high-mobility pentacene transistors with solution-processed high dielectric constant insulators. *Adv Mater* **1999,** *11* (16), 1372-1375.

[132] Shtein, M.; Mapel, J.; Benziger, J. B.; Forrest, S. R., Effects of film morphology and gate dielectric surface preparation on the electrical characteristics of organic-vapor-phase-deposited pentacene thin-film transistors. *Appl Phys Lett* **2002,** *81* (2), 268-270.

[133] Kitamura, M.; Arakawa, Y., Pentacene-based organic field-effect transistors *J. Phys.: Condens. Matter* **2008**, 20, 184011.

[134] Kang, S. J.; Chung, K. B.; Park, D. S.; Kim, H. J.; Choi, Y.; Jang, M. H.; Noh, M.; Whang, C. N., Fabrication and characterization of the pentacene thin film transistor with a Gd2O3 gate insulator. *Synthetic Met* **2004,** *146* (3), 351-354.

[135] Veres, J.; Ogier, S. D.; Leeming, S. W.; Cupertino, D. C.; Khaffaf, S. M., Low-k insulators as the choice of dielectrics in organic field-effect transistors. *Adv Funct Mater* **2003,** *13* (3), 199-204.

[136] Puigdollers, J.; Voz, C.; Martin, I.; Vetter, M.; Orpella, A.; Alcubilla, R., Electrical characterization of pentacene thin-film transistors with polymeric gate dielectric. *Synthetic Met* **2004,** *146* (3), 355-358.

[137] Jin, Y. B.; Rang, Z. L.; Nathan, M. I.; Ruden, P. P.; Newman, C. R.; Frisbie, C. D., Pentacene organic field-effect transistor on metal substrate with spin-coated smoothing layer. *Appl Phys Lett* **2004,** *85* (19), 4406-4408.

[138] Dimitrakopoulos, C. D.; Purushothaman, S.; Kymissis, J.; Callegari, A.; Shaw, J. M., Low-voltage organic transistors on plastic comprising high-dielectric constant gate insulators. *Science* **1999,** *283* (5403), 822-824.

[139] Kobayashi, S.; Nishikawa, T.; Takenobu, T.; Mori, S.; Shimoda, T.; Mitani, T.; Shimotani, H.; Yoshimoto, N.; Ogawa, S.; Iwasa, Y., Control of carrier density by self-assembled monolayers in organic field-effect transistors. *Nat Mater* **2004,** *3* (5), 317-322.

[140] Lin, Y. Y.; Gundlach, D. J.; Nelson, S. F.; Jackson, T. N., Stacked pentacene layer organic thin-film transistors with improved characteristics. *Ieee Electr Device L* **1997,** *18* (12), 606-608.

[141] Shankar, K.; Jackson, T. N., Morphology and electrical transport in pentacene films on silylated oxide surfaces. *J Mater Res* **2004,** *19* (7), 2003-2007.

[142] Street, R. A.; Knipp, D.; Volkel, A.; Ho, J., Pentacene thin film transistors on inorganic dielectrics: Morphology, structural properties, and electronic transport. *J Appl Phys* **2003,** *93* (1), 347-355.

[143] Kim, D. H.; Park, Y. D.; Jang, Y. S.; Yang, H. C.; Kim, Y. H.; Han, J. I.; Moon, D. G.; Park, S. J.; Chang, T. Y.; Chang, C. W.; Joo, M. K.; Ryu, C. Y., Enhancement of field-effect mobility due to surface-mediated molecular ordering in regioregular polythiophene thin film transistors. *Adv Funct Mater* **2005,** *15* (1), 77-82.

[144] Cho, K.; Kim, D. H.; Jang, Y.; Park, Y. D., Surface-induced conformational changes in poly(3-hexylthiophene) monolayer films. *Langmuir* **2005,** *21* (8), 3203-3206.

[145] Yagi, I.; Tsukagoshi, K.; Aoyagi, Y., Modification of the electric conduction at the pentacene/SiO2 interface by surface termination of SiO2. *Appl Phys Lett* **2005,** *86,* 103502-1-3.

[146] Knipp, D.; Street, R. A.; Volkel, A.; Ho, J., Pentacene thin film transistors on inorganic dielectrics: Morphology, structural properties, and electronic transport. *J Appl Phys* **2003,** *93* (1), 347-355.

[147] Boulas, C.; Davidovits, J. V.; Rondelez, F.; Vuillaume, D., Suppression of charge carrier tunneling through organic self-assembled monolayers. *Phys Rev Lett* **1996,** *76* (25), 4797-4800.

[148] Gundlach, D. J.; Jia, L. L.; Jackson, T. N., Pentacene TFT with improved linear region characteristics using chemically modified source and drain electrodes. *Ieee Electr Device L* **2001,** *22* (12), 571-573.

[149] Myny, K.; De Vusser, S.; Steudel, S.; Janssen, D.; Muller, R.; De Jonge, S.; Verlaak, S.; Genoe, J.; Heremans, P., Self-aligned surface treatment for thin-film organic transistors. *Appl Phys Lett* **2006,** *88*, 222103.

[150] Tang, C. W.; Vanslyke, S. A., Organic Electroluminescent Diodes. *Appl Phys Lett* **1987,** *51* (12), 913-915.

[151] Burroughes, J. H.; Bradley, D. D. C.; Brown, A. R.; Marks, R. N.; Mackay, K.; Friend, R. H.; Burns, P. L.; Holmes, A. B., Light-Emitting-Diodes Based on Conjugated Polymers. *Nature* **1990,** *347* (6293), 539-541.

[152] Bernanose, A.; Comte, M.; Vouaux, P., *Sur Un Nouveau Mode Demission Lumineuse Chez Certains Composes Organiques. *J Chim Phys Pcb* **1953,** *50* (1), 64-68.

[153] Hung, L. S.; Chen, C. H., Recent progress of molecular organic electroluminescent materials and devices. *Mat Sci Eng R* **2002,** *39* (5-6), 143-222.

[154] Muller, K.; Scherf, U. organic light emitting devices: synthesis, properties and applications. Wiley, 400 pp. ISBN: 3-527-31218-8

[155] J. A. Barltrop and J. D. Coyle, Excited states in organic chemistry. London; New York : Wiley-VCH, 1975.

[156] Forrest, S. R., The path to ubiquitous and low-cost organic electronic appliances on plastic. *Nature* **2004,** *428* (6986), 911-918.

[157] Kwong, R. C.; Weaver, M. S.; Lu, M. H. M.; Tung, Y. J.; Chwang, A. B.; Zhou, T. X.; Hack, M.; Brown, J. J., Current status of electrophosphorescent device stability. *Org Electron* **2003,** *4* (2-3), 155-164.

[158] Zhigang Li, Hong Meng, "Organic Light-Emitting Materials and Devices" Boca Raton : CRC/Taylor & Francis, c2007

[159] Kuwabara, Y.; Ogawa, H.; Inada, H.; Noma, N.; Shirota, Y., Thermally Stable Multilayered Organic Electroluminescent Devices Using Novel Starburst Molecules, 4,4',4"-Tri(N-Carbazolyl)Triphenylamine (Tcta) and 4,4',4"-Tris(3-Methylphenylphenyl-Amino)Triphenylamine (M-Mtdata), as Hole-Transport Materials. *Adv Mater* **1994,** *6* (9), 677-679.

[160] Bredas, J. L.; Hreha, R. D.; George, C. P.; Haldi, A.; Domercq, B.; Malagoli, M.; Barlow, S.; Kippelen, B.; Marder, S. R., 2,7-bis(diarylamino)-9,9-dimethylfluorenes as hole-transport materials for organic light-emitting diodes. *Adv Funct Mater* **2003,** *13* (12), 967-973.

[161] Tokito, S.; Tanaka, H.; Okada, A.; Taga, Y., High-temperature operation of an electroluminescent device fabricated using a novel triphenylamine derivative. *Appl Phys Lett* **1996,** *69* (7), 878-880.

[162] Zhao, J. M.; Zhan, Y. Q.; Zhang, S. T.; Wang, X. J.; Zhou, Y. C.; Wu, Y.; Wang, Z. J.; Ding, X. M.; Hou, X. Y., Mechanisms of injection enhancement in organic light-emitting diodes through insulating buffer. *Appl Phys Lett* **2004,** *84* (26), 5377-5379.

[163] Zhang, S. T.; Ding, X. M.; Zhao, J. M.; Shi, H. Z.; He, J.; Xiong, Z. H.; Ding, H. J.; Obbard, E. G.; Zhan, Y. Q.; Huang, W.; Hou, X. Y., Buffer-layer-induced barrier reduction: Role of tunneling in organic light-emitting devices. *Appl Phys Lett* **2004,** *84* (3), 425-427

[164] Geffroy, B.; Le Roy, P.; Prat, C., Organic light-emitting diode (OLED) technology: materials, devices and display technologies. *Polym Int* **2006,** *55* (6), 572-582.

[165] Lin, Y. J.; Chou, W. Y.; Lin, S. T., Enhanced efficiency in polymer light-emitting diodes due to the improvement of charge-injection balance. *Appl Phys Lett* **2006,** *88,* 71108.

[166] Yamasaki, T.; Sumioka, K.; Tsutsui, T., Organic light-emitting device with an ordered monolayer of silica microspheres as a scattering medium. *Appl Phys Lett* **2000,** *76* (10), 1243-1245.

[167] Parthasarathy, G.; Burrows, P. E.; Khalfin, V.; Kozlov, V. G.; Forrest, S. R., A metal-free cathode for organic semiconductor devices. *Appl Phys Lett* **1998,** *72* (17), 2138-2140.

[168] Baldo, M. A.; O'Brien, D. F.; Thompson, M. E.; Forrest, S. R., Excitonic singlet-triplet ratio in a semiconducting organic thin film. *Phys Rev B* **1999,** *60* (20), 14422-14428.

[169] Adachi, C.; Baldo, M. A.; Thompson, M. E.; Forrest, S. R., Nearly 100% internal phosphorescence efficiency in an organic light-emitting device. *J Appl Phys* **2001,** *90* (10), 5048-5051.

[170] Tanaka, D.; Sasabe, H.; Li, Y. J.; Su, S. J.; Takeda, T.; Kido, J., Ultra high efficiency green organic light-emitting devices. *Jpn J Appl Phys 2* **2007,** *46* (1-3), L10-L12.

[171] Tanaka, D.; Agata, Y.; Takeda, T.; Watanabe, S.; Kido, J., High luminous efficiency blue organic light-emitting devices using high triplet excited energy materials. *Jpn J Appl Phys 2* **2007,** *46* (4-7), L117-L119.

[172] Kuo, C. T.; Weng, S. Z., Integrated device based on conjugated oligoaniline. *Polym Advan Technol* **2002,** *13* (10-12), 753-758.

[173] Hepp, A.; Heil, H.; Weise, W.; Ahles, M.; Schmechel, R.; von Seggern, H., Light-emitting field-effect transistor based on a tetracene thin film. *Phys Rev Lett* **2003,** *91,* 157406-1-3.

[174] Cicoira, F.; Santato, C., Organic light emitting effect transistors: advances and perspectives. *Adv. Funct. Mater.* **2007**, *17*, 3421–3434

[175] Tessler, N.; Pinner, D. J.; Cleave, V.; Ho, P. K. H.; Friend, R. H.; Yahioglu, G.; Barny, P. L.; Gray, J.; de Souza, M.; Rumbles, G., Properties of light emitting organic materials within the context of future electrically pumped lasers. *Synthetic Met* **2000,** *115* (1-3), 57-62.

[176] Dinelli, F.; Capelli, R.; Loi, M. A.; Murgia, M.; Muccini, M.; Facchetti, A.; Marks, T. J., High-mobility ambipolar transport in organic light-emitting transistors. *Adv Mater* **2006,** *18* (11), 1416-420

[177] Zaumseil, J.; Friend, R. H.; Sirringhaus, H., Spatial control of the recombination zone in an ambipolar light-emitting organic transistor. *Nat Mater* **2006,** *5* (1), 69-74.

[178] Feng, M.; Holonyak, N.; Hafez, W., Light-emitting transistor: Light emission from InGaP/GaAs heterojunction bipolar transistors. *Appl Phys Lett* **2004,** *84* (1), 151-153.

[179] Huang, Y.; Zhang, X. B.; Ryou, J. H.; Dupuis, R. D.; Dixon, F.; Holonyak, N.; Feng, M., InAlGaAs/InP light-emitting transistors operating near 1.55 mu m. *J Appl Phys* **2008,** *103* (11).

[180] Muccini, M., A bright future for organic field-effect transistors. *Nat Mater* **2006,** *5* (8), 605-613.

[181] Barbarella, G.; Melucci, M.; Sotgiu, G., The versatile thiophene: An overview of recent research on thiophene-based materials. *Adv Mater* **2005,** *17* (13), 1581-1593.

[182] Yoon, M. H.; DiBenedetto, S. A.; Facchetti, A.; Marks, T. J., Organic thin-film transistors based on carbonyl-functionalized quaterthiophenes: High mobility N-channel semiconductors and ambipolar transport. *J Am Chem Soc* **2005,** *127* (5), 1348-1349.

[183] Loi, M. A.; Rost-Bietsch, C.; Murgia, M.; Karg, S.; Riess, W.; Muccini, M., Tuning optoelectronic properties of ambipolar organic light-emitting transistors using a bulk-heterojunction approach. *Adv Funct Mater* **2006,** *16* (1), 41-47.

[184] Cicoira, F.; Santato, C.; Dinelli, F.; Murgia, M.; Loi, M. A.; Biscarini, F.; Zamboni, R.; Heremans, P.; Muccini, M., Correlation between morphology and field-effect-transistor mobility in tetracene thin films. *Adv Funct Mater* **2005,** *15* (3), 375-380.

[185] Santato, C.; Capelli, R.; Loi, M. A.; Murgia, M.; Cicoira, F.; Roy, V. A. L.; Stallinga, P.; Zamboni, R.; Rost, C.; Karg, S. E.; Muccini, M., Tetracene-based organic light-emitting transistors: optoelectronic properties and electron injection mechanism. *Synthetic Met* **2004,** *146* (3), 329-334.

[186] Reynaert, J.; Cheyns, D.; Janssen, D.; Muller, R.; Arkhipov, V. I.; Genoe, J.; Borghs, G.; Heremans, P., Ambipolar injection in a submicron-channel light-emitting tetracene transistor with distinct source and drain contacts. *J Appl Phys* **2005,** *97* (11), 114501.

[187] Sakanoue, T.; Fujiwara, E.; Yamada, R.; Tada, H., Visible light emission from polymer-based field-effect transistors. *Appl Phys Lett* **2004,** *84* (16), 3037-3039.

[188]Ahles, M.; Hepp, A.; Schmechel, R.; von Seggern, H., Light emission from a polymer transistor. *Appl Phys Lett* **2004,** *84* (3), 428-430.

[189] H. Nakanotani, S. Akiyama, D. Ohnishi, M. Moriwake, M. Yahiro, T. Yoshihara, S. Tobita, and C. Adachi, "Extremely low-threshold amplified spontaneous emission of 9,9'-spirobifluorene derivates and electroluminescence from field-effect transistor structure," Adv. Funct. Mater. **2007**, 17, 2328–2335.

[190] Heeger, A. J.; Swensen, J.; Moses, D., Light emission in the channel region of a polymer thin-film transistor fabricated with gold and aluminum for the source and drain electrodes. *Synthetic Met* **2005,** *153* (1-3), 53-56.

[191] Cicoira, F.; Santato, C.; Dadvand, A.; Harnagea, C.; Pignolet, A.; Bellutti, P.; Xiang, Z.; Rosei, F.; Meng, H.; Perepichka, D. F., Environmentally stable light emitting field effect transistors based on 2-(4-pentylstyryl)tetracene. *J Mater Chem* **2008,** *18* (2), 158-161.

[192] Nakamura, K.; Ichikawa, M.; Fushiki, R.; Kamikawa, T.; Inoue, M.; Koyama, T.; Taniguchi, Y., Light emission from organic single-crystal field-effect transistors. *Japanese Journal of Applied Physics Part 2-Letters & Express Letters* **2005,** *44* (42-45), L1367-L1369.

[193]Takenobu, T.; Bisri, S. Z.; Takahashi, T.; Yahiro, M.; Adachi, C.; Iwasa, Y., High current density in light-emitting transistors of organic single crystals. *Phys Rev Lett* **2008,** *100* (6), 066601.

[194] Bisri, S. Z.; Takenobu, T.; Yomogida, Y.; Shimotani, H.; Yamao, T.; Hotta, S.; Iwasa, Y., High Mobility and Luminescent Efficiency in Organic Single-Crystal Light-Emitting Transistors. *Adv Funct Mater* **2009,** *19* (11), 1728-1735.

[195] Sawabe, K.; Takenobu, T.; Bisri, S. Z.; Yamao, T.; Hotta, S.; Iwasa, Y., High current densities in a highly photoluminescent organic single-crystal light-emitting transistor. *Appl Phys Lett* **2010,** *97* (4), 043307.

[196] Nakanotani, H.; Saito, M.; Nakamura, H.; Adachi, C., Highly balanced ambipolar mobilities with intense electroluminescence in field-effect transistors based on organic single crystal oligo(p-phenylenevinylene) derivatives. *Appl Phys Lett* **2009,** *95* (3), 033308.

[197] Nakanotani, H.; Kabe, R.; Yahiro, M.; Takenobu, T.; Iwasa, Y.; Adachi, C., Blue-light-emitting ambipolar field-effect transistors using an organic single crystal of 1,4-Bis(4-methylstyryl)benzene. *Appl Phys Express* **2008,** *1* (9), 091801.

[198] Oyamada, T.; Sasabe, H.; Adachi, C.; Okuyama, S.; Shimoji, N.; Matsushige, K., Electroluminescence of 2,4-bis(4-(2 '-thiophene-yl)phenyl)thiophene in organic light-emitting field-effect transistors. *Appl Phys Lett* **2005,** *86* (9) 093505.

[199] Cicoira, F.; Santato, C.; Melucci, M.; Favaretto, L.; Gazzano, M.; Muccini, M.; Barbarella, G., Organic light-emitting transistors based on solution-cast and vacuum-sublimed films of a rigid core thiophene oligomer. *Adv Mater* **2006,** *18* (2), 169-174.

[200] Capelli, R.; Dinelli, F.; Loi, M. A.; Murgia, M.; Zamboni, R.; Muccini, M., Ambipolar organic light-emitting transistors employing heterojunctions of n-type and p-type materials as the active layer. *J Phys-Condens Mat* **2006,** *18* (33), S2127-S2138.

[201] Dinelli, F.; Capelli, R.; Loi, M. A.; Murgia, M.; Muccini, M.; Facchetti, A.; Marks, T. J., High-mobility ambipolar transport in organic light-emitting transistors. *Adv Mater* **2006,** *18* (11), 1416-1420.

[202] Rost, C.; Karg, S.; Riess, W.; Loi, M. A.; Murgia, M.; Muccini, M., Ambipolar light-emitting organic field-effect transistor. *Appl Phys Lett* **2004,** *85* (9), 1613-1615.

[203] Loi, M. A.; Rost-Bietsch, C.; Murgia, M.; Karg, S.; Riess, W.; Muccini, M., Tuning optoelectronic properties of ambipolar organic light-emitting transistors using a bulk-heterojunction approach. *Adv Funct Mater* **2006,** *16* (1), 41-47.

[204] Di, C. A.; Yu, G.; Liu, Y. Q.; Xu, X. J.; Wei, D. C.; Song, Y. B.; Sun, Y. M.; Wang, Y.; Zhu, D. B., Organic light-emitting transistors containing a laterally arranged heterojunction. *Adv Funct Mater* **2007,** *17* (9), 1567-1573.

[205] Capelli, R.; Toffanin, S.; Generali, G.; Usta, H.; Facchetti, A.; Muccini, M., Organic light-emitting transistors with an efficiency that outperforms the equivalent light-emitting diodes. *Nat Mater* **2010,** *9* (6), 496-503.

[206] Swensen, J. S.; Soci, C.; Heeger, A. J., Light emission from an ambipolar semiconducting polymer field-effect transistor. *Appl Phys Lett* **2005,** *87* (25), 253511.

[207] Zaumseil, J.; Donley, C. L.; Kim, J. S.; Friend, R. H.; Sirringhaus, H., Efficient top-gate, ambipolar, light-emitting field-effect transistors based on a green-light-emitting polyfluorene. *Adv Mater* **2006,** *18* (20), 2708-2712.

[208] Naber, R. C. G.; Bird, M.; Sirringhaus, H., A gate dielectric that enables high ambipolar mobilities in polymer light-emitting field-effect transistors. *Appl Phys Lett* **2008,** *93* (2), 023301.

[209] Sakanoue, T.; Yahiro, M.; Adachi, C.; Uchiuzou, H.; Takahashi, T.; Toshimitsu, A., Ambipolar light-emitting organic field-effect transistors using a wide-band-gap blue-emitting small molecule. *Appl Phys Lett* **2007,** *90* (17), 171118.

CHAPTER 2

Materials and Experimental Techniques

The development and optimization of OTFTs is considered an important task that takes huge effort to solve a number of practical concerns. This chapter includes a short description of the various structures of transistors fabricated in our lab; the procedures for fabrication and characterization of the samples by various techniques.

2.1 Materials used in this thesis

The choice of the different OSCs based on the principal of π-conjugated molecular and materials were based on the novel organic compounds synthesized in Prof. Perepichka's laboratory at McGill University and by collaborators (DuPont Company, Moscow State University, Weizmann Institute of Science). Materials investigated during this PhD work, together with their HOMO and LUMO levels are presented in Figure 2.1.

Figure 2.1: The organic materials and their energy level studied in this work.
[a] DFT/B3LYP/6–31G(d) and [b] DFT/B3LYP/6–31G(2d,p) level of theory.

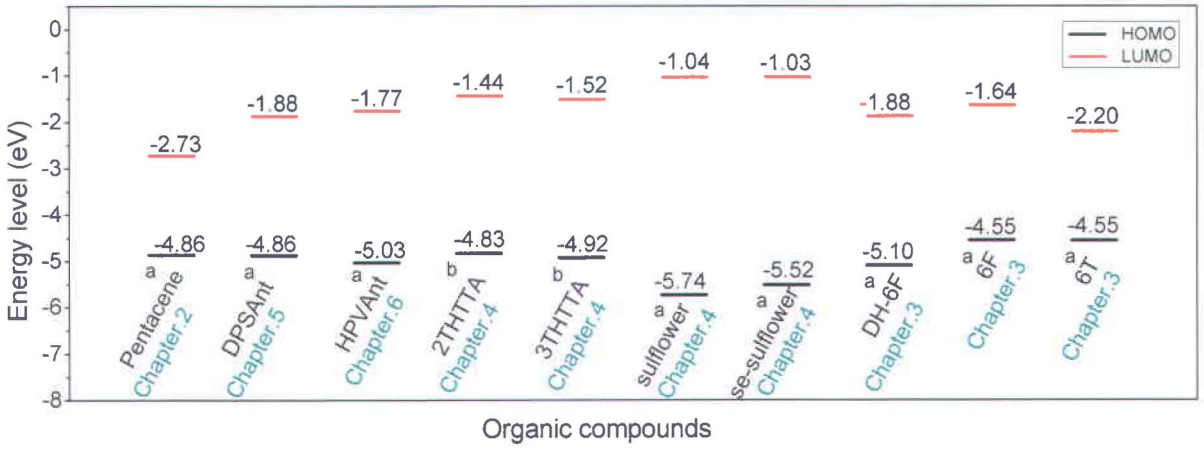

2.2. Cleaning procedure

Prior to deposition, the substrates are cleaned using different techniques to eliminate impurities from the surface. All samples are first rigorously sonicated in 2-propanol, and acetone for 5-10 min each to remove any dust and other physisorbed impurities, and then they are inserted in the oxygen[1] plasma cleaner (HARICK PDC-32G) for 10-15 min. In some cases instead of plasma cleaning, substrates were soaked in piranha solution (30% H_2O_2/ 70% H_2SO_4 v/v) for 15 min to remove all residual impurities, especially organics. Then substrates are thoroughly rinsed by sonication in water and dried in a stream of N_2.

2.3 Deposition process

High vacuum evaporation: Thermal evaporation of small molecule OSCs is the most common technique for depositing the active layer in OFETs. This technique allows good control of the film deposition, resulting in a highly homogeneous thin film and superior device performance. Optimisation of the substrate temperature and deposition rate can also promote favourable molecular ordering yielding better device performance. In this work organic films were mainly deposited at a low rate (0.1-0.3 Å/s) by vacuum evaporation. A pressure of about 10^{-6} to 10^{-7} Torr is achieved in the chamber by a turbo-molecular pump. To ensure a stable and reproducible deposition, the source temperature was risen slowly, at a rate of about 1°C/min. A thickness monitor with a 5 MHz quartz crystal (SQM-160 Thin Film Deposition Monitor) was used to measure the nominal deposition rate and the thickness. Thermal evaporation was also used to deposit different metals (mainly Au) as electrodes in top-contact devices. To ensure the uniform deposition of metals and also to prevent possible damages to the organic film, the evaporation rate was kept between 0.1-0.3 Å/s.

Solution processing: Solution processing is an effective method to deposit coating materials onto different type of substrates. Among different solution process techniques, spin-coating is widely used for fabrication of uniform thin films (both organic and inorganic) over a large area. This technique has various applications in microelectronics,[1,2] optical coating,[3] protective coating (against corrosion, UV light, humidity…),[4] paint coating,[5] sensors,[6] and membranes.[7] The fast evaporation of solvent and quick fluid flow, caused by rotation, result in rapid film formation. The films are sometimes annealed to promote an ordered structure.[8] In spin coating, the solution

[1] In some cases when oxygen was not available, air was used as inlet gas and cleaning time increased to 20-25 min.

is applied on a rotating disc, resulting in spreading, and evaporation of the solvent leaves a viscous liquid or a solid thin film. The adhesive forces at the interface between liquid and substrate result in strongly sheared liquid and consequently a radial flow and ejection of surplus solution from the substrate surface. See Figure (2.2)

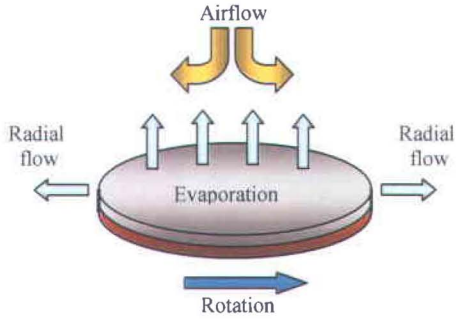

Figure 2.2: Schematic of spin-coat process

The thickness of the film is controlled by different parameters such as viscosity (or concentration) of the solution, angular velocity, rate of the deposition, and the acceleration method. For higher angular velocity and lower concentration the film thickness will decrease.[9,10] We used a Laurel spin coater (WS-650S/6NPP/LITE) for the deposition of the OSCs. Different rotation speeds (between 400- 2500 rpm), depending the solution concentration, were employed for 20 s to 2 min for coating the samples. The samples were dried under vacuum or flow of N_2 at 60 °C to 100 °C.

Vapour phase single crystal growth and deposition: In this process, an inert gas, such as argon, nitrogen, and helium, is flowed over the organic material as it is heated to its sublimation temperature. Then the vapour of material is carried along the tube by the gas and solidifies along a temperature gradient (Figure 2.3). The single crystal growth is affected by different factors, among which the type of inert gas, its flow velocity, and the temperature gradient are the major influences. Because the carrier gas always contains a small fraction of oxygen, the growth process should be performed in the dark to avoid the photoinduced oxidation of the organic material.1

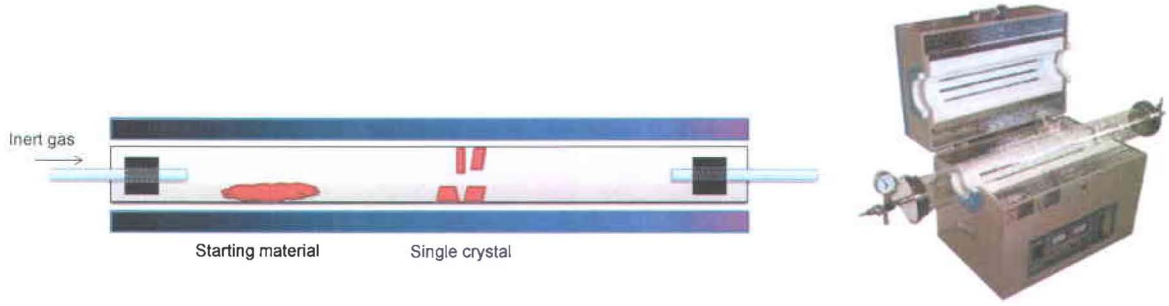

Figure 2.3 Schematic of zone furnace and image of 3" long four-zone tube furnace (OTF-1200X-V)

The crystal growth rate is influenced by the gas flow velocity and temperature gradient. Usually, faster gas flow and high temperature gradients accelerate the crystal growth. Crystals typically vary in size and shape, depending on crystal packing of the specific organic material. They grow either needle-like (1D) or plate-like (2D) with sizes from tens of nanometers to several micrometers in both lateral size and thickness.1 The sublimation temperature of the source material, total time of growth as well as the type and the rate of the transporting gas vary from one material to another. After the crystal growth, the crystal-containing tube are sealed and transferred into a glovebox to minimize the air exposure of the crystals. The quality, size and shape of the grown single crystals are verified under the polarized microscope and subsequently laminated onto the substrate by utilizing the electrostatic force between the crystal and the substrate. For a good adhesion of crystal on the substrate and to enhance the devices performance, it is preferable to choose thin crystals with thickness at sub-micrometre.[11]

2.4 OFETs fabrication

Bottom-Contact Configuration: Bottom contact devices in which an organic active film deposited on substrates pre-patterned with electrodes are suitable for fundamental studies since this geometry ensures high injection efficiency and prevents reaction between the metal and the organic film.[12] However, the growth of the organic film close to the edges of the metal contacts is often negatively affect the grain size is smaller at these critical locations thus altering the device performance. OFETs typically employ Au electrodes deposited on a SiO_2 gate dielectric. The poor adhesion of Au on SiO_2 requires the use of a thin metal film (such as Cr) as an adhesion layer. An important electrode geometry is that of circular interdigitated bottom-contact transistor in which the electrodes (Figure 2.4) are deposited on the gate dielectric prior to deposition of the OSC. The circular transistors have large channel width and thus provide a

higher drain-source current than that of other geometries. This geometry also maximizes the electroluminescence intensity of OLETs due to its large channel width and also circumvents parasitic currents because the drain electrode is isolated from the rest of the substrate.[13] In addition, in the case of a sensor application its larger contact surface may yield a higher sensitivity.

Figure 2.4: Linear and circular source and drain electrodes

Top-Contact Configuration: In the case of the top-contact structure, source and drain are deposited at the last stage after the deposition of the organic semiconductor. In general, since OSCs are sensitive to etching reagents and radiation, top contacts cannot be deposited by UV lithography. The most used method for top contact deposition is evaporation through a metal shadow mask. A general drawback of this method is the difficulty to properly place the mask and its attachment to the delicate organic thin film material. In shadow mask patterning, the resolution is limited by various parameters. The dimensions and edge sharpness of the deposited metal electrode can be influenced by the partial shadowing effects (penumbra) that occurs mainly due to the finite size of the evaporation source as illustrated for the interdigitated pattern in Figure (2.5a).

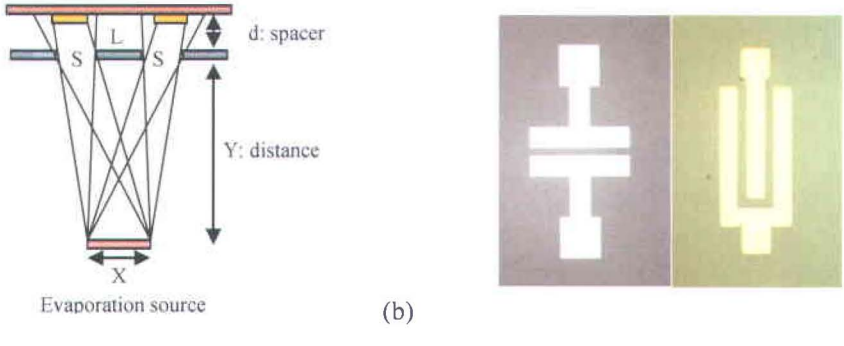

Figure 2.5: (a) schematic of shadow evaporation (b) optical micrograph evaporated Au-contacts on OSC through shadow mask

Various metals can be deposited through shadow masks by vacuum evaporation. The process of deposition should be carried out under vacuum, generally 10^{-5} to 10^{-7} Torr, to prevent scattering of the evaporated atoms by collisions and consequently to preserve a high accuracy the pattern.

During this work, OTFTs were fabricated in both **bottom-** and **top-contact** configurations using 190-200 nm thick SiO_2 as dielectric thermally grown on heavily n-doped (Sb, $\rho\sim$ 0.01–0.02 Ohm.cm) silicon substrate. In **bottom-contact** configuration, 25 nm Au electrodes were patterned by lift off technique and using a 5 nm thick Cr adhesion layer. The bottom-contact devices had channel lengths (L) of 6, 10, 40 μm and corresponding widths (W) of 1880 μm for single digit devices and W/L (μm/μm) of 42000/6, 41000/10, 18800/40 for interdigitated electrodes.

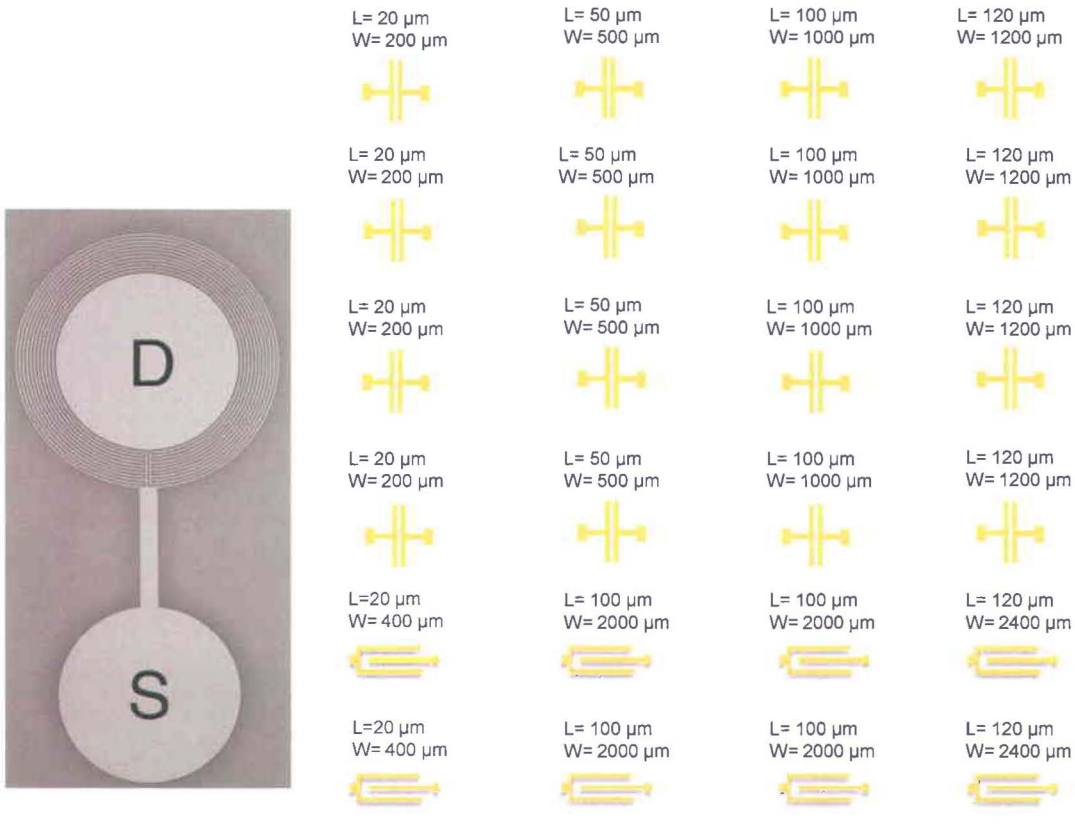

Figure 2.6: (left) Optical image of interdigitated concentric Au source and drain electrodes with W/L=18800/40 μm/μm and (right) schematic of shadow mask and W/L ratio.

In **top-contact** configuration, on the other hand, Au electrodes were deposited using the shadow mask technique. We used a stainless steel mask purchased from *Thin Metal Parts* Company (USA). **Top-contact** devices had channel lengths of 50, 100 μm and widths of 500, 1000 μm

(Figure 2.6). In some devices, the films of compound were deposited on hexamethyldisilazane (HMDS) treated substrates by vacuum sublimation (ultimate pressure ~10^{-6} Torr) at deposition rate of 0.1 to 1 Å/s until the nominal thickness of about 50 nm was reached.

For single crystal devices a highly doped silicon wafer with a 500 nm thermally grown SiO_2 layer was spin coated (1500-2000 rpm) with a 5 to 10 nm PMMA film obtained from a toluene solution. The films were maintained in an oven at 70 °C overnight and were subsequently annealed at 100 °C for 3h in an Ar or N_2 atmosphere. Then the crystals were transferred into the glove box without exposure to air and laminated onto the PMMA/SiO_2/Si substrates. Metal electrodes then were thermally evaporated through the shadow mask.

2.5 Characterization

2.5.1 Electrical characterization

Electrical characterisations of the devices were carried out using a Keithley 4200 Semiconductor Parameter Analyzer. In bias stress application, a continuous voltage is applied to the gate and/or drain for studying the transfer characteristic of the device. The measurements were performed using a lakeshore TTP4 probe station placed in an hermetically sealed chamber, under different environmental conditions of surrounding gas (under vacuum, nitrogen or ambient atmosphere) and at various temperatures. The latter were carried out using a thermal platform containing both a resistive heating element and a cooling system which are in thermal contact with a semiconductor wafer, and it is capable to reach temperatures from 4.5 K to 475 K. Cooling to such a low temperature helped us to study the activation energy (chapter 3). The tips, made of Cu/Be or tungsten with a diameter of 10 and 25 μm, were brought to contact with source, drain and gate electrodes by the help of optical microscope and video monitor. The back of the highly doped wafers are used as gate electrodes and for the wafers with double side oxide layer, a tiny spot of the wafer is scratched to remove the oxide get access to the highly doped silicon. Each single device should be separated from each other and the rest of the substrate to avoid parasitic. Patterning of devices was done by simple scratching OSC with a needle.

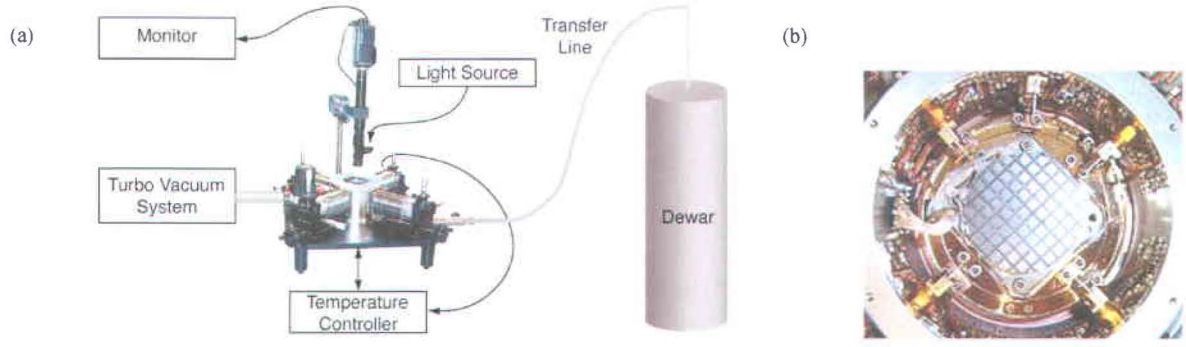

Figure 2.7: a) Lakeshore TTP-4 probe station, and b) characterisation chamber

2.5.2 Atomic Force Microscopy (AFM)

AFM is generally used to visualize the morphology of organic films and to determine the organization of the molecules. In this technique, a sharp tip is scanned over the sample surface with a feedback mechanism controlling a piezoelectric scanner such that the tip is maintained above the sample surface at a constant force or height to obtain height or force information respectively. Most common AFMs use a laser beam deflection system where a laser is reflected on the back of the reflective AFM cantilever onto a position-sensitive detector (Figure 2.8).When the tip is brought into proximity of a sample surface, forces between the tip and the sample lead to a deflection of the cantilever according to Hooke's law.

$$F = -Kz \qquad (2.1)$$

Where F is the force, K is the stiffness of the lever, and z is the distance the lever is bent. The total interaction force includes the mechanical contact force (such as repulsion, friction and adhesion), chemical bonding, electrostatic forces, Van der Waals forces, capillary forces, magnetic forces, etc. The sample is mounted on a piezoelectric tube, that moves the sample in the x and y directions for scanning the sample and in the z direction for maintaining a constant force. A tripod configuration of three piezo crystals, in which each piezo is responsible for scanning in the x, y and z directions, may be used to eliminate some of the distortion effects seen with a tube scanner. The resulting map of the area s = f(x,y) represents the topography of the sample.[14]

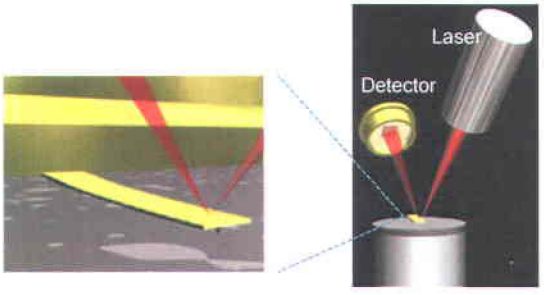

Figure 2.8: Reflection of the laser beam from the back of the reflective AFM cantilever onto a position-sensitive detector.[14]

The AFM can be operated in a number of modes, depending on the application. In general, possible imaging modes are divided into the static (also called Contact) mode and a variety of dynamic modes. Here we present the contact mode and tapping mode of AFM operation.

Contact mode is widely used in AFM operation. The tip is deflected as it is raster-scanned across the surface and over the surface corrugation. In this mode, the tip is constantly adjusted to keep a constant deflection, thus constant force above the surface. However, tracking the surface in this manner is limited by the feedback circuit. When the tip scans without this adjustment, (constant height mode), only the deflection can be measured. This is useful for small, high-speed atomic resolution scans, and is known as the variable-deflection mode. Because the tip is in hard contact with the surface, the stiffness of the cantilever needs to be less than the effective spring constant holding atoms together, which is on the order of 1 to10 N/m. Most contact mode cantilevers have a spring constant of less than 1 N/m.[14]

Tapping mode is also referred to as intermittent-contact or in more general terms the Dynamic Force Mode. The cantilever is oscillated at its resonance frequency, and maintaining a constant amplitude while scanning results in tapping the surface, thus the interaction time between tip and surface is only a very small fraction of its oscillation period, reducing dramatically the lateral forces are dramatically reduced as the tip moves over the surface. Thus, the lateral resolution is improved for soft samples, especially for poorly adsorbed specimens on a substrate surface.

Typically, in tapping mode cantilevers used are very stiff, as tips can get stuck in the water contamination layer. In this work, we used AFM (tapping mode) to characterize the topology of the surface (either OSC or gate dielectric) and measure the surface roughness, the grain size of

the polycrystalline organic materials.[14] This allowed us to study the film growth mechanisms of different types of organic semiconductors. The images were taken at the low scan rate (number of scan lines per second) of 0.3 Hz to 1 Hz with a resolution of 512×512 (sample/line). The integral gain of the feedback loop was typically 0.8 to 1.5 while the proportional gain varied between 1 and 2.

2.5.3 Optical characterization

Ultra Violet - Visible Spectroscopy (UV/VIS) is based on the absorption of electromagnetic radiation by the substances in the ultraviolet and visible regions of the spectrum that will result in changes in their electronic structure. Absorption may be presented as transmittance ($T=I/I_0$) or absorbance $A=\log (I/I_0)$, with I_0 and I being the intensities of the reference and sample beams, respectively. If no absorption has occurred in a sample, T = 1.0 and A= 0. The wavelength of an absorbance peak is a characteristic value of the compound and defined as λ_{max}.

Fluorescence Spectroscopy is an electromagnetic spectroscopy in which a molecule is promoted to an electronically excited state by absorption of ultraviolet, visible or near infrared light. Fluorescence occurs when the excited molecule returns to the electronic ground state by emission of a photon. Fluorescence measurements can be carried out on liquid, gaseous, and solid samples. Solvents may decrease the fluorescence efficiency if they absorb at the wavelength used to excite the sample. Moreover, any changes in the polarity of the solvent can significantly affect the fluorescence efficiency.

Photoluminescence quantum yield measurements: the ratio between the number of photons absorbed and the number of photons emitted via fluorescence is called fluorescence quantum yield (Φ_F). The quantum yield gives the probability of the excited state being deactivated by fluorescence rather than by other, non-radiative mechanisms. Photoluminescence quantum yield is defined as:

$$\Phi_F = \frac{number\ of\ the\ emitted\ photons}{number\ of\ the\ absorbed\ photons} \quad (2.2)$$

The most reliable technique for recording Φ_F is the comparative method[15] which involves the use of well characterised standard samples with known Φ_F values and absorption wavelength close to that of the test sample. A ratio of the integrated fluorescence intensities of the two solutions (recorded under identical conditions) will yield the ratio of the quantum yield values.

The fluorescence quantum yield is calculated with following equation:

$$\Phi_x = \Phi_{ST}\left(\frac{Grad_x}{Grad_{ST}}\right)\left(\frac{\eta_x}{\eta_{ST}}\right) \quad (2.3)$$

Where the subscripts ST and X denote standard and test respectively, Φ is the fluorescence quantum yield, Grad the gradient from the plot of integrated fluorescence intensity versus absorbance, and η the refractive index of the solvent.[16] In this work, the fluorescence spectra were taken by Cary Eclipse Fluorescent Spectrometry (Varian). All the fluorescence spectra are with constant slit widths since any change to this parameter between samples invalidates the quantum yield measurement. The samples were excited at different wavelength and in a 10 mm cuvette, while the fluorescence was recorded at a slow scan rate from 400 nm to 650 nm.

Measurement of the PLQY of thin films is a more complex compared to that of solution measurement. The high refractive index of films could result in substantial wave-guiding of the luminescence. To overcome the angular dependence of the emission from films, integrating spheres are generally used to collect the emitted light. The use of integrating spheres has usually required a laser as the excitation source in combination with a fibre coupled CCD camera as the luminescence detectors.[17] It has been shown that a commercial fluorimeter can also be used together with an integrating sphere to absolute measurement of the solid-state PLQY.[18] In this method the PLQY is calculated according to the Mello's formula: [19]

$$(2.4) \qquad \phi_{PL} = \frac{E_i(\lambda)-(1-A)E_0(\lambda)}{L_e(\lambda)A} \qquad \text{where} \qquad A = \frac{L_0(\lambda)-L_i(\lambda)}{L_0(\lambda)}$$

Where $E_i(\lambda)$ and $E_0(\lambda)$ are the integrated luminescence as a result of direct excitation of the film and secondary excitation, respectively. The lattermost luminescence is a result of the reflected excitation beam from the sphere walls hitting the sample. *A* is the film absorbance measured from the integrated excitation profile. $L_i(\lambda)$ is the integrated excitation when film is directly excited and $L_0(\lambda)$ is the integrated excitation when the film is indirectly excited by the reflected beam from the sphere wall. And finally $L_e(\lambda)$ is the integrated excitation spectrum from empty sphere.

To evaluate EL of OLETs and confirm the modulation of the emission, a photodiode (Hamamatsu 3137QB Si) was placed right above the working OLET and intensity of the EL was recorded while device was biased for output characteristics measurement.

2.6 Pentacene as a testing platform for novel semiconductors

In this project, pentacene ($C_{22}H_{14}$) was chosen to establish a reproducible and reliable process for the fabrication of OFETs. Pentacene is the benchmark material for OFETs with $\mu_h \geq 1$ cm^2/Vs. Impurities from the synthetic procedure and/or material degradation during the storage often exist in pentacene samples and its insolubility complicates the purification process. Exposing pentacene to oxygen and ultraviolet light can also result in photoinduced electron transfer, leading to [4+4] radical cataion species formation to an oxidized product (6,13-pentacenequinone), together with the photodimerized product (Scheme 2.1).[20] These impurities can act as trapping sites, influencing the electronic transport and decreasing the device performance.

Scheme 2.1: Impurities often found in pentacene: a) 6,13-pentacenequinone b) pentacene dimer

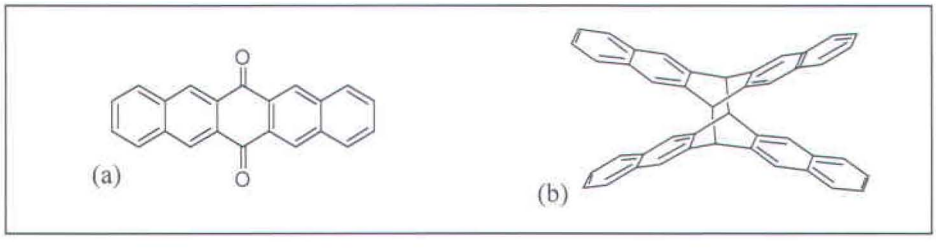

The thin film of pentacene has a wide range of different morphologies and structures on the substrates which can be due to different substrate materials, deposition rate, substrate temperature, film thickness, and purity of the pentacene. These effects can be conveniently studied by AFM. Figure 2.9 shows AFM micrographs (tapping mode) and the histogram of the step size of pentacene thin films deposited on silicon dioxide with deposition rate of 0.1 (A/s) while the substrates were kept at room temperature. The grains seem to be terraced and closely packed.

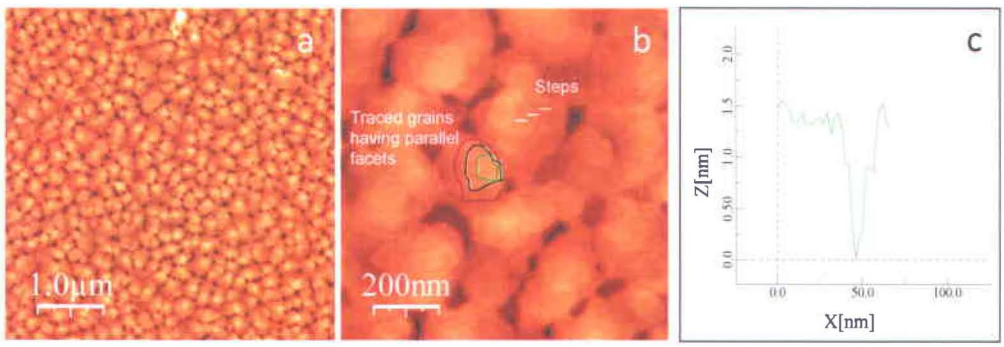

Figure 2.9: a) thin film and (b) magnified AFM images of vacuum deposited pentacene on SiO_2/Si (b) the step size histogram of the film

Moreover, the neighbouring facets are parallel showing the existence of long range ordering across the pentacene crystals which can contribute to charge carrier transport. The step-height of these terraces is a ~1.5 nm which agrees well with the length of the pentacene molecule, suggesting a perpendicular growth of the latter to the substrate along its long axis.

A plot of the output and transfer characteristics of top- and bottom-contact pentacene-FET prepared under high vacuum on SiO_2/Si substrate is shown in Figure 2.9 and 2.10. In the output plot, the drain-source current is depicted vs. the drain-source voltage (sweeping from 0 V to -60 V) at different gate bias (0 V to -60 V by the steps of -10 volts). Transfer characteristics of pentacene-FETs are plotted at the constant drain-source voltage of -60V while gate bias was swept from 0V to -60 V. On the left y axis of transfer characteristics, the square root of $|I_{DS}|$ is plotted as a function of gate voltage, allowing the calculation of the threshold voltage, and on the right y axis $|I_{DS}|$ is plotted vs. gate voltage on a logarithmic scale, which allows an estimation of the I_{on}/I_{off}. The output and transfer characteristics of a bottom-contact pentacene TFT evaporated under high vacuum on bare SiO_2/Si are shown in Figure 2.9. Device exhibits the characteristics of a p-type semiconductor with a field effect mobility of 0.2 cm^2/Vs, I_{on}/I_{off} ratios of 10^5 and threshold voltage of -12 V while V_G scanned from 60 V to -60 V and V_{DS} fixed at -60 V. Figure 2.10 also shows the unipolar transistor characteristics of top-contact devices having pentacene as the active layer deposited on bare SiO_2/Si substrate. In this device, the calculated saturation field effect mobility is 0.8 (cm^2/Vs) and the threshold voltage of -10 V with V_G scanned from 5 V to -60 V. In this study, we could promote the layer growth mechanism (which is necessary for good charge transport thus device performance) of pentacene on SiO_2/Si substrate. Moreover the FET characteristics of this molecule on bottom-and top-contact devices are comparable to the

literature. This assures the standard and reliable process for the fabrication of OFETs incorporating novel OSCs studied this thesis.

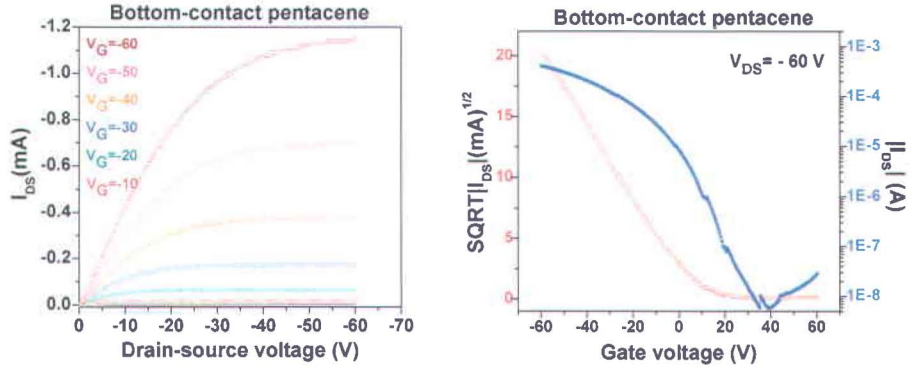

Figure 2.9: output (left) and transfer (right) characteristics of bottom-contact pentacene-FETs (deposition rate of 0.6 (A/s), nominal thickness = 50 nm)

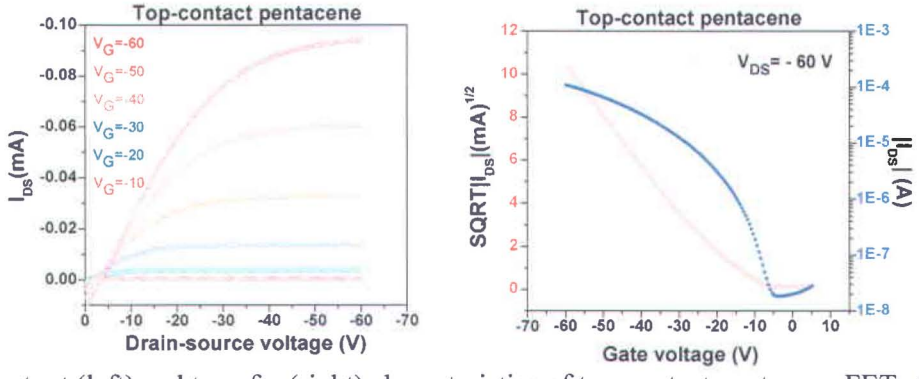

Figure 2.10: output (left) and transfer (right) characteristics of top-contact pentacene-FETs (deposition rate of 0.6 (A/s), nominal thickness = 50 nm)

References

[1] Sirringhaus, H.; Brown, P. J.; Friend, R. H.; Nielsen, M. M.; Bechgaard, K.; Langeveld-Voss, B. M. W.; Spiering, A. J. H.; Janssen, R. A. J.; Meijer, E. W., Microstructure-mobility correlation in self-organised, conjugated polymer field-effect transistors. *Synthetic Met* **2000,** *111*, 129-132.

[2] Burroughes, J. H.; Bradley, D. D. C.; Brown, A. R.; Marks, R. N.; Mackay, K.; Friend, R. H.; Burns, P. L.; Holmes, A. B., Light-Emitting-Diodes Based on Conjugated Polymers. *Nature* **1990,** *347* (6293), 539-541.

[3] Walheim, S.; Schaffer, E.; Mlynek, J.; Steiner, U., Nanophase-separated polymer films as high-performance antireflection coatings. *Science* **1999,** *283* (5401), 520-522.

[4] Chang, D.; Yoon, D.; Ro, M. D.; Hwang, I.; Park, I.; Shin, D., Synthesis and characteristics of protective coating on thin cover layer for high density-digital versatile disc. *Japanese Journal of Applied Physics Part 1-Regular Papers Short Notes & Review Papers* **2003,** *42* (2B), 754-758.

[5] Nelson, T. L.; Young, T. M.; Liu, J.; Mishra, S. P.; Belot, J. A.; Balliet, C. L.; Javier, A. E.; Kowalewski, T.; McCullough, R. D., Transistor paint: high mobilities in small bandgap polymer semiconductor based on the strong acceptor, diketopyrrolopyrrole and strong donor, dithienopyrrole. *Adv Mater* **2010,** *22* (41), 4617-21.

[6] Douglas, P.; Eaton, K., Response characteristics of thin film oxygen sensors, Pt and Pd octaethylporphyrins in polymer films. *Sensor Actuat B-Chem* **2002,** *82* (2-3), 200-208.

[7] Yan, X. H.; Liu, G. J.; Dickey, M.; Willson, C. G., Preparation of porous polymer membranes using nano- or micro-pillar arrays as templates. *Polymer* **2004,** *45* (25), 8469-8474.

[8] Norrman, K.; Kingshott, P.; Kaeselev, B.; Ghanbari-Siahkali, A., Photodegradation of poly(ether sulphone) Part 1. A time-of-flight secondary ion mass spectrometry study. *Surf Interface Anal* **2004,** *36* (12), 1533-1541.

[9] Bornside, D. E.; Macosko, C. W.; Scriven, L. E., On the Modeling of Spin Coating. *J Imaging Technol* **1987,** *13* (4), 122-130.

[10] Daughton, W. J.; Givens, F. L., An Investigation of the Thickness Variation of Spun-on Thin-Films Commonly Associated with the Semiconductor Industry. *J Electrochem Soc* **1982,** *129* (1), 173-179.

[11] Jiang, L.; Dong, H. L.; Hu, W. P., Organic single crystal field-effect transistors: advances and perspectives. *J Mater Chem* **2010,** *20* (24), 4994-5007.

[12] Santato, C.; Cicoira, F.; Cosseddu, P.; Bonfiglio, A.; Bellutti, P.; Muccini, M.; Zamboni, R.; Rosei, F.; Mantoux, A.; Doppelt, P., Organic light-emitting transistors using concentric source/drain electrodes on a molecular adhesion layer. *Appl Phys Lett* **2006,** *88* (16),

[13] Meijer, E. J.; Detcheverry, C.; Baesjou, P. J.; van Veenendaal, E.; de Leeuw, D. M.; Klapwijk, T. M., Dopant density determination in disordered organic field-effect transistors. *J Appl Phys* **2003,** *93* (8), 4831-4835.

[14] http://www.nanoscience.com/index.html

[15] Williams, A. T. R.; Winfield, S. A.; Miller, J. N. Relative fluorescence quantum yields using a computer controlled luminescence spectrometer, *Analyst*, **1983,** 108, 1067.

[16] www.jobinyvon.com

[17] http://www.horiba.com/scientific/products/fluorescence-spectroscopy/application-notes/quantum-yields/

[18] Palsson, L. O.; Monkman, A. P., Measurements of solid-state photoluminescence quantum yields of films using a fluorimeter. *Adv Mater* **2002,** *14* (10), 757-758.

[19] Rocheleau, C. E.; Downs, W. D.; Lin, R. L.; Wittmann, C.; Bei, Y. X.; Cha, Y. H.; Ali, M.; Priess, J. R.; Mello, C. C., Wnt signaling and an APC-related gene specify endoderm in early C-elegans embryos. *Cell* **1997,** *90* (4), 707-716.

[20] Maliakal, A.; Raghavachari, K.; Katz, H.; Chandross, E.; Siegrist, T., Photochemical stability of pentacene and a substituted pentacene in solution and in thin films. *Chem Mater* **2004,** *16* (24), 4980-4986.

CHAPTER 3

Linear oligomers*

3.1 Introduction

Conjugated oligomers (or polymers) are attracting considerable attention due to their potential application in organic light-emitting diodes (OLEDs),[1,2] photovoltaic cells,[3,4] organic field-effect transistors (OFETs),[5,6] and electrochromic devices.[7] One advantage of conjugated oligomers over polymers is the ability to prepare high-purity material and to form structurally ordered films, both which are important for the efficient charge transport. The electronic properties of polymers with different chalcogen atoms has already been studied systematically and compared to polythiophene. [7b,7c,8] Due to the variation of chain length of polymers, however, the comparison between the properties of polymers does not provide complete information about the contributions of chalcogen atoms into the electronic structure of conjugated systems. But the comparison between the similar structure of oligomers and their derivatives can provide some necessary information regarding the contribution of chalcogen atoms into the charge transport of the molecules.

The thiophene based π-conjugated systems have shown great achievements in the field of n and p type OFETs.[9] It has been debated that the superior polarizability of heavier chalcogens such as sulphur and selenium over oxygen improves the charge mobility of the oligomers and their derivatives.[10] Selenophene is the heavy member of chalcogenophenes series and its properties show similar to those of thiophene. The electron-donating[11] and polarizability[12] properties of selenophenes are higher than thereof thiophenes. These facts suggest that selenophene containing oligomers should be especially attractive as electronic materials. This perception extends to the field of conducting polymers, where the lower conductivity of polyfurans relative to polythiophenes was explained by the unfavorable electronic effects of the oxygen atom.[13]

* Parts of this chapter are published in: O. Gidron, A. Dadvand, Y. Sheynin, M. Bendikov, and D. F. Perepichka, "Towards "green" electronic materials. α-Oligofurans as semiconductors", *Chem. Commun.*, 2011, 47, 1976-1978.

However, the effect of an oxygen heteroatom on field effect properties has never been studied systematically.[14] This chapter will present the study of semiconducting properties of α-oligofurans in comparison with oligothiophenes/oligoselenophenes and provide experimental and theoretical evidence that the effect of the type of the chalcogen atom on the charge mobility of heteroaromatic semiconductors is surprisingly weak, and is within the usual device-to-device variation.

3.2 Oligoselenophenes

At the beginning of this study, the FET properties of a series of semiconducting oligomers having mixed hetero-units (hexamers of thiophene and selenophene) were studied (Scheme 3.1). All OTFTs were fabricated on bottom-contact configuration and the dielectric surface was treated by HMDS.

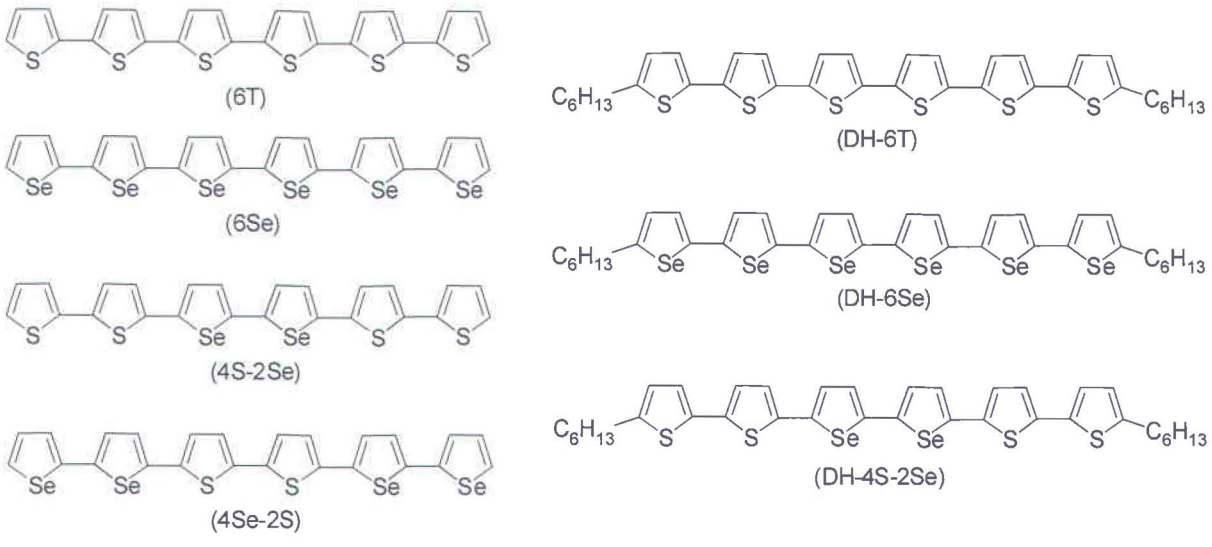

Scheme 3.1. Chemical structure of oligoselenophenes and oligothiophenes

The comparative FET characteristics of the oligoselenophenes and oligothiophenes are summarized in Table 3.1. The overall device characteristics suggested somewhat low effect of the type of the chalcogen atom on the charge mobility of heteroaromatic semiconductors. This is in contrast to the other reports regarding the greater contribution of the heavier chalcogens on the overall charge transport of π-conjugated systems. It should be noted that the presented data is based on limited number of devices and no optimization of the fabrication process was performed. This was mainly due to the poor stability of source materials at deposition

temperature that hindered the preparation of large amount of pure material. However, OTFTs were all fabricated under the similar condition to allow comparisons. To further investigate the role of heteroatom, this work was directed to the detailed study of FET characteristics of oligofurans in comparison with oligothiophenes.

Table 3.1. Comparative FET characteristics of the oligoselenophenes and oligothiophenes prepared in bottom-contact configuration

Compound	Max. Mobility (cm^2/Vs)	On/Off ratio	V_T (V)
α-6T	4×10^{-2}	10^6	-15
α-6Se	1.1×10^{-2}	10^6	-20
DH-6T	4×10^{-2}	10^3	-7
DH-6Se	4×10^{-3}	10^5	-18
α-4S-2Se	2×10^{-2}	10^6	-20
α-4Se-2S	4×10^{-2}	10^6	-20
DH-4S-2Se	0.1	10^3	+6

3.3 Oligofurans

Furan-only materials are biodegradable, and in addition, furans (in contrast to other types of conjugated materials) can be obtained from entirely renewable resources.[15]

α-Oligofurans, compared to oligothiophenes, have a relatively high HOMO energy (facilitating hole injection from a high workfunction electrode such as Au), efficient fluorescence, and high rigidity.[16] In addition, the tight herringbone packing of α-oligofurans and low calculated reorganization energy suggest them as possible candidates for OFET applications. Unlike oligothiophenes and other organic electronic materials, furan-based materials are biodegradable and can be obtained from renewable resources.

In this section, we study the film morphology and FET characteristics of **6F**, **DH-6F**, and **8F** (Scheme 3.2). These structures were chosen to enable a direct comparison with some of the most studied and well-understood oligothiophene analogues **6T**, **DH-6T,** and **8T**.[17,18,19,20,21] The comparative study of OTFTs based on **6T** and **8T** shows that **8T** possesses higher mobility[22,23] Linear alkyl groups at terminal α-position in **DH-6T** induce preferred molecular orientation thereby enhancing mobility up to one order of magnitude.[24] This has been demonstrated in an increase of mobility from 0.01 cm^2/Vs to for un-substituted 6T to 0.13 cm^2/Vs for alkylated **6T**.[24]

The heteroatom effect is therefore evaluated for oligomers of different lengths (which affects HOMO/LUMO levels and reorganization energy) and for alkyl chain-substituted molecules (which usually possess an improved morphology in thin films).[25] Surprisingly, we found that the field effect mobility of oligofurans is very similar to that of the corresponding oligothiophenes. Thus, the presence of heavier polarizable elements such as sulfur is not a prerequisite for successful OFET materials based on conjugated heterocyclic molecules.

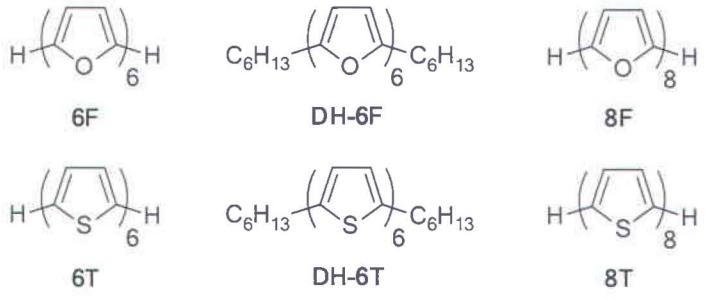

Scheme 3.2. Chemical structure of oligothiophene and oligofurane derivatives

3.3.1 Thin film morphologies of oligofurans

Thin film morphologies of oligofurans vacuum deposited on Si/SiO_2 were studied by atomic force microscopy (AFM) and X-ray diffraction (XRD). AFM images of **DH-6F** show a layer-by-layer deposition, with a layer thickness of ~2.8–3.0 nm (Figure 3.1a). This is in agreement with XRD measurements on these films, which reveal only a set of *h00* diffraction peaks for **DH-6F** with a corresponding *d*-spacing of 2.75 nm. This distance corresponds to the calculated length of **DH-6F** (3.89 nm) at a tilt angle of 45°. The film growth proceeds in a layer-by-layer fashion, at least for the first three monolayers. For **8F**, layer-by-layer deposition is observed as well, with a layer thickness of ~3 nm (the calculated length is 3.09 nm), (Figure 3.1c). Again, the layer-by-layer deposition is confirmed by XRD, which shows a set of *h00* peaks (up to eighth order), with *d*-spacing of 2.54 nm, indicating that the surface molecules lie at a ~55° tilt. The morphology of **6F** films is very different from that of **8F** and **DH-6F** films. AFM shows the formation of 1D 'wires' (Figure 3.1e), which pack in bundles at longer deposition times. The XRD pattern of such a film shows no selective alignment of the crystallographic planes of **6F** vs. the substrate. (Figure 3.2)

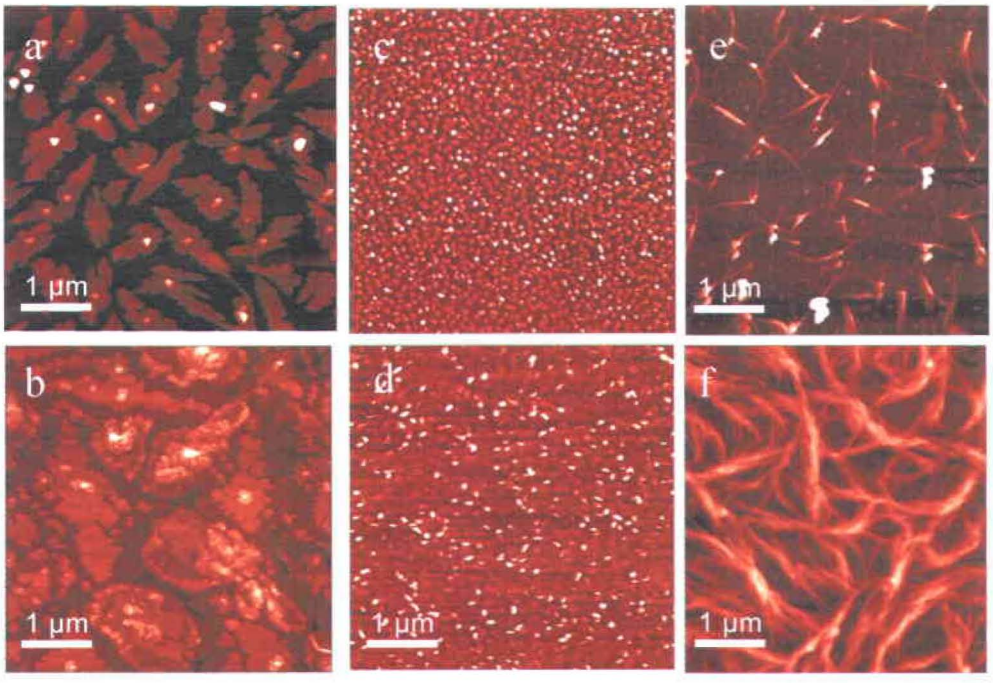

Figure 3.1. AFM images and cross section diagrams of (a) **DH-6F** after a deposition time of 20 s (sub-monolayer regime), (b) **DH-6F** after a 120 s deposition time (thickness of 3 layers), (c) **8F** after a deposition time of 20 s, (d) **8F** after a deposition time of 60 s, (e) **6F** after a deposition time of 20 s, and (f) **6F** after a deposition time of 60 s, on Si/SiO_2.

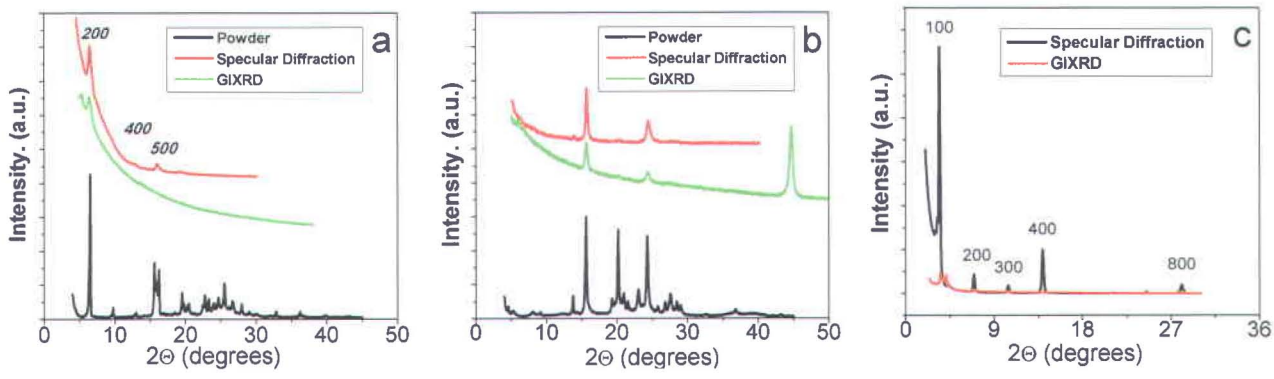

Figure 3.2. XRD patterns for vacuum deposited films of (a) **DH-6F** (b) **6F**, and (c) **8F**.

3.3.2 OFETs based on oligofurans

OFET devices based on **6F**, **DH-6F**, and **8F** were fabricated in a bottom and top-contact geometry, and all the devices showed only *p*-type behavior (Table 3.1 and Figure 3.3 and 3.4). The hole mobility of **DH-6F** (up to 0.05 cm^2/Vs) is very similar to values measured for **DH-6T** (0.04–0.09 cm^2/Vs) in this work as well as by others (10^{-2}–10^{-1} cm^2/Vs)[17,18b,19,20,26] under similar conditions.[†] **8F** shows a somewhat higher mobility (up to 0.07 cm^2/Vs) that is still similar to the previously measured mobilities of **8T** (although the transport properties of **8T**[17c] were found to be highly field-dependent).[17e] In contrast, the mobility of **6F** is significantly lower (4×10^{-4} cm^2/Vs compared with 0.04–0.09 cm^2/Vs for **6T** in this work and 0.02–0.06 cm^2/Vs by others under similar conditions[18a]), which is in accordance with the poor film morphology of **6F** mentioned above. Despite the lower (photo)oxidative stability of oligofurans, the devices remain operational after prolonged exposure to ambient laboratory conditions (mobility drops by less than a factor of two for **DH-6F** OFETs stored in air in the dark for one month; mobility drops by a factor of ~8 when same storage involves direct exposure to light).

Table 3.1. Comparative FET characteristics of the oligofurans and oligothiophenes prepared in this work.

Compound	Substrate temperature	Mobility cm^2/Vs	on/off ratio	Threshold voltage (V)
6F	RT	6.4×10^{-4}	10^5	–14
6T	RT	0.04	4×10^5	–12
	(90°C)	(0.09)	(2×10^5)	(–15)
DH-6F	RT	0.034	5×10^5	–10
	(70°C)	(0.05)	(2×10^5)	(–15)
DH-6T	RT	0.045	3×10^5	–17
	(100°C)	(0.098)	(5×10^5)	(–10)
8F	RT	0.014	1×10^5	–6
	(70 °C)	(0.066)	(8×10^5)	(–14)

[†] The mobility of 1.1 cm^2/Vs was reported for **DH-6T** [26] when a poly(4-vinylphenol) film was used as a dielectric but there was an uncertainty on measuring the capacity of the polymer dielectric.

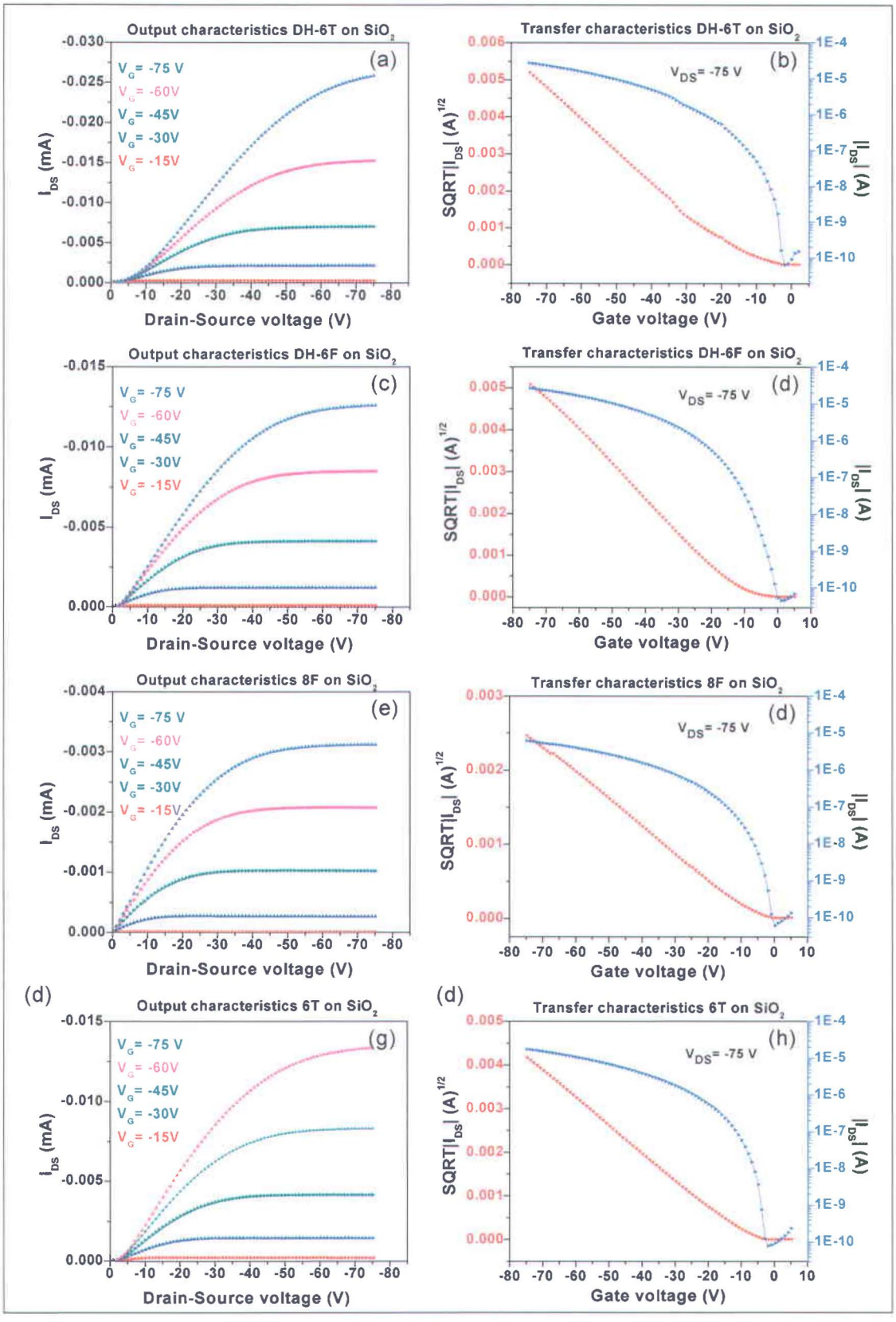

Figure 3.3: Output (a,c,e,g) and transfer (b,d,f,h) characteristics of OFETs based on **DH-6T** (a, b) **DH-6F** (c, d), **8F** (e, f) and **6T** (g, h) prepared at RT (W/L=1000/50 μm).

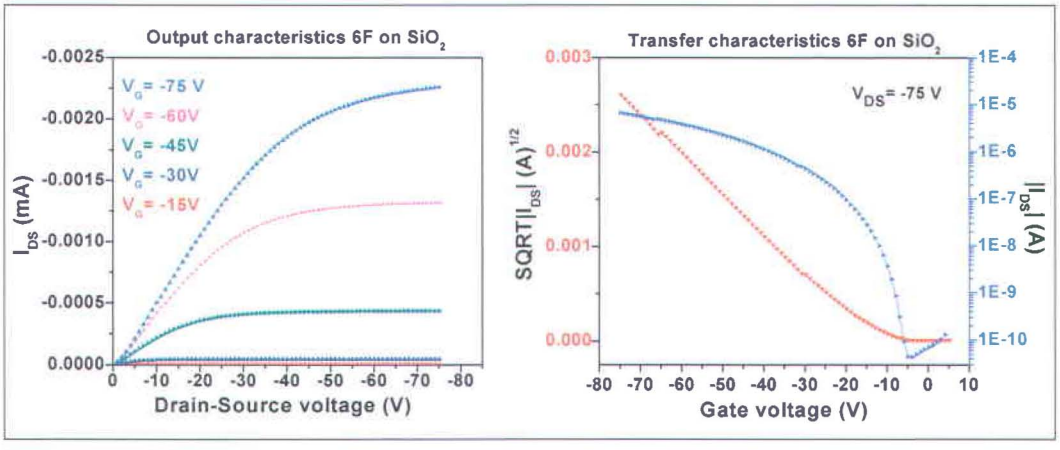

Figure 3.4: Output (left) and transfer curves (right) of bottom-contact TFT (W/L= 1880/6 μm) based on a vacuum sublimed film (~50 nm) of **6F** (at room temperature).

One of the advantages of oligofurans is their relatively efficient emission properties that are of potential interest for the development of organic light-emitting transistors (OLET).[27] Thus, the quantum yield of **DH-6F** (72%) is substantially higher than that of **DH-6T** (38%, measured in this work under the same conditions). Optical microscopy on the OFET with **DH-6F** revealed appearance of greenish-yellow electroluminescence (Figure 3.5) upon biasing the devices (when the gate voltage was "on"). The emission intensity is quite weak as most of the recombination zone is buried under the top gold contact (the cathode), which is due to exciton generation being limited by electron injection.[28] Nevertheless, the observation sets a starting point for future OLET development.

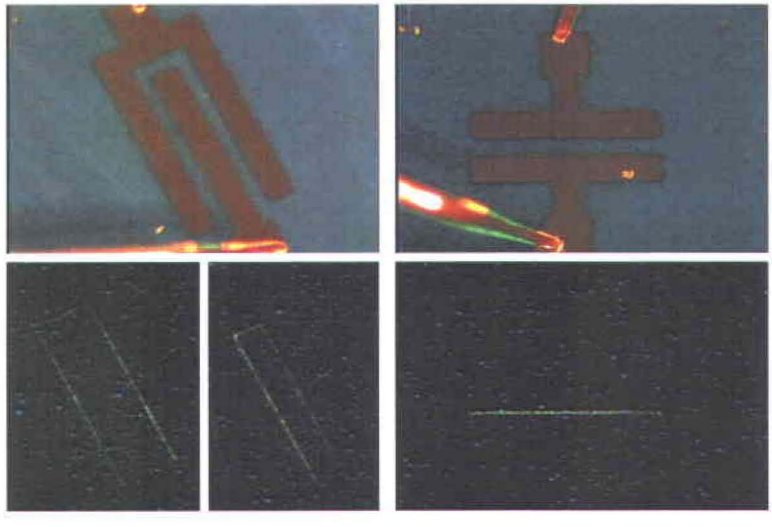

Figure 3.5: Electroluminescence of a top-contact OFET based on **DH-6F**. (W/L= 1000/50 and 500/50 μm). The top images show the device under external illumination. The bottom images show electroluminescence appearing in the vicinity of the cathode upon biasing of the gated device.

The linear shape of the output curves for oligofuran-based OFETs (Figure 3.3c,3.3e) in the low drain voltage (V_{DS}) region indicates a good (ohmic) contact with the electrodes.[29] This is in contrast with the nonlinear current increase observed for the corresponding oligothiophenes under these conditions. The difference may arise from the higher HOMO of oligofurans and subsequently lower contact resistance with the Au electrodes (e.g, HOMO = –4.55 eV for **6F** and –4.80 eV for **6T** at the B3LYP/6-31G(d) level).

3.3.3 Temperature dependence of the mobility of DH6F

The temperature dependence of the mobility of transistors based on **DH6F** is summarized in Figure 3.6 which includes an Arrhenius plot of the field-effect mobility as a function of the temperature from 300 K down to 4.6 K.‡ The device behavior in region I (15 K < T < 300 K) is in accordance with Arrhenius relation $\mu_{eff} \alpha \exp(-E_a / kT)$, where E_a, k, and T are the activation energy, Boltzmann constant, and temperature, respectively.[30] At temperatures lower than 15 K (region II), tunneling (*band-like transport*) is a dominant charge transport mechanism and mobility becomes almost temperature independent. Band-conduction at low temperature might be explained by kT becoming much lower than valence band width. At high gate bias, *however*, traps can be presented in conducting channel of field-effect transistors. At the temperatures ranging from 63K to 300 K, thermally activated hopping becomes the dominant means of charge transport. From the analysis of the slope of the Arrhenius logarithmic plot, the activation energy was estimated to be 14 meV. This value is more than two[31] and three[32] times lower than previously reported for devices based on **DH6T**. Both oligothiophenes and oligofurans show herringbone packing but shorter inter-plane distances with oligofurans[16] make the hopping distance much smaller and it can explain the lower activation energy. This has also been manifested in the lower threshold voltage and excellent output characteristics of the oligofuran based devices.

‡ Similar experiments are reported only down to 10 K

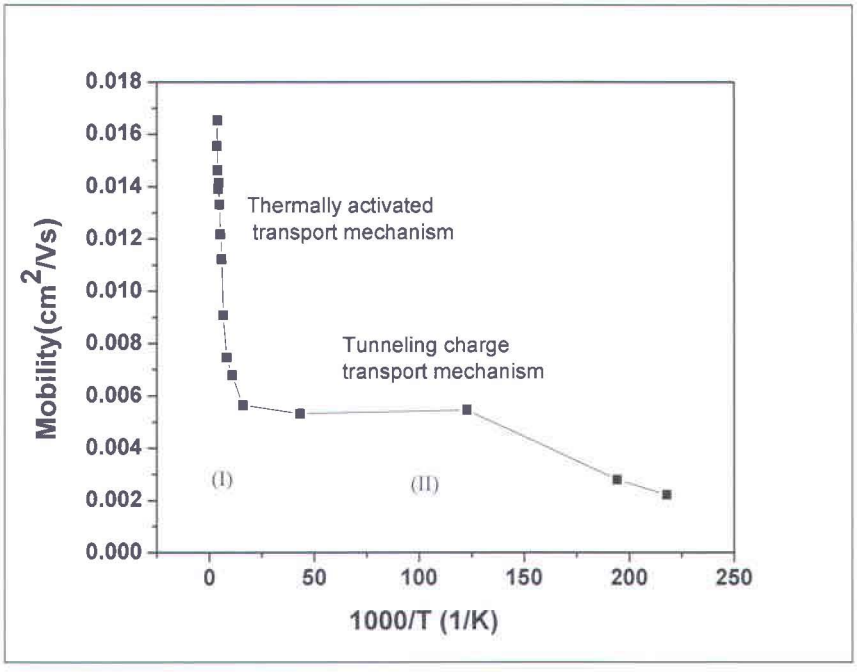

Figure 3.6. The temperature dependence of the mobility of transistors based on **DH6F**

3.4 Conclusion

We showed that oligofurans can be used as *p*-type semiconductors in OFET. Tighter packing of oligofurans vs. oligothiophenes compensates the effect of the larger/more diffuse orbitals of the sulfur vs. oxygen. As a result, field-effect mobilities measured for **DH-6F** and **8F** of 0.05–0.07 cm^2/Vs are very similar to those of their thiophene analogs. *Clearly, the effect of the heteroatom is small* compared to those of the functional groups and film morphology. Oligofurans are more electron-rich than the respective thiophenes, and are therefore more easily oxidized. By virtue of the intrinsically higher fluorescence, higher HOMO, better processability, biodegradability, and renewable feed-stock for furan derivatives, oligofurans appear to be promising new materials for scalable optoelectronic applications. Therefore, the substitution of sulfur with oxygen in many known materials could lead to the development of new efficient organic semiconductors.

References

[1](a) Burroughes, J. H.; Bradley, D. D. C.; Brown, A. R.; Marks, R. N.; Mackay, K.; Friend, R. H.; Burns, P. L.; Holmes, A. B., Light-Emitting-Diodes Based on Conjugated Polymers. *Nature* **1990,** *347* (6293), 539-541; (b) Ho, P. K. H.; Kim, J. S.; Burroughes, J. H.; Becker, H.; Li, S. F. Y.; Brown, T. M.; Cacialli, F.; Friend, R. H., Molecular-scale interface engineering for polymer light-emitting diodes. Nature **2000**, 404 (6777), 481-484.

[2] (a) Perepichka, I. F.; Perepichka, D. F.; Meng, H.; Wudl, F., Light-emitting polythiophenes. *Adv Mater* **2005,** *17* (19), 2281-2305; (b) Tanaka, H.; Herland, A.; Lindgren, L. J.; Tsutsui, T.; Andersson, M. R.; Inganas, O., Enhanced current efficiency from bio-organic light-emitting diodes using decorated amyloid fibrils with conjugated polymer. *Nano Lett* **2008,** *8* (9), 2858-2861; (c) Schols, S.; McClatchey, C.; Rolin, C.; Bode, D.; Genoe, J.; Heremans, P.; Facchetti, A., Organic Light-Emitting Diodes with Field-Effect-Assisted Electron Transport Based on alpha,omega-Diperfluorohexyl-quaterthiophene. *Adv Funct Mater* **2008,** *18* (22), 3645-3652; (d) Zhou, Y.; He, Q. G.; Yang, Y.; Zhong, H. Z.; He, C.; Sang, G. Y.; Liu, W.; Yang, C. H.; Bai, F. L.; Li, Y. F., Binaphthyl-Containing Green- and Red-Emitting Molecules for Solution-Processable Organic Light-Emitting Diodes. *Adv Funct Mater* **2008,** *18* (20), 3299-3306; (e) Choudhury, K. R.; Lee, J. W.; Chopra, N.; Gupta, A.; Jiang, X. Z.; Amy, F.; So, F., Highly Efficient Hole Injection Using Polymeric Anode Materials for Small-Molecule Organic Light-Emitting Diodes. *Adv Funct Mater* **2009,** *19* (3), 491-496; (f) Takizawa, S. Y.; Montes, V. A.; Anzenbacher, P., Phenylbenzimidazole-Based New Bipolar Host Materials for Efficient Phosphorescent Organic Light-Emitting Diodes. *Chem Mater* **2009,** *21* (12), 2452-2458.

[3] (a) Sariciftci, N. S.; Smilowitz, L.; Heeger, A. J.; Wudl, F., Photoinduced Electron-Transfer from a Conducting Polymer to Buckminsterfullerene. *Science* **1992,** *258* (5087), 1474-1476; (b) Yu, G.; Gao, J.; Hummelen, J. C.; Wudl, F.; Heeger, A. J., Polymer Photovoltaic Cells - Enhanced Efficiencies Via a Network of Internal Donor-Acceptor Heterojunctions. *Science* **1995,** *270* (5243), 1789-1791.

[4] (a) Hoppe, H.; Sariciftci, N. S., Organic solar cells: An overview. *J Mater Res* **2004,** *19* (7), 1924-1945; (b) Tang, C. W., 2-Layer Organic Photovoltaic Cell. *Appl Phys Lett* **1986,** *48* (2), 183-185; (c) Liu, P.; Li, Q.; Huang, M. S.; Pan, W. Z.; Deng, W. J., High open circuit voltage organic photovoltaic cells based on oligothiophene derivatives. *Appl Phys Lett* **2006,** *89* (21), 213501-213503; (d) Reyes-Reyes, M.; Kim, K.; Dewald, J.; Lopez-Sandoval, R.; Avadhanula, A.; Curran, S.; Carroll, D. L., Meso-structure formation for enhanced organic photovoltaic cells. *Org Lett* **2005,** *7* (26), 5749-5752.

[5] (a) Koyanagi, T.; Muratsubaki, M.; Hosoi, Y.; Shibata, T.; Tsutsui, K.; Wada, Y.; Furukawa, Y., Organic field-effect transistor based on a thin film of polydiacetylene prepared from 10,12-pentacosadiynoic acid. *Chem Lett* **2006,** *35* (1), 20-21; (b) Valiyev, F.; Hu, W. S.; Chen, H. Y.; Kuo, M. Y.; Chao, I.; Tao, Y. T., Synthesis and characterization of anthra[2,3-b]thiophene and tetraceno[2,3-b]thiophenes for organic field-effect transistor applications. *Chem Mater* **2007,** *19* (12), 3018-3026.

[6] (a) Drury, C. J.; Mutsaers, C. M. J.; Hart, C. M.; Matters, M.; de Leeuw, D. M., Low-cost all-polymer integrated circuits. *Appl Phys Lett* **1998,** *73* (1), 108-110; (b) arnier, F.; Hajlaoui, R.; El Kassmi, M., Vertical device architecture by molding of organic-based thin film transistor. *Appl Phys Lett* **1998,** *73* (12), 1721-1723; (c) Sirringhaus, H.; Tessler, N.; Friend, R. H., Integrated optoelectronic devices based on conjugated polymers. *Science* **1998,** *280* (5370), 1741-1744; (d) Li, X. C.; Sirringhaus, H.; Garnier, F.; Holmes, A. B.; Moratti, S. C.; Feeder, N.; Clegg, W.; Teat, S. J.; Friend, R. H., A highly pi-stacked organic semiconductor for thin film transistors based on fused thiophenes. *J Am Chem Soc* **1998,** *120* (9), 2206-2207; (e) Bao, Z. A.; Lovinger, A. J.; Brown, J., New air-stable n-channel organic thin film transistors. *J Am Chem Soc* **1998,** *120* (1), 207-208; (f) Bao, Z. N.; Lovinger, A. J., Soluble regioregular polythiophene derivatives as semiconducting materials for field-effect transistors. *Chem Mater* **1999,** *11* (9), 2607-2612.

[7] (a) Beaujuge, P. M.; Ellinger, S.; Reynolds, J. R., The donor-acceptor approach allows a black-to-transmissive switching polymeric electrochrome. *Nat Mater* **2008,** *7* (10), 795-799; (b) Li, M.; Sheynin, Y.; Patra, A.; Bendikov, M., Tuning the Electrochromic Properties of Poly(alkyl-3,4-ethylenedioxyselenophenes) Having High Contrast Ratio and Coloration Efficiency. *Chem Mater* **2009,** *21* (12), 2482-2488; (c) Li, M.; Patra, A.; Sheynin, Y.; Bendikov, M., Hexyl-Derivatized Poly(3,4-ethylenedioxyselenophene): Novel Highly Stable Organic Electrochromic Material with High Contrast Ratio, High Coloration Efficiency, and Low-Switching Voltage. *Adv Mater* **2009,** *21* (17), 1707-1711.

[8] Gonzalez-Tejera, M. J.; de la Blanca, E. S.; Carrillo, I., Polyfuran conducting polymers: Synthesis, properties, and applications. *Synthetic Met* **2008,** *158* (5), 165-189.

[9] (a) Murphy, A. R.; Frechet, J. M. J., Organic semiconducting oligomers for use in thin film transistors. *Chem Rev* **2007,** *107* (4), 1066-1096; (b) Takimiya, K.; Kunugi, Y.; Otsubo, T., Development of new semiconducting materials for durable high-performance air-stable organic field-effect transistors. *Chem Lett* **2007,** *36* (5), 578-583; (c) Sakamoto, Y.; Komatsu, S.; Suzuki, T., Tetradecafluorosexithiophene: The first perfluorinated oligothiophene. *J Am Chem Soc* **2001,** *123* (19), 4643-4644; (d) Facchetti, A.; Deng, Y.; Wang, A. C.; Koide, Y.; Sirringhaus, H.; Marks, T. J.; Friend, R. H., Tuning the semiconducting properties of sexithiophene by alpha,omega-substitution - alpha,omega-diperfluorohexylsexithiophene: The first n-type sexithiophene for thin-film transistors. *Angew Chem Int Edit* **2000,** *39* (24), 4547-4551; (e) Facchetti, A.; Mushrush, M.; Katz, H. E.; Marks, T. J., n-type building blocks for organic electronics: A homologous family of fluorocarbon-substituted thiophene oligomers with high carrier mobility. *Adv Mater* **2003,** *15* (1), 33-38; (f) Dholakia, G. R.; Meyyappan, M.; Facchetti, A.; Marks, T. J., Monolayer to multilayer nanostructural growth transition in N-type oligothiophenes on Au(111) and implications for organic field-effect transistor performance. *Nano Lett* **2006,** *6* (11), 2447-2455; (g) Ando, S.; Murakami, R.; Nishida, J.; Tada, H.; Inoue, Y.; Tokito, S.; Yamashita, Y., n-Type organic field-effect transistors with very high electron mobility based on thiazole oligomers with trifluoromethylphenyl groups. *J Am Chem Soc* **2005,** *127* (43), 14996-14997.

[10] (a) Hutchison, G. R.; Ratner, M. A.; Marks, T. J., Intermolecular charge transfer between heterocyclic oligomers. Effects of heteroatom and molecular packing on hopping transport in organic semiconductors. *J Am Chem Soc* **2005,** *127* (48), 16866-16881; (b) Takimiya, K.; Kunugi, Y.; Konda, Y.; Niihara, N.; Otsubo, T., 2,6-diphenylbenzo[1,2-b : 4,5-b ']dichalcogenophenes: a new class of high-performance semiconductors for organic field-effect transistors. *J Am Chem Soc* **2004,** *126* (16), 5084-5085; (c) Okamoto, T.; Kudoh, K.; Wakamiya, A.; Yamaguchi, S., General synthesis of thiophene and selenophene-based heteroacenes. *Org Lett* **2005,** *7* (23), 5301-5304.

[11] Djumanazarova, A. Z.; Litvinov, V. P.; Konar, A., Charge-Transfer Complexes of Some 5-Membered Condensed Heteroaromatic Systems with Tetracyanoethylene. *Chem Scripta* **1982,** *20* (5), 214-218.

[12] Kamada, K.; Ueda, M.; Sakaguchi, T.; Ohta, K.; Fukumi, T., Femtosecond optical Kerr study of heavy atom effects on the third-order optical nonlinearity of thiophene homologues: Purely electronic contribution. *Chem Phys Lett* **1996,** *263* (1-2), 215-222.

[13] Politis J. K., Nemes, J. C., Curtis, M. D., Synthesis and Characterization of Regiorandom and Regioregular Poly(3-octylfuran). *J. Am. Chem. Soc.* **2001**, *123*, 2537.

[14] The charge mobility of alternating furan/thiophene oligomers was studied by Kumatsu's group and mobility values similar to those of oligothiophenes were obtained. (a) Miyata, Y.; Nishinaga, T.; Komatsu, K., Synthesis and structural, electronic, and optical properties of oligo(thienylfuran)s in comparison with oligothiophenes and oligofurans. *J Org Chem* **2005,** *70* (4), 1147-1153; (b) Miyata, Y.; Terayama, M.; Minari, T.; Nishinaga, T.; Nemoto, T.; Isoda, S.; Komatsu, K., Synthesis of oligo(thienylfuran)s with thiophene rings at both ends and their structural, electronic, and field-effect properties. *Chem-Asian J* **2007,** *2* (12), 1492-1504.

[15] (a) Okada, M.; Tachikawa, K.; Aoi, K., Biodegradable polymers based on renewable resources. III. copolyesters composed of 1,4 : 3,6-dianhydro-D-glucitol, 1,1-bis(5-carboxy-2-furyl)ethane and aliphatic dicarboxylic acid units. *J Appl Polym Sci* **1999,** *74* (14), 3342-3350; (b) Gandini, A., Polymers from Renewable Resources: A Challenge for the Future of Macromolecular Materials. *Macromolecules* **2008,** *41* (24), 9491-9504.

[16] (a) Gidron, O.; Diskin-Posner, Y.; Bendikov, M., alpha-Oligofurans. *J Am Chem Soc* **2010,** *132* (7), 2148.

[17] (a) Horowitz, G.; Fichou, D.; Peng, X. Z.; Xu, Z. G.; Garnier, F., A Field-Effect Transistor Based on Conjugated Alpha-Sexithienyl. *Solid State Commun* **1989,** *72* (4), 381-384; (b) Garnier, F.; Yassar, A.; Hajlaoui, R.; Horowitz, G.; Deloffre, F.; Servet, B.; Ries, S.; Alnot, P., Molecular Engineering of Organic Semiconductors - Design of Self-Assembly Properties in Conjugated Thiophene Oligomers. *J Am Chem Soc* **1993,** *115* (19), 8716-8721; (c) Hajlaoui, R.; Fichou, D.; Horowitz, G.; Nessakh, B.; Constant, M.; Garnier, F., Organic transistors using alpha-octithiophene and alpha,omega-dihexyl-alpha-octithiophene: Influence of oligomer length versus molecular ordering on mobility. *Adv Mater* **1997,** *9* (7), 557; (d) Garnier, F.; Hajlaoui, R.; El Kassmi, A.; Horowitz, G.; Laigre, L.; Porzio, W.; Armanini, M.; Provasoli, F., Dihexylquaterthiophene, a two-dimensional liquid crystal-like organic semiconductor

with high transport properties. *Chem Mater* **1998,** *10* (11), 3334-3339; (e) Horowitz, G.; Hajlaoui, M. E., Mobility in polycrystalline oligothiophene field-effect transistors dependent on grain size. *Adv Mater* **2000,** *12* (14), 1046-1050.

[18] (a) Ortiz, R. P.; Casado, J.; Hernandez, V.; Navarrete, J. T. L.; Letizia, J. A.; Ratner, M. A.; Facchetti, A.; Marks, T. J., Thiophene-Diazine Molecular Semiconductors: Synthesis, Structural, Electrochemical, Optical, and Electronic Structural Properties; Implementation in Organic Field-Effect Transistors. *Chem-Eur J* **2009,** *15* (20), 5023-5039; (b) Seo, H. S.; Zhang, Y.; Jang, Y. S.; Choi, J. H., Performance and transport characteristics of alpha,omega-dihexylsexithiophene-based transistors with a high room-temperature mobility of 0.16 cm(2)/V s. *Appl Phys Lett* **2008,** *92* (22), 223310.

[19] Dodabalapur, A.; Torsi, L.; Katz, H. E., Organic Transistors - 2-Dimensional Transport and Improved Electrical Characteristics. *Science* **1995,** *268* (5208), 270-271.

[20] Dimitrakopoulos, C. D.; Furman, B. K.; Graham, T.; Hegde, S.; Purushothaman, S., Field-effect transistors comprising molecular beam deposited alpha,omega-di-hexyl-hexathienylene and polymeric insulator. *Synthetic Met* **1998,** *92* (1), 47-52.

[21] Fichou, D., Structural order in conjugated oligothiophenes and its implications on opto-electronic devices. *J Mater Chem* **2000,** *10* (3), 571-588.

[22] Horowitz, G.; Hajlaoui, R.; Fichou, D.; El Kassmi, A., Gate voltage dependent mobility of oligothiophene field-effect transistors. *J Appl Phys* **1999,** *85* (6), 3202-3206.

[23] Hajlaoui, R.; Fichou, D.; Horowitz, G.; Nessakh, B.; Constant, M.; Garnier, F., Organic transistors using alpha-octithiophene and alpha,omega-dihexyl-alpha-octithiophene: Influence of oligomer length versus molecular ordering on mobility. *Adv Mater* **1997,** *9* (7), 557-561.

[24] Garnier, F.; Yassar, A.; Hajlaoui, R.; Horowitz, G.; Deloffre, F.; Servet, B.; Ries, S.; Alnot, P. Molecular Engineering of Organic Semiconductors: Design of Self-assembly Properties in Conjugated Thiophene Oligomers. *J. Am. Chem. Soc.* **1993**, *115*, 8716–8721.

[25] (a) Murphy, A. R.; Frechet, J. M. J., Organic semiconducting oligomers for use in thin film transistors. *Chem Rev* **2007,** *107* (4), 1066-1096.

[26] M. Halik, H. Klauk, U. Zschieschang, G. Schmid, S. Ponomarenko, S. Kirchmeyer, W. Weber, Relationship Between Molecular Structure and Electrical Performance of Oligothiophene Organic Thin Film Transistors. *Adv. Mater.* **2003**, *15,* 917.

[27] (a) Capelli, R.; Toffanin, S.; Generali, G.; Usta, H.; Facchetti, A.; Muccini, M., Organic light-emitting transistors with an efficiency that outperforms the equivalent light-emitting diodes. *Nat Mater* **2010,** *9* (6), 496-503. (b) Cicoira, F.; Santato, C., Organic light emitting field effect transistors: Advances and perspectives. *Adv Funct Mater* **2007,** *17* (17), 3421-3434.

[28] (a) Hepp, A.; Heil, H.; Weise, W.; Ahles, M.; Schmechel, R.; von Seggern, H., Light-emitting field-effect transistor based on a tetracene thin film. *Phys Rev Lett* **2003,** *91* (15), *91*, 157406; (b) Cicoira, F.; Santato, C.; Dadvand, A.; Harnagea, C.; Pignolet, A.; Bellutti, P.; Xiang, Z.; Rosei, F.; Meng, H.; Perepichka, D. F., Environmentally stable light emitting field effect transistors based on 2-(4-pentylstyryl)tetracene. *J Mater Chem* **2008,** *18* (2), 158-161.

[29] Herasimovich, A.; Scheinert, S.; Horselmann, I., Influence of traps on top and bottom contact field-effect transistors based on modified poly(phenylene-vinylene). *J Appl Phys* **2007,** *102* (5), 054509 and refs therein.

[30] Minari, T.; Nemoto, T.; Isoda, S., Temperature and electric-field dependence of the mobility of a single-grain pentacene field-effect transistor. *J Appl Phys* **2006,** *99* (3), 034506.

[31] Seo, H. S.; Zhang, Y.; Jang, Y. S.; Choi, J. H., Performance and transport characteristics of alpha,omega-dihexylsexithiophene-based transistors with a high room-temperature mobility of 0.16 cm^2/Vs. *Appl Phys Lett* **2008,** *92* (22), 223310.

[32] Horowitz, G.; Hajlaoui, R.; Bourguiga, R.; Hajlaoui, M., Theory of the organic field-effect transistor. *Synthetic Met* **1999,** *101* (1-3), 401-404.

CHAPTER 4

Fused Oligothiophenes*

Conjugated oligomers and based on aromatic and heteroaromatic moieties have attracted considerable attention as the most viable materials for OTFTs. Among these, linear acenes and oligothiophenes are the two most studied classes of OSCs to date.[1,2] The charge carrier mobility in organic materials generally increases with the extention of conjugation. For example, hole mobilities (μ_h) of 0.12 cm^2/Vs and 3.0 cm^2/Vs have been reported for thin films of tetracene (**2**)[2] and pentacene (**3**),[3] respectively, whereas no discernable mobility has been observed for thin films of anthracene (**1**). Unfortunately, an increased conjugation length is often associated with decreased stability, predominantly because of the significantly raised HOMO in these molecules. It is interesting to mention that in aromatic hydrocarbon OSCs, the change of the connection between the benzene ring from linear (oligophenylenes) to fused (oligoacenes) structure results in substantial increase of conjugation and charge carrier mobility and chemical instability, particularly towards oxidation.[4] Thus, pentacene, the current benchmark semiconductor for OTFTs, is a very reactive molecule, so as non-encapsulated devices should be measured and even stored under inert atmosphere, to avoid degradation. At the same time, fused thiophene oligomers seem to enjoy an increased stability in comparison with linearly linked structures, together with a more efficient conjugation.[5] In recognition of this fact, a significant focus in organic materials research was lately given to synthesis and device studies of fused thienothiophene and benzothiophene derivatives. Bis(dithienobenzene) **4** represents one of the earliest reports of an air stable organic semiconductor which exhibited reasonable thin film mobility (0.04 cm^2/Vs).[6] Similar

* Parts of this chapter are published in: (a) Brusso, J. L.; Hirst, O. D.; Dadvand, A.; Ganesan, S.; Cicoira, F.; Robertson, C. M.; Oakley, R. T.; Rosei, F.; Perepichka, D. F., Two-dimensional structural motif in thienoacene semiconductors: Synthesis, structure, and properties of tetrathienoanthracene isomers. *Chem Mater* **2008,** *20*, 2484-2494. (b) Dadvand, A.; Cicoira, F.; Chernichenko, K. Y.; Balenkova, E. S.; Osuna, R. M.; Rosei, F.; Nenajdenko, V. G.; Perepichka, D. F., Heterocirculenes as a new class of organic semiconductors. *Chem Commun* **2008,** 5354-5356.

results were obtained from the fully heterocyclic bis(dithienothiophene) **5** in which thin film devices exhibited mobilities of 0.05 cm^2/Vs.[7] More recently, remarkable thin-film mobilities of μ_h = 0.4 cm^2/Vs and even ~2.0 cm^2/Vs for related diphenyl(dithienothiophene) **6**[8] and diphenyl(dibenzothienothiophene) **7**,[9] respectively, have been reported.

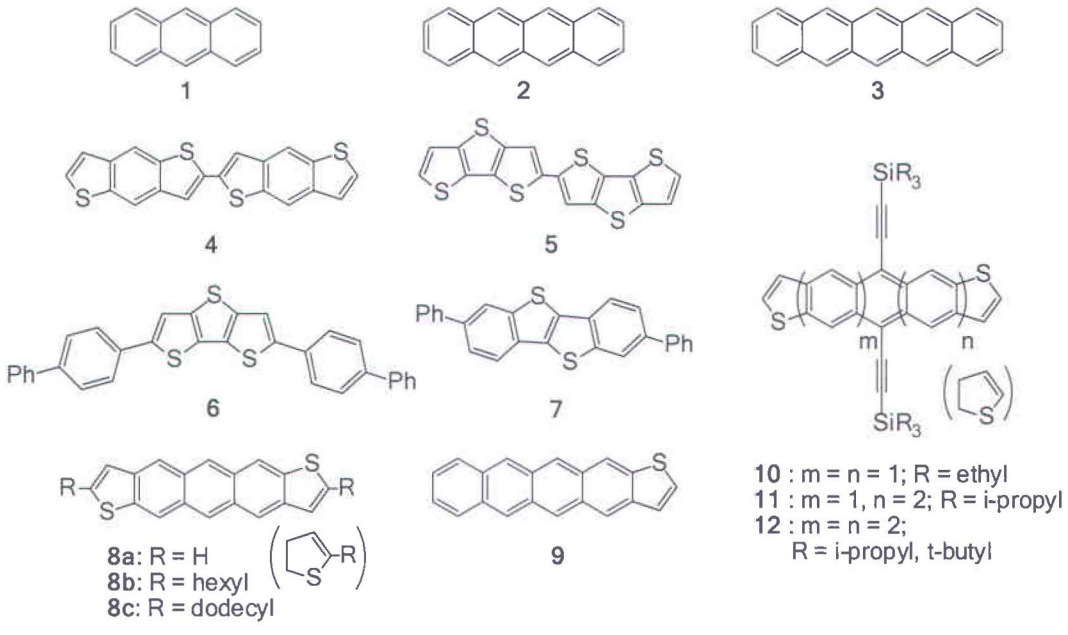

Scheme 4.1. Chemical structure of fused oligoacenes and oligothiophenes

Combining thiophene and oligoacene building blocks has been another extensively studied approach in design of OSCs. Substantial hole mobilities in OTFT devices have been demonstrated for a series of dithienoanthracenes **8** ($\mu_h \sim 10^{-1}$ cm^2/Vs),[10] monothienotetracenes **9** ($\mu_h \sim 10^{-1}$ cm^2/Vs),[11] and trialkylsilyl acetylene functionalized dithienoanthracene **10** ($\mu_h \sim 1.0$ cm^2/Vs).[12] However, further extension of the conjugation, as in dithienotetracene **11**, resulted in rather low mobility ($\mu_h \sim 10^{-5}$ cm^2/Vs) and no transistor function was found in dithienopentacene derivatives **12**.[2c,13] The difficulties in separation of these anti- and syn- isomers in dithienoacene structures **10–12**, and also lower stability for longer dithienoacenes, could be responsible for their poor performance.

Remarkably, in most cases, modulation of the conjugation in OSC molecules was attained through a linear (1D) elongation of the molecule. Much less is known about the effect of the 2D conjugation extension on the properties of molecular semiconductors. One could expect that for 2D aromatic molecules, the packing in the solid state should favor $\pi\cdots\pi$ stacks vs

π···H–C herringbone packing, common for linear oligoacene and thiophene oligomers.[14] Important examples of such molecules include hexa-peri-hexabenzocoronenes,[15] supertriphenylene,[16] and phthalocyanines.[17]

In this chapter, we set to answer some of the questions regarding the structure-property relationships and solid state packing tendencies of 2D conjugated fused systems through studies of the fused heteroaromatic isomers of tetrathienoanthracene and heterocirculenes.

4.1 A New Structural Motif in Thienoacene Semiconductors: Structure and Properties of Tetrathienoanthracene Isomers

In this section, the structure-property of the fused heteroaromatic isomers of **13** and **14** will be studied. It was of particular interest to see if and how the position of a heteroatom in the heteroacene structure (two isomeric parent tetrathienoanthracenenes **13a** and **14a** and their hexylated derivatives **13b** and **14b**) affects the molecular properties and solid state packing. The comparative studies of their electronic properties by UV-visible and fluorescence spectroscopy reveal an important role of the position of the sulfur atoms. The semiconducting properties of the two isomeric hexylated compounds **13b** and **14b** are studied as active layer in OTFT configuration.

Scheme 4.2

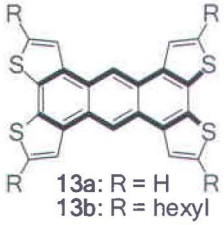

13a: R = H
13b: R = hexyl

14a: R = H
14b: R = hexyl

Thermogravimetric analysis (TGA) revealed very high stability of compounds **13b** and **14b**, with onset decomposition temperatures, T_{dec} of ~400 °C in air. The same experiment under nitrogen showed no decomposition until sublimation of the compounds at 450–500 °C. Such a remarkable stability (for thiophene derivatives) is particularly important for application of these compounds in OTFTs, where the stability of organic semiconductors is still a major limitation.

Absorption and emission spectroscopy: UV-Vis spectra of DCM solutions of **13** and **14** reveal a strong absorption band at ~300–350 nm and a weaker band at ~350–450 nm, both with pronounced vibronic structure, characteristic of rigid acene molecules (Table 4.1 and Figure 4.1). A large bathochromic shift of ~30 nm is observed between the isomeric structures **13** and **14** (where R = H or hexyl) which is attributed to longer "effective conjugation" of **13** vs. **14**. Indeed, the electronic structure of oligoacenes, although having many features of an aromatic system, can also be represented as two bridged polyene chains.[18] Thus, fusion of the thiophene units to anthracene as in **14** extends the conjugation by two double bonds, while in **13** the conjugation formally is only extended by the lone pairs of the sulfur atoms (shown as bold lines in scheme 3). While this is certainly an oversimplified approach, the expected trend is also predicted by Density Functional Theory (DFT) calculations showing lower HOMO-LUMO gaps for **14** and supported by experimental observations (Table 4.1).

Table 4.1. Theoretical[a] and photophysical properties for **13** and **14**.

	E_{HOMO}^{calc} [eV]	E_g^{calc} [eV]	$E_{HOMO}^{electrochem.}$ [eV]	λ_{max}^{abs} [nm][b]	E_g^{opt} [eV][c]	λ_{max}^{PL} [nm][d]	Stokes shift [eV]
13a	-5.14	3.52	-6.22	379	3.27	398	0.16
13b	-4.83[g]	3.37[g]	-5.91	405	3.06	421	0.12
14a	-5.23	3.50	-6.69	414	2.97	422	0.03
14b	-4.92[g]	3.40[g]	-5.95	428	2.90	436	0.05

[a] DFT/B3LYP/6-31G(2d,p) level of theory. [b] In DCM. [c] Calculated from λ_{max} of the longest wavelength transition in the absorption spectrum. [d] In DCM, upon excitation at 370 nm for **13** and 324 nm for **14**

The trends noted in the absorption spectra were also observed in the emission spectra with bathochromic shifts between **13** and **14** as well as between the respective unsubstituted (R = H) and substituted (R = hexyl) derivatives. Furthermore, increased photoluminescence quantum yields were obtained for **14** vs. **13**. The Stokes shifts of the fluorescence band were rather low and they were lower for the isomer **14** (0.03–0.05 eV) than for the isomer **13** (0.12–0.16 eV), which is in agreement with the longer effective conjugation in **14**. These numbers compare very favorably to typically large Stoke shifts of linear oligothiophenes (0.61 eV for quaterthiophene)[19] and even fused thienoacenes (0.28 eV for pentathienoacene),[19] although even lower Stoke shifts are observed for homo-acenes (0.02 eV for anthracene under the same conditions). The low Stokes shifts are indicative of a small structural difference between the excited and ground states

and also strongly suggest that the reorganization energy of the charge carrier (polaron or radical cation), which limits the intrinsic mobility of organic semiconductors, will be low.

The photophysical properties of drop-cast films of **13b** and **14b** were investigated and compared with that in solution. As expected, the absorption and emission spectra are bathochromically shifted (by 9 nm for absorption and by 64-69 nm for emission). Also, the peaks become broader and the vibronic structure is almost completely lost (Figure 4.2).

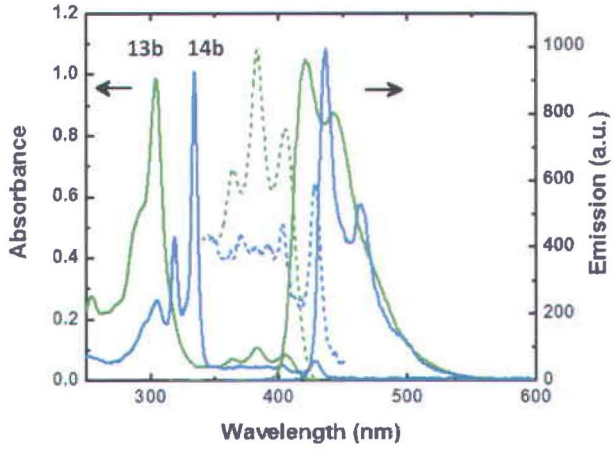

Figure 4.1: Absorption and emission spectra of **13b** (green line) and **14b** (blue line). The long-wavelength region of the absorbance spectra is shown enlarged (×10, dashed lines)

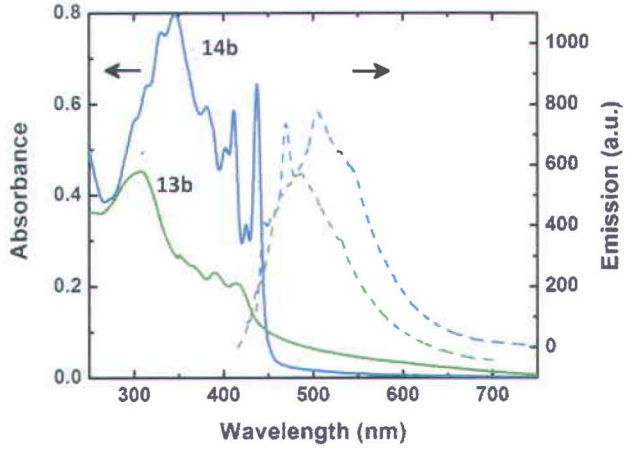

Figure 4.2: Absorption (solid line) and emission (dotted line) spectra of drop-cast films of **13b** (green line) and **14b** (blue line).

X-ray crystallography: Long-range molecular ordering is of paramount importance to obtain high charge mobilities in OSCs. In particular, the amount of π-orbital overlap is expected to have a strong influence on the mobility, as has been recently illustrated in structurally related pentacene derivatives.[20] To shed light on supramolecular organization, the crystal structures of **13a** and **14a**

have been determined by single crystal X-ray diffraction (Table 4.2). Crystals of **13a** and **14a** consist of slipped π-stacks (along *y*) which are aligned into herringbone arrays running along the *z*-direction. The molecules are completely planar, despite the slight steric strain due to interaction between the hydrogen of the central anthracene ring with the hydrogen of the thiophene (2.30 Å) for **13a** and with sulfur (2.80 Å) for **14a**. Two views of the crystal structure, showing the unit cell packing and the π-stacked structures, are provided in Figure 4.3. Such packing is similar to that found in most linear (hetero)acenes and their derivatives. However, the "wider" conjugation framework of **13a** and **14a** still provides for close π···π contacts (3.388(3) Å and 3.354(3) Å, respectively) within the slipped stack. Moreover, for compound **13a** the intermolecular interaction within these π-stacked arrays and between the stacks is reinforced by close intermolecular S···S contacts (3.635(1) Å, 3.719(1) Å and 3.773(1) Å). Among these, only one contact (3.635 Å) is slightly lower than double the van-der-Waals radius of sulfur (3.68 Å).[21] The only S···S contacts observed in the crystal structure of **14a** was 3.769 (1) Å.

Growing quality single crystals of hexylated molecules **13b** and **14b** was not successful. However, considering that the sulfur atoms in the isomer **13** are more exposed than in **14** (where they are almost buried inside the molecule) one could expect more (if any) intermolecular S···S contacts in the hexylated isomer **13b** as compared to **14b**. XRD patterns of both films of **13b** and **14b** grown on glass substrate at room temperature are highly crystalline which can lead to decent charge mobility in OTFT configuration (Figure 4.4).

Table 4.2. Crystal data and intermolecular contacts.

Compound	**13a**	**14a**
a (Å)	12.3815 (14)	11.2784 (24)
b (Å)	5.2570 (6)	5.0330 (11)
c (Å)	12.7975 (15)	14.3066 (31)
β (deg)	97.753 (2)	92.006 (4)
S1 - S1' (Å)	3.635(1)	---
S2 - S2' (Å)	3.719(1)	3.769 (1)
S1 - S2' (Å)	3.773(1)	---

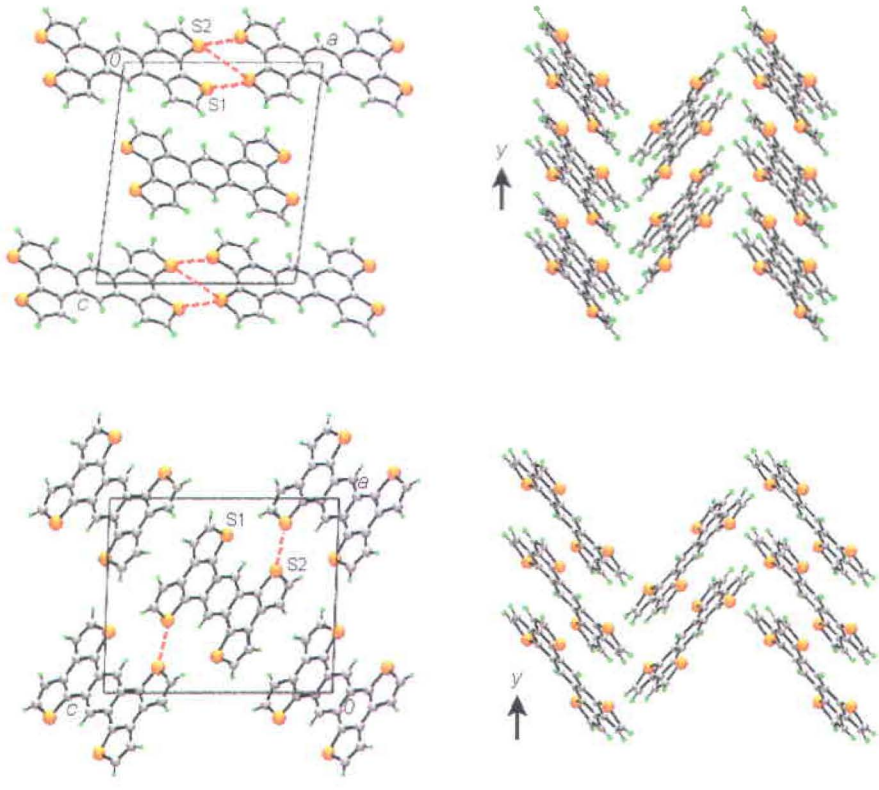

Figure 4.3: Unit cell (left) and slipped π-stack (right) drawings of **13a** (top) and **14a** (bottom). Intermolecular S···S' contacts are defined in Table 4.2.

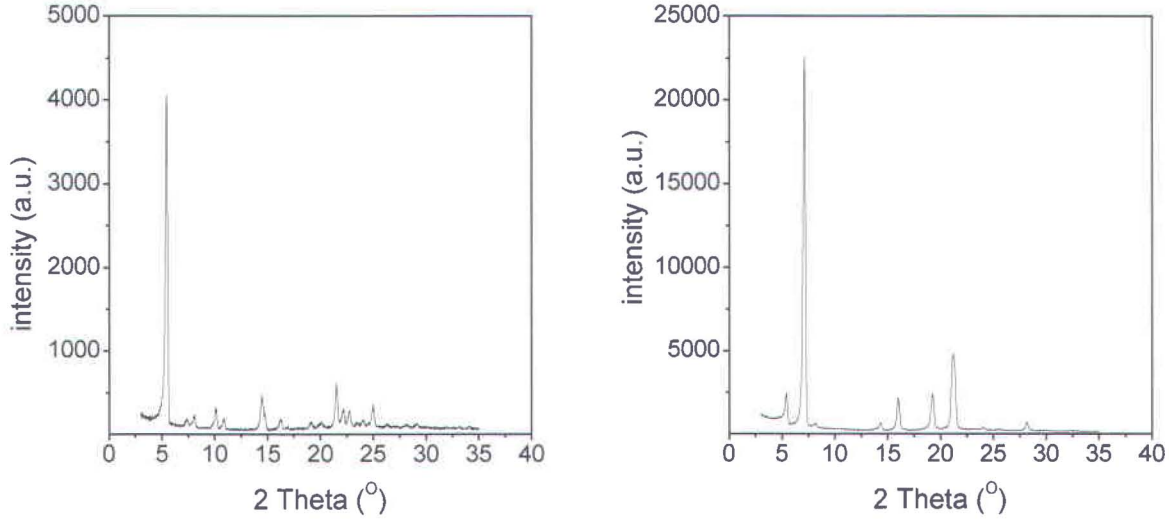

Figure 4.4: XRD patterns of (left) **13b** and (right) **14b** are presented. Films grown on glass substrate at room temperature (thickness~200 nm, deposition rate=1 Å/s)

Fabrication of thin-film transistors: OTFTs were prepared in bottom-contact configuration by vacuum deposition and drop-casting from chlorobenzene solution. The unsubstituted tetrathienoanthracene **13a** showed no transistor behavior, presumably due to poor quality of the films. **14a** was not tested due to the amount of available pure material. However, pronounced hole mobilities were found for the hexylated derivatives **13b** and **14b**, in both vacuum-deposited and solution-casted films. The transistor output and transfer characteristics are shown in the Figure 4.5 and the data are summarized in Table 4.3. Keeping the substrate temperature at 75 °C during the deposition improves the order in the films, resulting in a substantial increase of the hole mobility (one orders of magnitude).

Table 4.3. FET characteristics of **13b** and **14b**.

	Drop-cast[a]			Vacuum-sublimed[b]		
	μ_h (cm^2/Vs)	On/Off	V_T (V)	μ_h (cm^2/Vs)	On/Off	V_T (V)
13b	3.5×10^{-3}	10^4	-18	7.4×10^{-2}	10^8	-33
14b	2.5×10^{-4}	10^4	-25	1.9×10^{-2}	10^6	-30

[a] Annealed as described above. [b] Evaporated on a substrate kept at 75°C.

Vacuum-deposited films reveal field-effect mobilities of 7.4×10^{-2} cm^2/Vs and 2.0×10^{-2} cm^2/Vs, for **13b** and **14b**, respectively. While the mobilities of $\leq 10^{-1}$ cm^2/Vs are certainly far from the highest values observed in OSCs, the on-off ratio observed for vacuum-deposited **13b** (10^8) is very remarkable. Pentacene OTFTs prepared under identical conditions show a mobility of $\sim2\times10^{-1}$ cm^2/Vs and it is expected that higher mobility values can be obtained upon device optimization (top-contact configuration, optimized deposition conditions, SiO_2 modification with organic monolayers, etc.).

For solution processed films, an increased order can be achieved by rapid (several seconds) heating to the melting point. Although the prepared films are quite rough, even upon optical microscopy inspection, they are also highly crystalline. The best saturated hole mobilities were 3.5×10^{-3} cm^2/Vs for **13b** and 2.5×10^{-4} cm^2/Vs for **14b**, with an on-off ration $\sim10^4$ for both.

In both solution-processed and vacuum-deposited films, isomer **13b** showed higher hole mobility than **14b**. This is, however, in contrast with the lower reorganization energy (Stoke shift) and HOMO-LUMO gaps of **14b**.

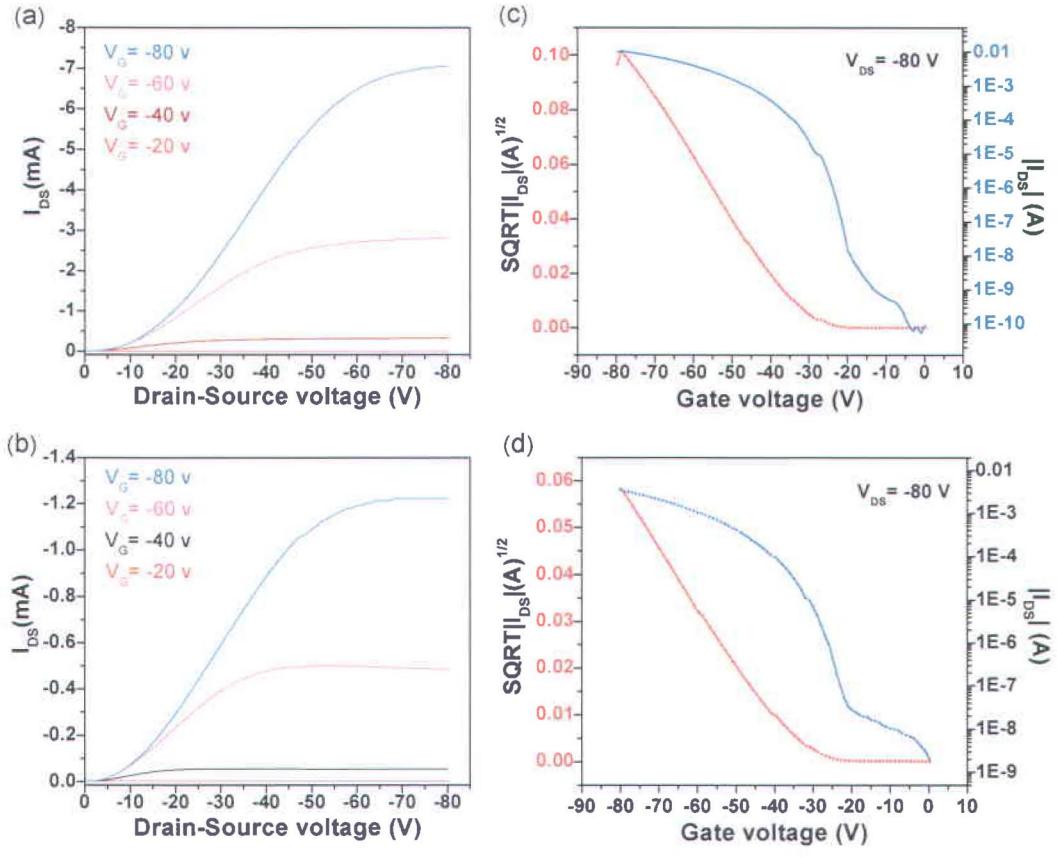

Figure 4.5: Output (a,b) and transfer (c,d) characteristics of compound **13b** (top) and **14b** (bottom) vacuum-sublimed on SiO_2/Si substrates pre-patterned with circular Au source and drain electrodes (W/L=42000/6 (μm/μm)). I_{DS} is the drain/source current, and V_{DS} and V_G are the drain/source and the gate/source voltage, respectively.

4.2 Heterocirculenes as a new class of organic semiconductors

Circulenes are an interesting class of polyaromatics which are built from arenes annulated into macrocycles.[22] Coronene is the only planar benzenoid circulene that has been used as a building block for surface nanotemplates and sensor fabrication.[23]

The higher symmetry of such molecules (as compared to linear structures) is potentially more favorable for solid state packing, although a practical advantage of this property is yet to be demonstrated. No OFETs have been reported for the parent circulene, coronene **15**, although discotic liquid crystalline derivatives of π-extended hexabenzocoronene have been employed as semiconductors in OFETs and photovoltaic cells and showed a hole mobility of up to 10^{-3} cm^2/Vs.[24] In the condensed state, coronene and its derivatives form π-stacked columns with strong electronic coupling (and facile charge transport) along the column, but little or no electronic communication between the columns, which is responsible for pronounced one-dimensional charge transport.[24]

Scheme 4.3

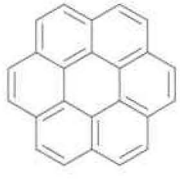

15

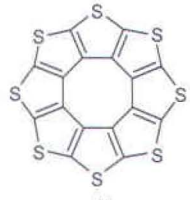

16

17

Introducing heteroatoms, such as S or Se, on the periphery of the circulene core, can induce intercolumnar interactions and, possibly, improve the charge-carrier mobility in such OSCs. The first all-heterocyclic octathio[8]circulene **16** (sulflower) has been recently synthesized.[25] Sulflower can also be considered as a fused oligothiophene, thus establishing a structural similarity with oligothiophenes **5-7**.[26]

X-ray crystallographic analysis confirms that sulflower is a flat molecule while their smaller and larger homologues form bowl-shape or saddle-shape curvatures.[26] In the solid state, sulflower shows tilted stacks with strong π–π interactions with a interplane distance 3.5-3.6 Å. Each column of sulflower is surrounded by six other neighboring columns, resulting in numerous close S-S contacts, 3.2–3.3 Å; considering the van der Waals radii (vdW) of S...S ~3.8 Å (Figure 4.6). The strong intermolecular interaction and the packing mode of sulflower molecules make it an interesting candidate material for OTFT application.

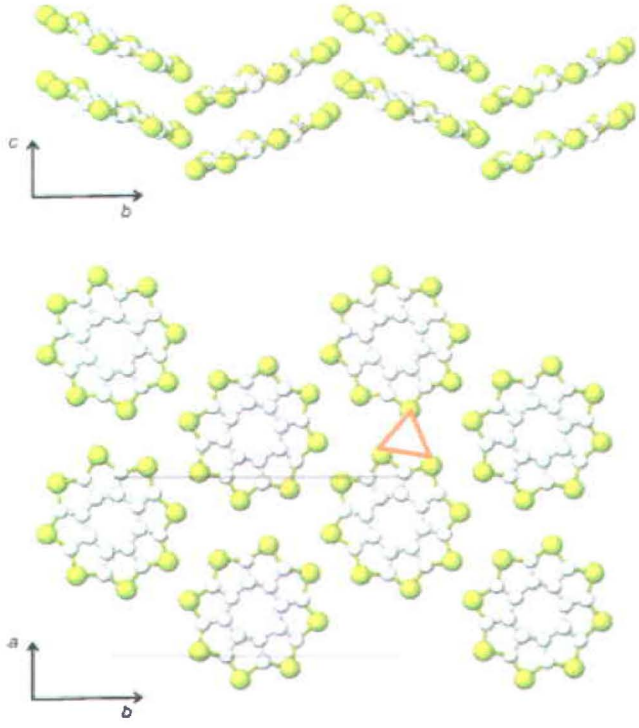

Figure 4.6: crystal structure of sulflower[25] **16**

This work demonstrates the applicability of **16** and its selenium analogue tetraselenotetrathio[8]circulene **17** (selenosulflower)[27] as OSCs by successfully fabricating organic thin film transistors with these materials. Both compounds **16** and **17** show a remarkable thermal and chemical stability in accordance with a large HOMO-LUMO gap (>4 eV) and rather low HOMO (<–5 eV).[25,27] According to density functional theory (DFT) calculations at B3LYP/6-31G(d,p) level, the HOMOs are at –5.7 eV and –5.2 eV for **16** and **17**, respectively. TGA of compounds **16** and **17** showed very high thermal stability, with onset decomposition temperatures of >400 °C in air (Figure 4.7).

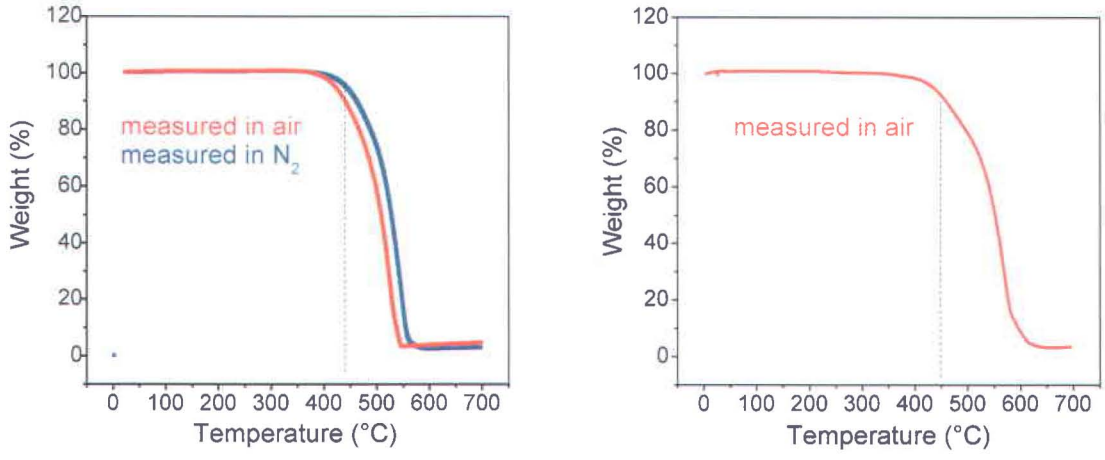

Figure 4.7: TGA of (left) sulflower and (right) selenosulflower

Fabrication of thin-film transistors: Thin films of heterocircuclenes **16** and **17** were prepared by vacuum deposition on SiO_2/Si substrates pre-patterned with Au circular electrodes.[28] The performance of the resulting OFETs was measured in a nitrogen atmosphere and the output and transfer characteristics are displayed in Figure 4.8 and summarized in Table 4.4.

Table 4.4: OFET characteristics of sulflower **16** and selenosulflower **17** films fabricated at room temperature

Compound	μ_h (cm^2/Vs)	V_T (V)	on/off
Sulflower, **16**	9×10^{-3}	-45	10^6
Selenosulflower, **17**	1×10^{-3}	-10	10^6

OFETs with sulflower **16** as OSC showed a hole field effect mobility and on/off current ratio of about 9×10^{-3} cm^2/Vs and 10^6, respectively. A rather high threshold voltage, ranging from –40 V to –46 V was measured for these devices. This can be explained by the very low HOMO of **16** (–5.7 eV, see above) and the resulting hole injection barrier into the Au electrode (workfunction –5.1 eV). Selenosulflower **17** OFETs showed a lower mobility of about 1×10^{-3} cm^2/Vs albeit with much lower threshold voltage of –10 V, in accordance with the higher HOMO of **17** (–5.2 eV). High device stability and on/off ratio were also observed for this OSC. The optimization efforts by changing the substrate temperature (20–130 °C) during deposition showed no increase in hole mobility (Table 4.5).

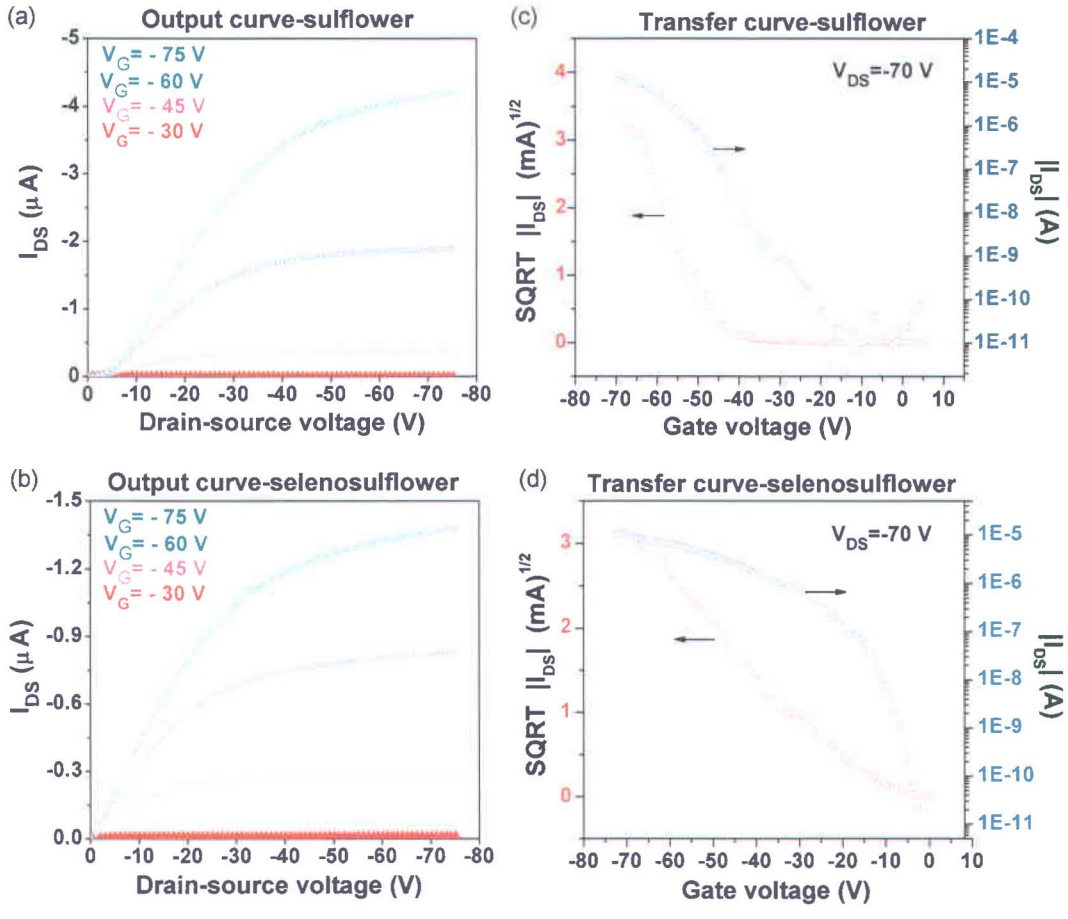

Figure 4.8: (a) and (b): output characteristics of bottom-contact OFET of **16** and **17**, respectively; (c) and (d): transfer characteristics of the same devices (**16** and **17**, respectively). Deposition rate 0.2 Å/s, nominal thickness ~ 36 nm, W/L=1880/6 μm/μm). I_{DS} is the drain/source current, and V_{DS} and V_G are the drain/source and the gate/source voltage, respectively.

Table 4.5: OFET characteristics of selenosulflower **17** films fabricated at different substrate temperature

Temperature (Ċ)	μ_h (cm^2/Vs)	V_T (V)	on/off
25	1×10^{-3}	-10	10^6
55	2×10^{-4}	-26	10^6
75	1×10^{-4}	-18	10^6
90	3×10^{-4}	-26	10^6
125	9×10^{-5}	-32	10^6

The lower mobility of selenosulflower **17** vs. sulflower **16** is surprising. The more polarizable selenium atoms are generally expected to provide for stronger intermolecular interactions as evidenced by increased conductivity and charge mobility, and reduced band gap in selenium-containing molecular solids and polymers, as compared to their sulfur analogues.[29,30] X-ray diffraction (XRD) patterns for the vacuum deposited films of **16** and **17** show characteristic reflections at the same angles as those obtained from the single crystal X-ray structure of these compounds (Figure 4.9). The strongest XRD peaks for **16** and **17** are at a *d*-spacing of 3.52 Å and 3.61 Å, respectively, which correspond to the π-stacking interaction in these solids. The sharper and higher intensity XRD peaks of **16** (ca. 0.25°) vs. **17** (ca. 0.5°) infer better crystallinity of its films, which might partially explain the higher hole mobility.

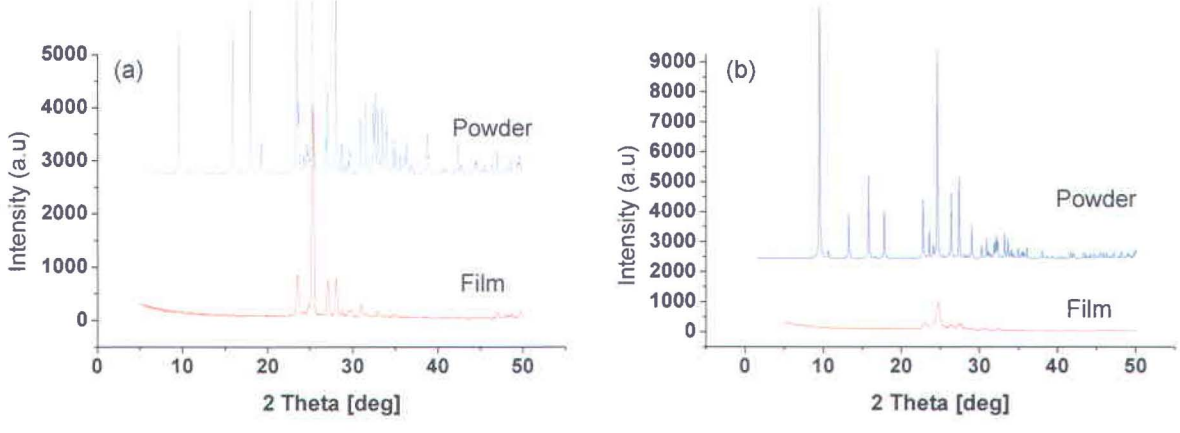

Figure 4.9: XRD patterns of (a) sulflower **16** and (b) selenosulflower **17** are presented. FWHM-XRD and *d*-spacing values of the strongest peaks for sulflower and selenosulflower are 0.2755 and 0.51, 3.52 Å and 3.61 Å, respectively. Films grown on glass substrate at room temperature (thickness ~200nm, deposition rate =1 Å/s)

Thin film morphology: The largest difference, however, was observed in the morphology of vacuum deposited films of **16** and **17**, as revealed by atomic force microscopy (AFM). The sulflower exhibits pronounced one-dimensional growth morphology (Figure 4.10). At very low coverage (Figure 4.10a) randomly-oriented joint needles with an average area of 12000 nm^2 and an average height of ca. 10-12 nm were observed. As the substrate coverage and grain size increases (Figure 4.10b), the grains keep growing one-dimensionally and the needle density increases. When the growing needles coalesce, continuing this linear growth

is no longer possible, and they start growing perpendicularly to the substrate (Figure 4.10 c). This growth mode hampers the formation of a continuous film directly on the surface of a dielectric, thus limiting the charge mobility. Films of **17** follow a different growth mode compared to the **16**. The early stages growth of **17** involve the nucleation of much smaller grains compared with the **16**, with a round shape (area ~1200 nm^2 and 2-5 nm height, Figure 4.10d). As the deposition time increases, the grains continue growing in the direction perpendicular to the substrate (height 6-14 nm), and their density increases (Figure 4.10e). Thus, no substantial lateral growth of the grains is observed, resulting in a large number of grain boundaries, and negatively affecting the charge mobility. Such unfavorable growth is caused by the very low energy of molecule-surface interactions as compared to molecule-molecule interactions this can be tuned by modifying the surface with organic monolayers, however, our preliminary experiments with hexamethyldisilazane-modified SiO_2/Si surfaces showed no significant change in the growth mode.

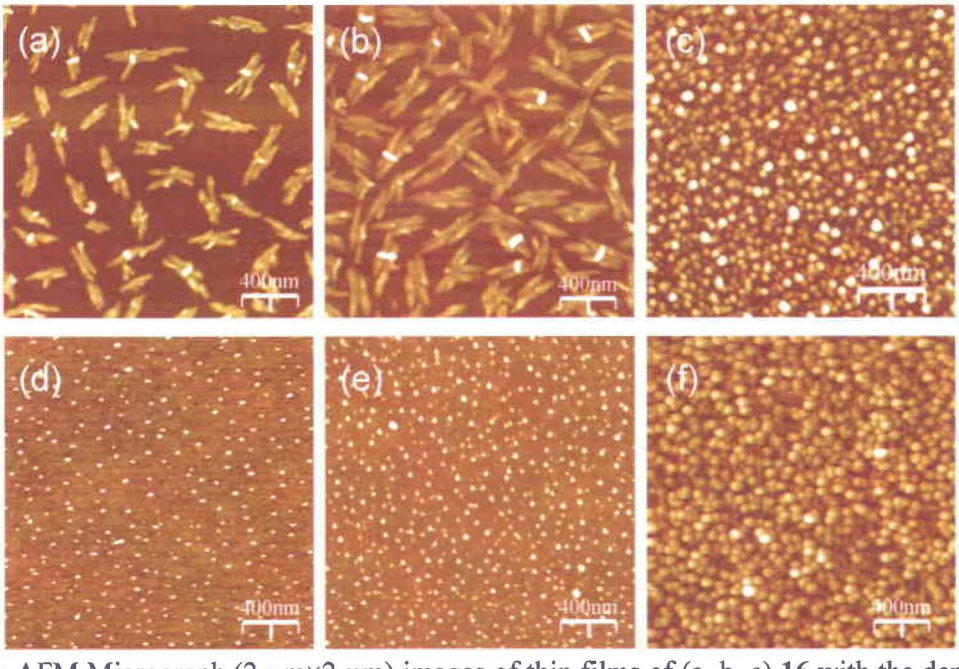

Figure 4.10: AFM Micrograph (2 μm×2 μm) images of thin films of (a, b, c) **16** with the deposition time of 1, 2, and 10 min, respectively; (d, e, f) **17** with the deposition time of 1, 2, and 8 min, respectively. Films grown on SiO_2/Si substrate at room temperature (deposition rate 0.2 Å/s)

Conclusion: This chapter demonstrates that the 2D extension of the conjugation through ring fusion is a viable approach to design novel OSCs with very high stability. Despite very large HOMO-LUMO of studied OSCs in this work, ~3.5 eV for TTA derivatives and >4eV for circulenes, they can be used as active semiconducting layer in OFET configuration. In line with a high HOMO-LUMO gap, TGA results reveal an exceptional thermal stability of all compounds in air.

TTA derivatives present a particular convenient building block to access a variety of related semiconducting molecules through substitution at the thiophene α-position. The OFET characteristics of the compounds can also be improved through different device preparation.

This chapter also presents the first demonstration of a heterocirculene acting as a semiconductor. The observed field-effect mobility of circulenes, however, is most likely limited by the one-dimensional growth mode of molecules in thin films which results in a very high density of grain boundaries. In line with the previous studies in chapter 3 on the contributions of chalcogen atoms into the electronic structure of conjugated OSCs, heavier chalcogene atoms have no obvious effect on the enhancement of conductivity and charge mobility. This chapter can provide valuable information toward the rational design of semiconducting materials based on 2D π–conjugated system.

References

[1]Facchetti, A.; Yoon, M. H.; Stern, C. L.; Hutchison, G. R.; Ratner, M. A.; Marks, T. J., Building blocks for N-type molecular and polymeric electronics. Perfluoroalkyl- versus alkyl-functionalized ligothiophenes (nTs; n=2-6). Systematic synthesis, spectroscopy, electrochemistry, and solid-state organization. *J Am Chem Soc* **2004,** *126* (41), 13480-13501.

[2] Gundlach, D. J.; Nichols, J. A.; Zhou, L.; Jackson, T. N., Thin-film transistors based on well-ordered thermally evaporated naphthacene films. *Appl Phys Lett* **2002,** *80* (16), 2925-2927.

[3] Kelley, T. W.; Boardman, L. D.; Dunbar, T. D.; Muyres, D. V.; Pellerite, M. J.; Smith, T. Y. P., High-performance OTFTs using surface-modified alumina dielectrics. *J Phys Chem B* **2003,** *107* (24), 5877-5881.

[4] Reddy, A. R.; Bendikov, M., Diels-Alder reaction of acenes with singlet and triplet oxygen theoretical study of two-state reactivity. *Chem Commun* **2006,** (11), 1179-1181.

[5] (a) Lee, K.; Sotzing, G. A., Poly(thieno[3,4-b]thiophene). A new stable low band gap conducting polymer. *Macromolecules* **2001,** *34* (17), 5746-5747. (b) Lee, B.; Yavuz, M. S.; Sotzing, G. A., Poly(thieno[3,4-b]thiophene)s from three symmetrical thieno[3,4-b]thiophene dimers. *Macromolecules* **2006,** *39* (9), 3118-3124.

[6] Laquindanum, J. G.; Katz, H. E.; Lovinger, A. J.; Dodabalapur, A., Benzodithiophene rings as semiconductor building blocks. *Adv Mater* **1997,** *9* (1), 36

[7] Li, X. C.; Sirringhaus, H.; Garnier, F.; Holmes, A. B.; Moratti, S. C.; Feeder, N.; Clegg, W.; Teat, S. J.; Friend, R. H., A highly pi-stacked organic semiconductor for thin film transistors based on fused thiophenes. *J Am Chem Soc* **1998,** *120* (9), 2206-2207.

[8] Sun, Y. M.; Ma, Y. W.; Liu, Y. Q.; Lin, Y. Y.; Wang, Z. Y.; Wang, Y.; Di, C. G.; Xiao, K.; Chen, X. M.; Qiu, W. F.; Zhang, B.; Yu, G.; Hu, W. P.; Zhu, D. B., High-performance and stable organic thin-film transistors based on fused thiophenes. *Adv Funct Mater* **2006,** *16* (3), 426-432.

[9]Takimiya, K.; Ebata, H.; Sakamoto, K.; Izawa, T.; Otsubo, T.; Kunugi, Y., 2,7-Diphenyl[1]benzothieno[3,2-b]benzothiophene, a new organic semiconductor for air-stable organic field-effect transistors with mobilities up to 2.0 cm(2) V-1 s(-1). *J Am Chem Soc* **2006,** *128* (39), 12604-12605.

[10] Laquindanum, J. G.; Katz, H. E.; Lovinger, A. J., Synthesis, morphology, and field-effect mobility of anthradithiophenes. *J Am Chem Soc* **1998,** *120* (4), 664-672.

[11] (a) Tang, M. L.; Okamoto, T.; Bao, Z. N., High-performance organic semiconductors: Asymmetric linear acenes containing sulphur. *J Am Chem Soc* **2006,** *128* (50), 16002-16003; (b) Valiyev, F.; Hu, W. S.; Chen, H. Y.; Kuo, M. Y.; Chao, I.; Tao, Y. T., Synthesis and characterization of anthra[2,3-b]thiophene and tetraceno[2,3-b]thiophenes for organic field-effect transistor applications. *Chem Mater* **2007,** *19* (12), 3018-3026.

[12] Payne, M. M.; Parkin, S. R.; Anthony, J. E.; Kuo, C. C.; Jackson, T. N., Organic field-effect transistors from solution-deposited functionalized acenes with mobilities as high as 1 cm(2)/V-s. *J Am Chem Soc* **2005,** *127* (14), 4986-4987.

[13] Payne, M. M.; Odom, S. A.; Parkin, S. R.; Anthony, J. E., Stable, crystalline acenedithiophenes with up to seven linearly fused rings. *Org Lett* **2004,** *6* (19), 3325-3328.

[14] Reese, C.; Bao, Z. N., Organic single crystals: tools for the exploration of charge transport phenomena in organic materials. *J Mater Chem* **2006,** *16* (4), 329-333.

[15] (a) Wu, J. S.; Baumgarten, M.; Debije, M. G.; Warman, J. M.; Mullen, K., Arylamine-substituted hexa-peri-hexabenzocoronenes: Facile synthesis and their potential applications as "coaxial" hole-transport materials. *Angew Chem Int Edit* **2004,** *43* (40), 5331-5335; (b) Dou, X.; Yang, X. Y.; Bodwell, G. J.; Wagner, M.; Enkelmann, V.; Mullen, K., Unexpected phenyl group rearrangement during an intramolecular Scholl reaction leading to an alkoxy-substituted hexa-peri-hexabenzocoronene. *Org Lett* **2007,** *9* (13), 2485-2488.

[16] Iyer, V. S.; Wehmeier, M.; Brand, J. D.; Keegstra, M. A.; Mullen, K., From hexa-peri-hexabenzocoronene to "superacenes". *Angew Chem Int Ed.* **1997,** *36* (15), 1604-1607.

[17] a) Schlettwein, D.; Tada, H.; Mashiko, S., Substrate-induced order and multilayer epitaxial growth of substituted phthalocyanine thin films. *Langmuir* **2000,** *16* (6), 2872-2881.

b) Ali-Adib, Z.; Clarkson, G. J.; McKeown, N. B.; Treacher, K. E.; Gleeson, H. F.; Stennett, A. S., Molecular assemblies of novel amphiphilic phthalocyanines: an investigation irate the self-ordering properties of complex functional materials. *J Mater Chem* **1998,** *8* (11), 2371-2378.

[18] Houk, K. N.; Lee, P. S.; Nendel, M., Polyacene and cyclacene geometries and electronic structures: Bond equalization, vanishing band gaps, and triplet ground states contrast with polyacetylene. *J Org Chem* **2001,** *66* (16), 5517-5521.; Bendikov, M.; Duong, H. M.; Starkey, K.; Houk, K. N.; Carter, E. A.; Wudl, F., Oligoacenes: Theoretical prediction of open-shell singlet diradical ground states. *J Am Chem Soc* **2004,** *126* (24), 7416-7417.

[19] Zhang, X. N.; Matzger, A. J., Effect of ring fusion on the electronic absorption and emission properties of oligothiophenes. *J Org Chem* **2003,** *68* (25), 9813-9815.

[20] Sheraw, C. D.; Jackson, T. N.; Eaton, D. L.; Anthony, J. E., Functionalized pentacene active layer organic thin-film transistors. *Adv Mater* **2003,** *15* (23), 2009-2011.

[21] Zefirov, Yu. V.; Zorkii, P. M. *Zh. Strukt. Khimii* **1976**, *17*, 745 (in russian)

[22] Dopper, J. H.; Wynberg, H., Synthesis and Properties of Some Heterocirculenes. *J Org Chem* **1975,** *40* (13), 1957-1966.

[23] Yoshimoto, S.; Tsutsumi, E.; Narita, R.; Murata, Y.; Murata, M.; Fujiwara, K.; Komatsu, K.; Ito, O.; Itaya, K., Epitaxial supramolecular assembly of fullerenes formed by using a coronene template on a Au(111) surface in solution. *J Am Chem Soc* **2007,** *129* (14), 4366-4376.

[24] (a) van de Craats, A. M.; Stutzmann, N.; Bunk, O.; Nielsen, M. M.; Watson, M.; Mullen, K.; Chanzy, H. D.; Sirringhaus, H.; Friend, R. H., Meso-epitaxial solution-growth of self-organizing discotic liquid-crystalline semiconductors. *Adv Mater* **2003,** *15* (6), 495-499; (b) Pisula, W.; Menon, A.; Stepputat, M.; Lieberwirth, I.; Kolb, U.; Tracz, A.; Sirringhaus, H.; Pakula, T.; Mullen, K., A zone-casting technique for device fabrication of field-effect transistors based on discotic hexa-peri-hexabenzoeoronene. *Adv Mater* **2005,** *17* (6), 684.

[25] Chernichenko, K. Y.; Sumerin, V. V.; Shpanchenko, R. V.; Balenkova, E. S.; Nenajdenko, V. G., "Sulflower": A new form of carbon sulfide. *Angew Chem Int Edit* **2006,** *45* (44), 7367-7370.

[26] A. Patra, Y. H. Wijsboom, L. J. W. Shimon and M. Bendikov, *Angew Chem Int Ed* 2008, **46**, 8814.

[27] Ivasenko, O.; MacLeod, J. M.; Chernichenko, K. Y.; Balenkova, E. S.; Shpanchenko, R. V.; Nenajdenko, V. G.; Rosei, F.; Perepichka, D. F., Supramolecular assembly of heterocirculenes in 2D and 3D. *Chem Commun* **2009,** (10), 1192-1194.

[28] Santato, C.; Cicoira, F.; Cosseddu, P.; Bonfiglio, A.; Bellutti, P.; Muccini, M.; Zamboni, R.; Rosei, F.; Mantoux, A.; Doppelt, P., Organic light-emitting transistors using concentric source/drain electrodes on a molecular adhesion layer. *Appl Phys Lett* **2006,** *88* (16), 163511.

[29] (a) Takimiya, K.; Kunugi, Y.; Konda, Y.; Niihara, N.; Otsubo, T., 2,6-diphenylbenzo[1,2-b:4,5-b']dichalcogenophenes: a new class of high-performance semiconductors for organic field-effect transistors. *J Am Chem Soc* **2004,** *126* (16), 5084-5085; (b Takimiya, K.; Ebata, H.; Sakamoto, K.; Izawa, T.; Otsubo, T.; Kunugi, Y., 2,7-Diphenyl[1]benzothieno[3,2-b]benzothiophene, a new organic semiconductor for air-stable organic field-effect transistors with mobilities up to 2.0 cm^2/Vs. *J Am Chem Soc* **2006,** *128* (39), 12604-12605.

[30] (a) Patra, A.; Wijsboom, Y. H.; Zade, S. S.; Li, M.; Sheynin, Y.; Leitus, G.; Bendikov, M., Poly(3,4-ethylenedioxyselenophene). *J Am Chem Soc* **2008,** *130* (21), 6734; (b) Heeney, M.; Zhang, W.; Crouch, D. J.; Chabinyc, M. L.; Gordeyev, S.; Hamilton, R.; Higgins, S. J.; McCulloch, I.; Skabara, P. J.; Sparrowe, D.; Tierney, S., Regioregular poly(3-hexyl) selenophene: a low band gap organic hole transporting polymer. *Chem Commun* **2007,** (47), 5061-5063.

CHAPTER 5

Bis(styryl)anthracenes as Active Semiconducting and Emissive Layer for OLETs

5.1 Introduction: Organic field-effect transistors (OTFTs) are of great current interest because they can potentially be fabricated at low cost, over large areas, and on flexible substrates.[1,2] Organic light-emitting transistors (OLETs) are devices that combine two functionalities, electrical switching and light emission.[3] Potential applications of OLETs include flat-panel display technologies, lighting, and, ultimately, electrically pumped organic lasers.[4]

Pentacene, a benchmark p-type OSC, demonstrates a charge carrier mobility greater than 1.0 (cm^2/Vs) in OTFT configuration.[5,6] The high charge carrier mobility of pentacene is attributed to its flat, symmetric molecular structure, that leads to highly ordered thin crystalline film morphology with large grain size when deposited at proper substrate temperatures. However, pentacene suffers from the disadvantages of poor oxidative instability and extreme insolubility that will limit its commercial potential.[7] Most of the polycyclic fused aromatic organic semiconductors (tetracene, rubrene) including pentacene also show rather weak or no photoluminescence. Therefore, there still exists a need for identifying π-conjugated semiconductors with high mobility, robust environmental stability and efficient luminescence. Several strategies have been explored to improve the stability and luminescence properties of OSCs through the design of large band gap (~3 eV) semiconductor materials, such as anthracene derivatives.[8,9] Principally, a combination of high charge mobility and high solid state luminescence efficiency in an OSC is required for OLET application.

Obviously the chemical structure of the OSCs together with the nature of their intermolecular electronic coupling in solid-state are two important parameters defining the optoelectronic properties of π-conjugated systems as well as their device characteristics. In planar π-conjugated

OSCs, the greater overlap between π-orbitals of neighbouring molecules leads to charge carrier mobilities but provides nonradiative decay pathway for excitons resulting in the quenching of solid-state emission. In other words, achieving *high charge mobility* and *high solid-state luminescence efficiency* is, so far, mutually exclusive in present OSCs.[10]

Substituted anthracenes are considered good candidates for OLET application due to their high fluorescence quantum yields and extended conjugation length. For example, 9,10-diphenyl-substituted anthracene has quantum yield about unity.[11] Substitution at 2 and 6 positions of anthracene core with styryl groups offer a planar extended π-conjugated system. Recently high charge mobility and remarkable stability were reported for 2,6-bis[2-(4-pentylstyryl)] anthracene, **2,6-DPSAnt**.[8] We earlier studied a green-emitting OLET based on 2-(4-pentylstyryl)tetracene (**PSTet**)[12], (scheme 5.1). While **PSTet** based OLETs showed a reasonable hole mobility of ~0.2 cm^2/Vs, its low solid state PLQY of ~7% was a drawback for OLET application. However, the material and the devices incorporating **PSTet** showed higher luminescence and also greater thermal and environmental stability compared to non-substituted tetracene and pentacene. By shrinking the acene core from tetracene to anthracene, one should expect even higher stability for the material. Anthracene core can also provide an enhanced PL efficiency of the molecule.

This chapter presents the light-emitting and charge transport properties of conjugated *trans*-styryl anthracenes substituted at 2,6- and 9,10- positions (Scheme 5.1) in an OLET configuration. It investigates the influence of the positions of styryl-alkyl anthracenes in the optoelectronic properties of the molecule and also device characteristics.

In this work, OTFTs incorporate a single layer of organic material as active semiconducting and emissive layer as well as symmetric source and drain metal electrodes to simplify the device fabrication.

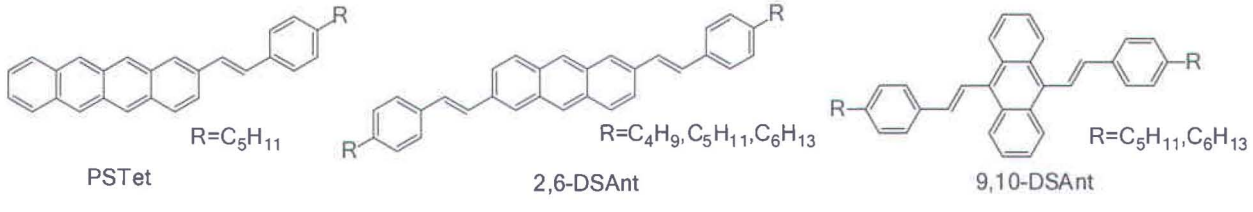

Scheme 5.1. Chemical structure of alkylted styryl-oligoacenes

5.2 Material characterization: Thermogravimetric analysis (TGA) revealed high stability of **2,6-DPSAnt** and **9,10-DPSAnt**, with onset decomposition temperatures (T_{dec}) of ~ 355 °C and 330 °C in air, respectively. The same experiment under nitrogen showed no decomposition until sublimation of the compounds at 410 °C for **2,6-DPSAnt** and 350 °C for compound **9,10-DPSAnt** (Figure 5.1). Such a remarkable stability is particularly important for application of these compounds in OTFTs, where the stability of organic semiconductors is still a major limitation.

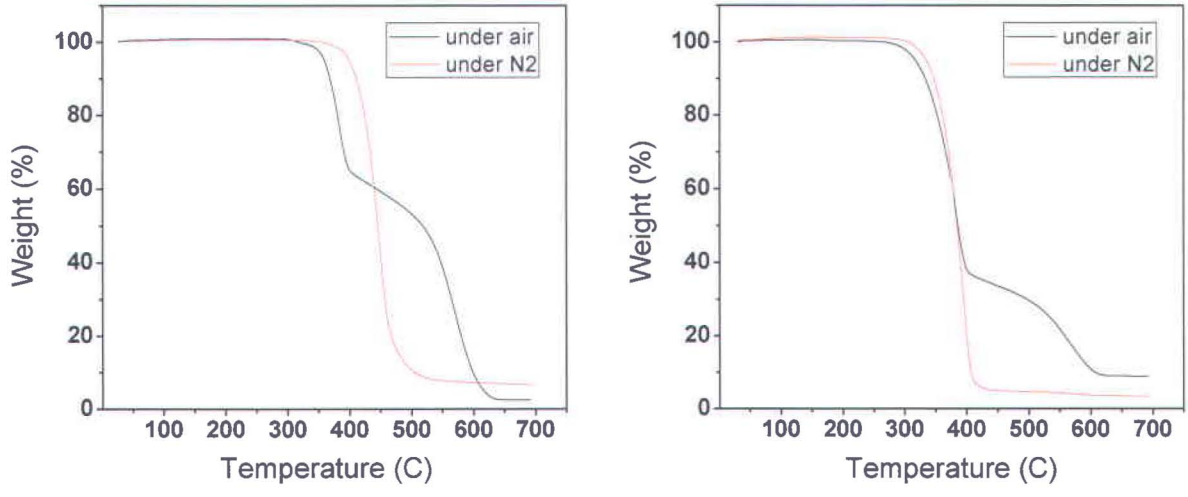

Figure 5.1: TGA of of **2,6-DPSAnt** (left) and **9,10-DPSAnt** (right) performed under N_2 and ambient conditions

We performed density functional theory (DFT) calculations to compare the energy level of both compounds. The calculations at B3LYP/6-31G(d) basis set suggest the HOMO and LUMO of **2,6-DPSAnt** at -4.87 eV and -1.88 eV, respectively. A similar HOMO-LUMO gap (3.03 eV) was obtained from the solution absorption spectrum of **2,6-DPSAnt** that shows vibronically structured bands at λ_{max}= 341, 356, 374 and 395 nm (Figure 5.2). The PL spectrum of **2,6-DPSAnt** is also vibronically structured at λ_{max}= 409 nm and 428 nm with a Stokes shift of 14 nm (0.11 eV). The solution PLQY for **2,6-DPSAnt** is 0.49. In the solid state, intermolecular interactions result in a red-shift of both absorption and PL (Fig. 1b) with a PLQY of 0.14. The optical band gap of **9,10-DPSAnt** obtained from the onset absorption (λ_{max}=415 nm) was slightly lower (2.64 eV). The larger Stocks shift of **9,10-DPSAnt** (0.81 eV) compared to **2,6-DPSAnt** is in line with higher reorganization energy of the **9,10-DPSAnt**. For **9,10-DPSAnt**, we obtained a higher PLQY of 0.58 and 0.18 in solution and in solid state, respectively. This is in contrast to

the previously reported value of <1% for solution of **9,10-DMSAnt**.

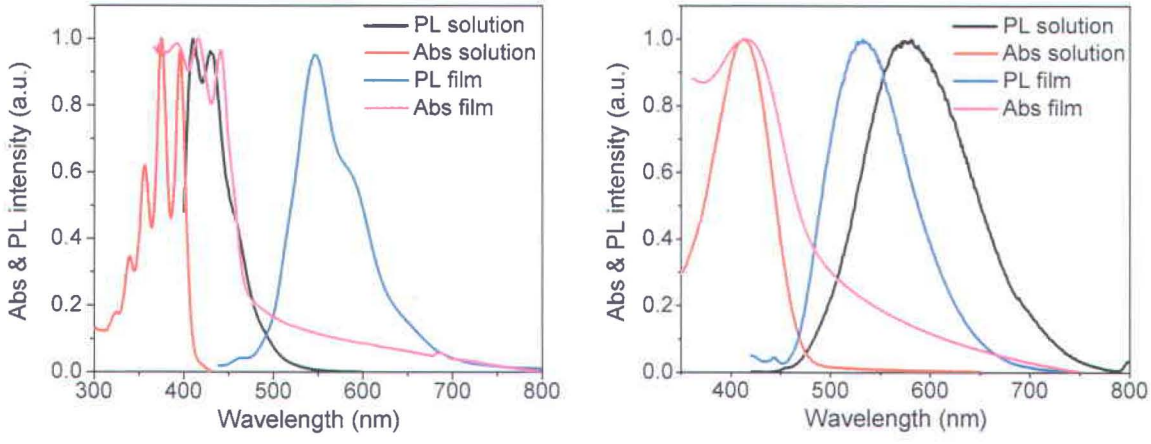

Figure 5.2: Absorbance and PL spectra of **2,6-DPSAnt** and **9,10-DPSAnt** in the solution and in the solid state

Table 5.1: Photophysical properties of bis(styryl) anthracenes

	E_{HOMO}^{calc} (eV)	E_{LUMO}^{calc} (eV)	E_g^{calc} (eV)	λ_{max}^{abs} (nm)	E_g^{opt} (eV)	Stokes shift (eV)	Reorg. Energy (eV)	PLQY
2,6-DPSAnt	–4.87	-1.88	2.99	395	3.03	0.11	0.198	0.49 (solution) 0.14 (film)
9,10-DPSAnt	–4.81	-1.84	2.97	415	2.64	0.81	0.321	0.58 (solution) 0.18 (film)

Similar to pentacene, single crystals of **2,6-DPSAnt** adapts herringbone arrangement but more densely packed.* This can explained by the extended conjugation length of **2,6-DPSAnt** and high intermolecular interactions between alkyl groups and planar aromatic rings in neighbouring molecular layers (Figure 5.3). The packing arrangement in crystal lattice of **9,10-DPSAnt** is, however, governed by CH…π hydrogen bonds interaction and not π…π interactions which is the result of non-planar molecular conformation. The x-ray data of **9,10-DPSAnt** showed small extent of orbital overlap (π-π interaction), which can lead to a poor charge transport property.

The styryl groups in **2,6-DPSAnt** are co-planar with an anthracene core but in **9,10-DPSAnt** they form torsional angle of 54° and 67° in the gas phase (calculation) and solid-state, respectively. The higher rotational freedom of syryl groups in solution compared to solid state

* Crystal packing of **pentacene** (a =7.79 Å, b= 6.27Å) and **2,6-DSAnt** (a= 7.23 Å, b=5.85 Å)[8]

leads to more effective π-conjugation with anthracene core and explains the red shift of the PL spectrum of **9,10-DPSAnt** in solution (Figure 5.3).

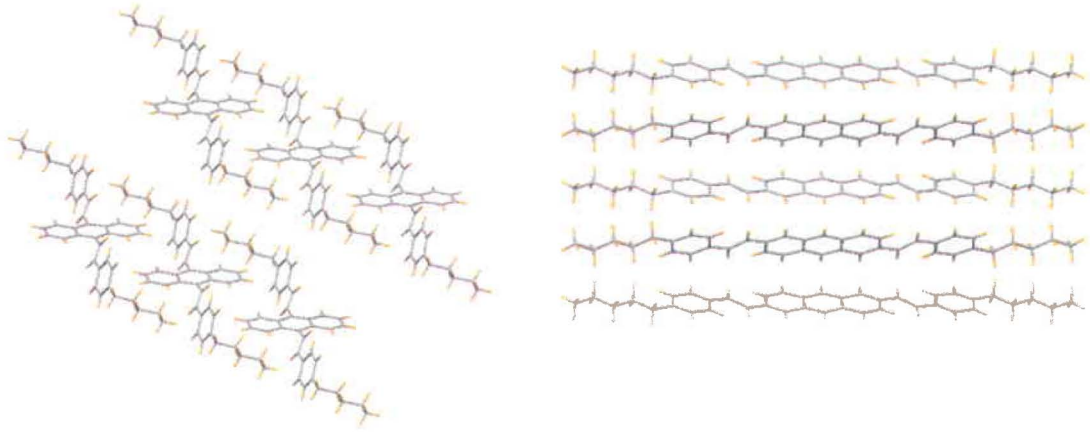

Figure 5.3: Intermolecular interactions in crystals of (left) **9,10-DPSAnt** and (right) **2,6-DPSAnt**[8]

5.3 Thin film characterization: Atomic force microscopy (AFM) in the standard tapping mode was used to study the surface morphology of **2,6-DPSAnt** and **9,10-DSAnt**. Vacuum-sublimed films of both materials were analyzed in their early growth stage (sub-monolayer) and also fully covered samples. Figure 5.4 and 5.5 present the AFM micrographs and the histogram of the height profile of thin films of **2,6-DPSAnt** and **9,10-DSAnt** deposited on SiO_2/Si at the deposition rate of 0.1 (Å/s) while the substrates were kept at room temperature. From AFM analysis of early growth films, typical Volmer-Weber (VW) growth was observed. It seems that molecule-molecule interactions in both materials are stronger than molecule-surface interactions, leading to the formation of three-dimensional islands.[13]

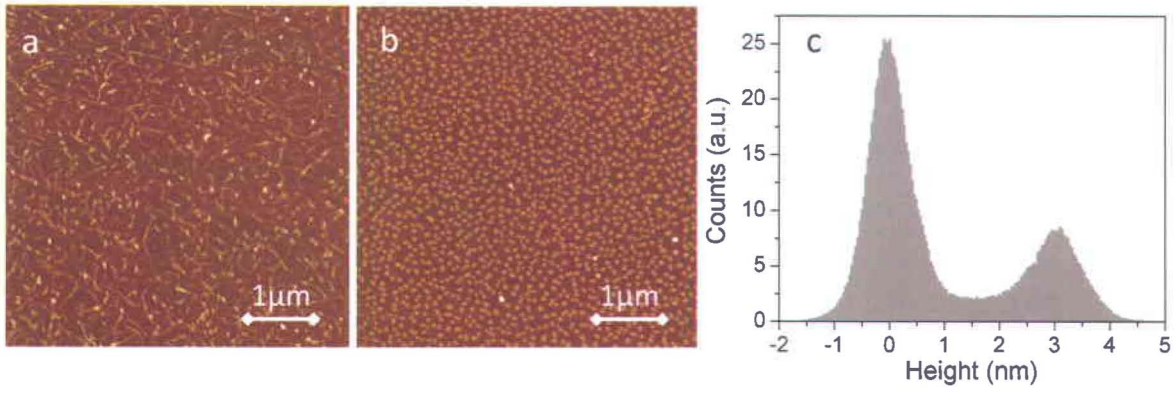

Figure 5.4: (a) AFM images of 35 nm and (b) early growth and film of **2,6-DPSAnt** on SiO_2/Si and corresponding (c) height profile of "b".

The early stages growth of the film of **2,6-DPSAnt** consists of sub-monolayers with an average height of 3 nm and average size of 0.005 μm^2 that do not have good interconnection across the surface (Figure 5.4b). By increasing the surface coverage, the grains seem to continue growing in one dimension with no substantial lateral growth and cover the entire surface with number of grain boundaries (Figure 5.4a). The early stage growth of the film of **9,10-DPSAnt** also includes the nucleation of small grains with the average height of 10-15 nm (Figure 5.5a). At a higher nominal film thickness of between 10 nm and 85 nm, still separated islands are observed (Figure 5.5b). This is due to the high surface energy leading to the greater affinity of the molecules to each other. The full coverage surface was observed for the film with higher thicknesses (Figure 5.5c). Principally, the continuous films formed at low nominal thickness, where the conducting channel is formed, are important for transistor applications since the grain boundaries are minimized. Thus, the growth mode of **9,10-DPSAnt** is detrimental for the charge transport within this material in OTFT configuration. We could not promote layer films growth of neither of materials through surface treatment and deposition at different substrate temperature which could limit the performance of resulting OTFTs.

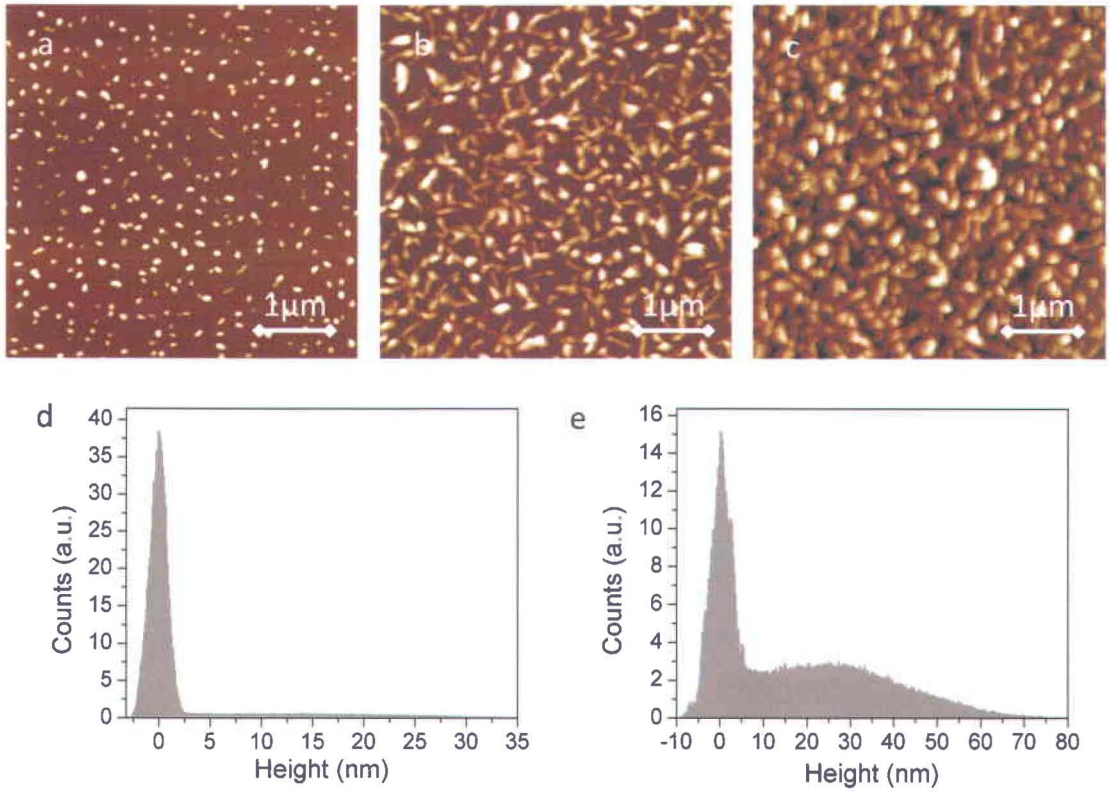

Figure 5.5: (a) AFM images of early growth and (b) 50 nm (c) 120 nm film of **9,10-DPSAnt** on SiO_2/Si and corresponding (d) height profile of "a" and (e) that of "b".

5.4 Device Characterization: OTFTs were fabricated in a top-contact configuration (with symmetric drain and source electrodes thermally evaporated through a shadow mask) and films were grown in room temperatures. Thin film of both molecules were grown by vacuum deposition (~10^{-6} mbar, deposition rate 0.1–0.4 Å/sec) on hexamethyldisilazane (HMDS) treated SiO_2/Si. SiO_2 was thermally grown (200 nm-thick) on heavily n-doped (Sb) Si ($\rho \approx$ 0.01 Ohm cm). Typical transfer characteristics and current density (derived from output characteristics) of the TFTs based on **2,6-DPSAnt** are shown in Figure 5.6. The devices incorporating **2,6-DPSAnt** showed a combination of high charge carrier mobility, environmental stability, and device repeatability. Typical hole mobility in the range of 0.1-0.78 cm^2/Vs was measured in OTFT configuration and in the vacuum. Threshold voltage and on-off ratio were -18±2 V and 10^5-10^7, respectively. Pentacene OTFTs prepared under identical conditions show a similar mobility as high as 0.8 cm^2/Vs and threshold voltage of -10±2 V (Chapter 2). The higher threshold voltages of the **2,6-DPSAnt** transistor compared to the pentacene OTFTs is related to the higher ionization potential of **2,6-DPSAnt** that, in turn, can lead to higher stability of the **2,6-DPSAnt** and consequently devices incorporating this material. Such combination of stability and high

performance in OSC materials are critical for the development of low cost organic electronics.

Current density in these devices reached up to 5 kA/cm^2 (assuming an accumulation layer of 1 nm thick). This relatively high value is due to the high charge mobility of the OTFTs based on **2,6-DPSAnt**. Similar values have already been reported for single crystal-FETs based on tetracene and rubrene at very high device bias.[14]

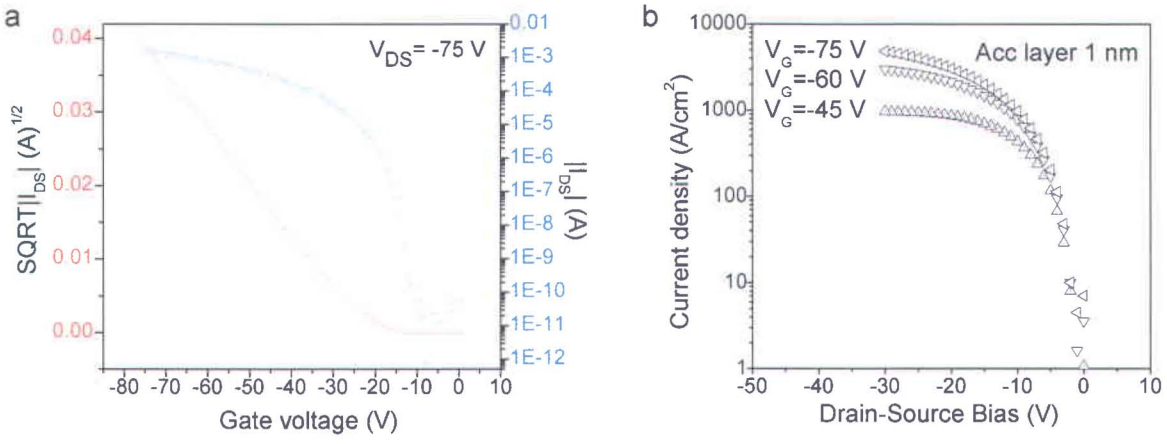

Figure 5.6: (a) transfer and (b) the current density (assuming channel thickness of 1 nm) of LET based on a vacuum sublimed film of **2,6-DPSAnt**.

We have also studied OTFTs incorporating butyl- and hexyl-substituted **2,6-DSAnt**. These devices, however, showed a lower performance compared to that of pentyl substituted **2,6-DSAnt**. This can be related to the different packing, film morphology, or the purity of materials.

In similar work carried out by H. Meng et al.,[8] top-contact OTFTs based on **2,6-DPSAnt** showed mobility in the range of 0.1-1.28 cm^2/Vs and on/off current ratios of 10^6-10^7, depending on the substrate temperature. They observed the highest values of charge mobility when the substrate temperature was kept in the range of 60-80°C. However, we did not observe any significant enhancement of the performance for the OTFTs prepared at different substrate temperatures. For **DSAnt**, Klauk et al.,[15] reported a maximum mobility of 1.3 cm^2/Vs for top-contact devices prepared at 80°C.

The good device performance of *styryl-substituted of anthracene in 2 and 6 positions*, in general, is attributed to the planar conformation of the molecule and strong π-π interaction in solid-state. It should be noted that the growth mechanism of **2,6-DPSAnt** film (Figure 5.4) that results in a large number of grain boundaries negatively affects the charge mobility. We expect a further enhancement in device performance by optimizing the deposition condition and promoting the

layer growth of the film. On the other hand, devices incorporating **9,10-DPSAnt** did not show any FET-mobility under similar conditions. This is mainly due the crystal structure and packing arrangements of **9,10-DPSAnt** (Table 5.1).[16,17] Moreover, as discussed earlier, the growth of the film of **9,10-DPSAnt** includes the nucleation of small grains and separated islands even at the nominal thickness of up to 85 nm. As a result, there should be no effective charge transport within the films of **9,10-DPSAnt** in OTFT configuration where the average film thickness of OSC is ~50 nm.

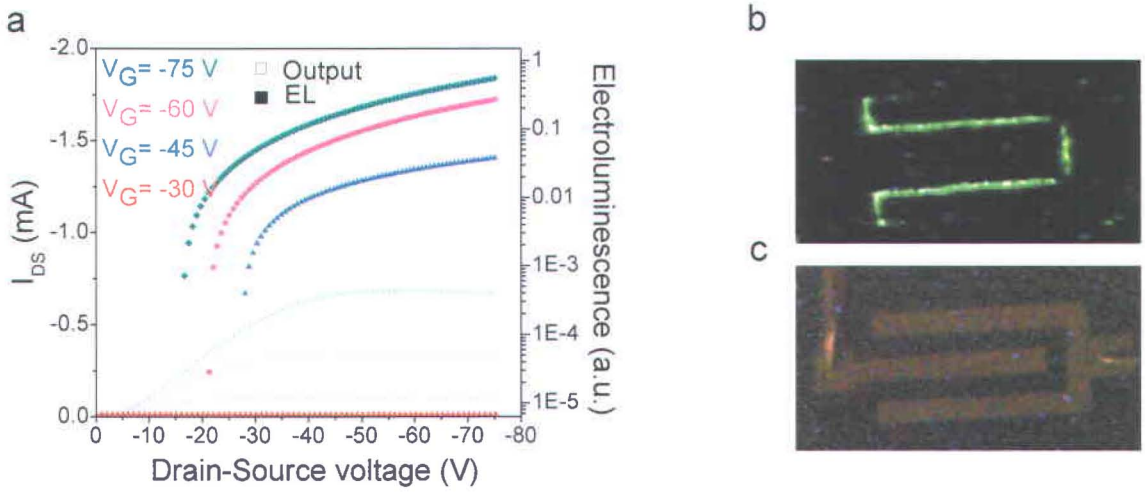

Figure 5.7: (a) output and modulated EL current characteristics (b) and (c) optical images of EL and biased LET based on a vacuum sublimed film of **2,6-DPSAnt**.

The transistor current and the EL were simultaneously recorded as a function of the drain-source voltage (V_{ds}) for different gate voltages (V_g). All devices (bottom- and top-contact configurations) based on **2,6-DPSAnt** showed p-type transistor behaviour and gate and drain modulated electroluminescence (Figure 5.7 a). The detection of EL was achieved using a Hamamatsu Si-photodiode. We also used a Toshiba IK-1000 charged coupled device (CCD) camera mounted on an optical microscope objective for EL imaging The optical image of the working device and green emission are shown in (Figure 5.7 b,c). The emission was sufficiently intense to be detected from the single channel OLETs. EL is mainly localized at the drain electrode which is consistent with unipolar p-type characteristics of **2,6-DPSAnt**. The asymmetric positions of the HOMO and LUMO of **2,6-DPSAnt** with respect to the work function of Au (~ –5 eV) create a high energy barrier for electron injection into the channel. Therefore, the preferential hole injection in this device configuration results in the confinement of EL in the vicinity of the electron injecting electrode.

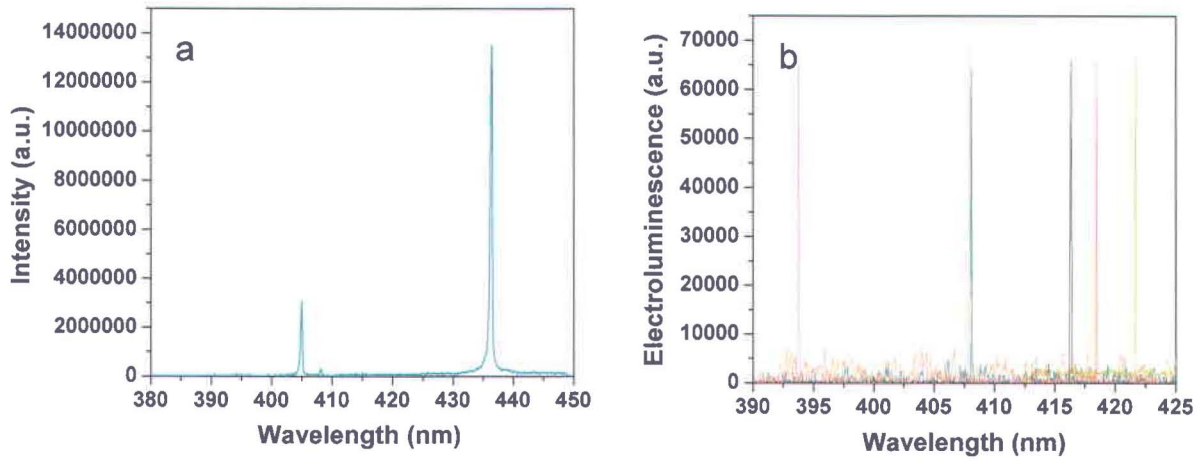

Figure 5.8: EL spectrum of OLETs based on a vacuum sublimed film of **2,6-DPSAnt** (FWHM of 1-3nm)

Surprisingly, a blue emission was also observed from the first series of devices while the green EL was quenched due to the lower FET mobility of **2,6-DPSAnt** in early devices. We set the detecting range of spectrometer between 350 nm and 500 nm and recorded the EL from different interdigitated devices having the channel length of 6, 10 and 40 μm. The recorded EL had a full width at half maximum (FWHM) of 1 nm to 3 nm (Figure 5.8 a,b). Different positions of the EL spectra between 395 nm and 436 nm could be due to different self-created resonators with the optical length of equal to an integer number of emission wavelengths[10].

The blue emission can be due to the "glow-discharge effects". In this process, the gas (N2) around the dielectric maybe ionized and emits characteristic narrow linewidth (Destriau effect).[18,19] Then the blue emission from the gas can be reabsorbed by the **2,6-DPSAnt** during device operation.

To eliminate any artifacts in the blue EL spectrum, we recorded the emission spectrum of intentionally created discharge (Figure 5.9) and confirmed that none of the spectra were similar to that of blue EL.

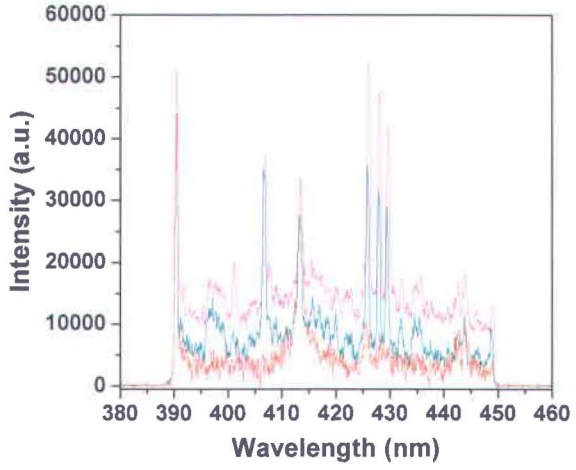

Figure 5.9: (a) Emission spectra from intentionally created discharges

PL spectral narrowing was not observed upon photo-pumping the film of **2,6-DPSAnt** on quartz with the excitation wavelength of 350 nm and maximum energy of 90 ($\mu j/cm^2$), Figure 5.10. We expect a collapse of the PL spectrum (Amplified Spontaneous Emission, ASE) of **2,6-DPSAnt** at higher photo-pumping energy.

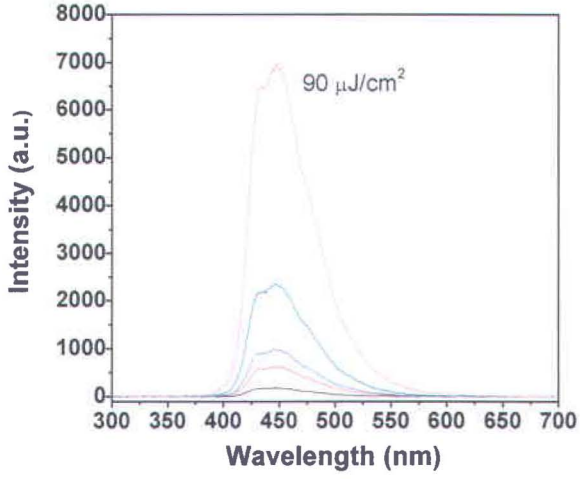

Figure 5.10: (a) evolution of PL spectrum of LET based on a vacuum sublimed film of **2,6-DPSAnt**

The narrow linewidth EL could be the indication of a lasing OLET based on **2,6-DPSAnt**. However, to recognize the lasing especially the electrically driven lasers, sufficient evidences should be provided. In addition to narrow linewidth emission, it should be the characteristic of the specific gain medium and resonator and possesses a clear threshold in both the output power and linewidth.[10] Detailed characterizations are required for a better understanding of the origin of the observed narrow linewidth blue emission from OTFTs based on **2,6-DPSAnt**. This might be useful for the rational design of OSCs capable of electrically-pumped lasing.

One hypothesis for the lattermost results could be the presence of *mono-substituted* styryl anthracene (as impurity) which introduces a bathochromic shift to EL. Only a small amount of mono-styryl anthracene could have existed in the first batch of **2,6-DPSAnt** since we did not observe the si4milar results for other fabricated OLETs. These results led us to the design and synthesis of mono-styryl substituted anthracene which combines necessary requirements for an high-performance OLETs including very high current density. This part will be fully covered in ***chapter 6.***

5.5 Conclusions: The optoelectronic and photophysical properties of styryl-substituted of anthracenes in two different positions were studied. 9,10 substituted anthracene showed high PLQY with no FET charge mobility. The poor charge transport in **9,10-DPSAnt** presumably is due to the low π-π interaction between neighbouring molecules in the solid state as well as very poor film forming of the molecule. **2,6-DPSAnt** showed high charge mobilities and moderate photoluminescence quantum yield. The optoelectronic properties of **2,6-DPSAnt** and OLETs characteristics based on **2,6-DPSAnt** are superior compared to our previous study on **PSTet.**[12]

Tuning of the optoelectronic properties of OSCs and thus the device characteristics requires a better understanding of the dependence of the charge transport and luminescence properties on the factors that determine the nature of molecular packing in the solid state.

As a perspective, apart from the investigation on the origin and the nature of the blue emission observed from OLETs based on **2,6-DPSAnt**, this work can also be directed to the study of the structure-property relationships and solid-state packing of the anthracene substituted by donor-styryl groups in 1,5 positions as well as extended anthracene in 2D (2,3,6,7-tetrastyrylanthracene).

References

[1] Mitzi, D. B.; Kosbar, L. L.; Murray, C. E.; Copel, M.; Afzali, A., High-mobility ultrathin semiconducting films prepared by spin coating. *Nature* **2004,** *428* (6980), 299-303.

[2] Reese, C; Roberts, M.; Ling, M.; Bao, Z., Organic thin film transistors. *Mater.Today* **2004**, 7, 20-27.

[3] Hepp, A.; Heil, H.; Weise, W.; Ahles, M.; Schmechel, R.; von Seggern, H., Light-emitting field-effect transistor based on a tetracene thin film. *Phys Rev Lett* **2003,** *91*, 157 406.

[4] Dinelli, F.; Capelli, R.; Loi, M. A.; Murgia, M.; Muccini, M.; Facchetti, A.; Marks, T. J., High-mobility ambipolar transport in organic light-emitting transistors. *Adv Mater* **2006,** *18* (11), 1416-1420.

[5] Klauk, H.; Halik, M.; Zschieschang, U.; Schmid, G.; Radlik, W.; Weber, W., High-mobility polymer gate dielectric pentacene thin film transistors. *J Appl Phys* **2002,** *92* (9), 5259-5263.

[6] Lin, Y. Y.; Gundlach, D. J.; Nelson, S. F.; Jackson, T. N., Stacked pentacene layer organic thin-film transistors with improved characteristics. *Ieee Electr Device L* **1997,** *18* (12), 606-608.

[7] Yamada, M.; Ikemoto, I.; Kuroda, H., Photooxidation of the Evaporated-Films of Polycyclic Aromatic-Hydrocarbons Studied by X-Ray Photoelectron-Spectroscopy. *B Chem Soc Jpn* **1988,** *61* (4), 1057-1062.

[8] Meng, H.; Sun, F. P.; Goldfinger, M. B.; Gao, F.; Londono, D. J.; Marshal, W. J.; Blackman, G. S.; Dobbs, K. D.; Keys, D. E., 2,6-bis[2-(4-pentylphenyl)vinyl]anthracene: A stable and high charge mobility organic semiconductor with densely packed crystal structure. *J Am Chem Soc* **2006,** *128* (29), 9304-9305.

[9] Merlo, J. A.; Newman, C. R.; Gerlach, C. P.; Kelley, T. W.; Muyres, D. V.; Fritz, S. E.; Toney, M. F.; Frisbie, C. D., p-channel organic semiconductors based on hybrid acene-thiophene molecules for thin-film transistor applications. *J Am Chem Soc* **2005,** *127* (11), 3997-4009.

[10] Samuel, I. D. W.; Turnbull, G. A., Organic semiconductor lasers. *Chem Rev* **2007,** *107* (4), 1272-1295.

[11] Xu, B.; Fang, H. H.; Dong, Y. J.; Chen, F. P.; Chen, Q. D.; Sun, H. B.; Tian, W. J., Solid state emission enhancement of 9,10-distyrylanthracene derivatives and amplified spontaneous emission from a large single crystal. *New J Chem* **2010,** *34* (9), 1838-1842.

[12] Cicoira, F.; Santato, C.; Dadvand, A.; Harnagea, C.; Pignolet, A.; Bellutti, P.; Xiang, Z.; Rosei, F.; Meng, H.; Perepichka, D. F., Environmentally stable light emitting field effect transistors based on 2-(4-pentylstyryl)tetracene. *J Mater Chem* **2008,** *18* (2), 158-161.

[13] Oura, K.; V.G. Lifshits, A.A. Saranin, A.V. Zotov, and M. Katayama (2003). Surface Science: An Introduction. Berlin: Springer. ISBN 3-540-00545-5.

[14] Sawabe, K.; Takenobu, T.; Bisri, S. Z.; Yamao, T.; Hotta, S.; Iwasa, Y., High current densities in a highly photoluminescent organic single-crystal light-emitting transistor. *Appl Phys Lett* **2010,** *97* (4) 043307.

[15] Klauk, H.; Zschieschang, U.; Weitz, R. T.; Meng, H.; Sun, T.; Nunes, G.; Keys, D. E.; Fincher, C. R.; Xiang, Z., Organic transistors based on di(phenylvinyl)anthracene: Performance and stability. *Adv Mater* **2007,** *19* (22), 3882-3887.

[16] Da Silva, D. A.; Kim, E. G.; Bredas, J. L., Transport properties in the rubrene crystal: Electronic coupling and vibrational reorganization energy. *Adv Mater* **2005,** *17* (8), 1072-1076

[17] Hutchison, G. R.; Ratner, M. A.; Marks, T. J., Intermolecular charge transfer between heterocyclic oligomers. Effects of heteroatom and molecular packing on hopping transport in organic semiconductors. *J Am Chem Soc* **2005,** *127* (48), 16866-16881.

[18] Gautier-Thianche, E.; Sentein, C.; Lorin, A.; Nunzi, J. M., Field-effect electroluminescence in a polymer channel. *Opt Mater* **1999,** *12* (2-3), 295-299.

[19] Charra, F.; Bouchel, S.; Plessis, O.; Nunzi, J. M.; Raimond, P.; Denis, C.; Gautier-Thianche, E., Near-field electroluminescence probe of polymer light-emitting diodes. *Opt Mater* **1999,** *12* (2-3), 249-253.

CHAPTER 6

Organic Light Emitting Transistors based on Styrylanthracenes*

6.1 Introduction: Tunable multifunctional properties accessible through synthetic design and facilitated device fabrication are the key advantages of organic semiconductors (OSC) vs. silicon and other inorganic materials. A tandem of light-emitting and charge-transporting properties in OSC has been widely explored, and already commercialized, in organic light-emitting diodes (OLED) and displays.[1,2] At the same time, it proved to be very difficult to maximize the charge mobility (μ) and luminescence efficiency in the same OSC. Due to short electrical channel length, OLEDs do not require $\mu > 10^{-4}...10^{-2}$ cm^2/Vs, however, a number of technological opportunities could arise if highly emissive OSC with $\mu > 1$ cm^2/Vs were available. These include organic light-emitting transistors (OLETs),[3] which combine electroluminescence (EL) and current control function of a field-effect transistor (FET) allowing to simplify the structure of active matrix displays. Larger current densities, attainable in transistor configuration vs. that in OLED,[3d] are highly desirable for the development of electrically pumped organic lasers.[4] However, this demands new materials with high μ.

Achieving mobility over 1 cm^2/Vs in OSC generally requires crystalline materials with strong π-π interactions. However, the latter most often lead to suppression or even complete quenching of the luminescence upon aggregation, particularly in the solid state.[5] Most efficient EL organic materials are amorphous. There are several reasons for luminescence quenching in the crystalline state, including fission of a singlet exciton (process that converts one singlet exciton to a pair of non-emissive triplet),[6] as well as exciton quenching on the defect sites. On the other hand, some conjugated molecules, *e.g.* tetraarylethylenes,[7] show enhancement of photoluminescence (PL) in the solid state (aggregation-enhanced emission).[8] One of the simplest blue emitters, anthracene,

* Parts of this chapter are published in: Dadvand, A.; Moiseev, A. G.; Sawabe, K.; Sun, W-H.; Djukic, B.; Chung, I.; Takenobu, T.; Rosei, F.; Perepichka. D. F., Maximizing Field-Effect Mobility and Solid-State Luminescence in Organic Semiconductors. **2012**, *Angew. Chem. Int. Ed.* 51, 1 – 6.

exhibits a PL quantum yield (PLQY) of 64% in crystals,[9] but no thin film transistors have been reported for this material. The larger aromatic core in tetracene gives rise to reasonable charge mobility ~0.1 cm^2/Vs in thin-film FET[10] but solid state PLQY drops down to 0.8%, mostly due to the singlet fission.[11] Its tetraphenyl derivative, rubrene, shows highest FET mobility of up to 10–20 cm^2/Vs (in single crystals)[12] but also very low (<1%) PL in the solid state, also attributed to the singlet fission.[6b] A number of other high mobility OSC have been reported,[13] including the record-breaking dinaphthothienothiophene and its derivatives, with mobility of up to 8 cm^2/Vs in thin film[14] and up to 16 cm^2/Vs in single crystals.[15] However, they all show either no or low emission in the solid state. The overall picture emerging from the literature is that maximizing charge mobility in OSC necessarily leads to decreased emission efficiency.

This work breaks this paradigm by showing that a charge mobility of >1 cm^2/Vs can be achieved in a structurally simple OSC that also shows blue EL and PL with PLQY of 70% in the crystalline state. Recently, styrylacenes have emerged as a promising subclass of OSC in which extending the conjugation through the styrene group and keeping the (less stable) acene moiety short allows achieving high field-effect mobility together with good stability.[16] In the previous chapter, a green-emitting OLET based on 2,6-DPSAnt was presented. While a reasonably high hole mobility of ~0.8 cm^2/Vs was measured DPSAnt based OLET, the relatively low solid state PLQY of ~15% suggests emission quenching in the film of this material.

This chapter presents the surprising finding that shrinking the length of the OSC (from bis-styryl substitute of anthracene that of mono-substitute) leads to a new OSC, HPVAnt, with even higher charge mobility and solid state PLQY of 70%. These are the key properties for the development of high-current light emitting devices demonstrating a blue-emitting OLET based on HPVAnt.

6.2 Material characterization: Due to small acene core and lack of reactive moieties, HPVAnt shows high thermal and chemical stability. Density functional theory (DFT) calculations at B3LYP/6-31G(d) level predict the HOMO and LUMO at –5.05 eV and –1.78 eV, respectively. HOMO and LUMO of HPVAnt obtained experimentally from electrochemical redox potentials are –5.47eV and –2.57 eV, respectively (assuming ferrocene at –4.80 eV).

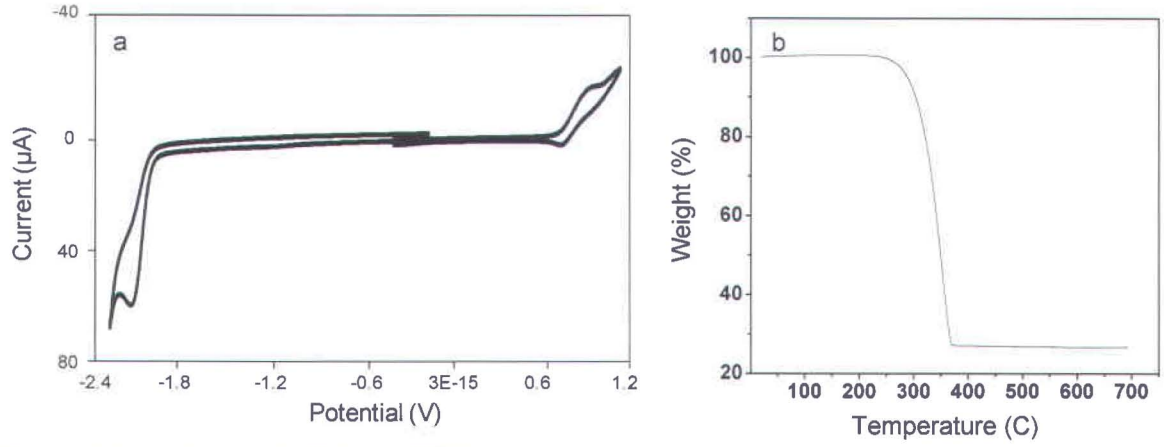

Figure 6.1: a) CV and (b) TGA of **HPVAnt**

A similar HOMO-LUMO gap (3.12 eV) was obtained from the solution absorption spectrum that shows vibronically structured bands at λ_{max}= 362, 378 and 397 nm (Figure 6.2). The PL spectrum is also vibronically structured (λ_{max} = 422 and 438 nm), with a Stokes shift of 0.18 eV. Both absorption and emission are red-shifted in the solid state and the band gap determined from onset absorption is 2.8 eV. High absolute PLQY of 70% measured in integrating sphere in single crystals (up from 55% in solution) makes HPVAnt a good candidate for OLET applications. A lower PLQY of ~20% was observed from thin films, likely due to exciton quenching on surface defects. The same trend was reported for anthracene which exhibits PLQY of 64%, 28% and 18% in single crystal, solution and powder, respectively.[9]

The high observed solid state PLQY might be due to elimination of the singlet fission process in HPVAnt. Indeed, DFT calculations predict that energy of singlet exciton S_1 of styrylanthracene (3.04 eV) is insufficient for generating two triplets (T_1 = 1.74 eV). The calculations are in excellent agreement with experimental measurements for S_1 state (3.06 eV[17]) and the reported triplet energy of 1.77 eV for 2-(4-metylphenylvinyl)antracene,[18] which confirms an endothermic nature of singlet fission and explain high PLQY of HPVAnt crystals. On the other hand, this is in contrast to the discussed above tetracene derivative PPVTet, for which the S_1 energy (2.39 eV) almost exactly matches the energy of two triplets (T_1 = 1.20 eV) thus explaining its low PLQY. Analysis of published photophysical data and our calculations reveals the same trend ($S_1 > 2T_1$) for other high mobility acene semiconductors, including tetracene[6a], pentacene[6a] and rubrene.[19] Accordingly, all of these display strong luminescence quenching in the solid state.

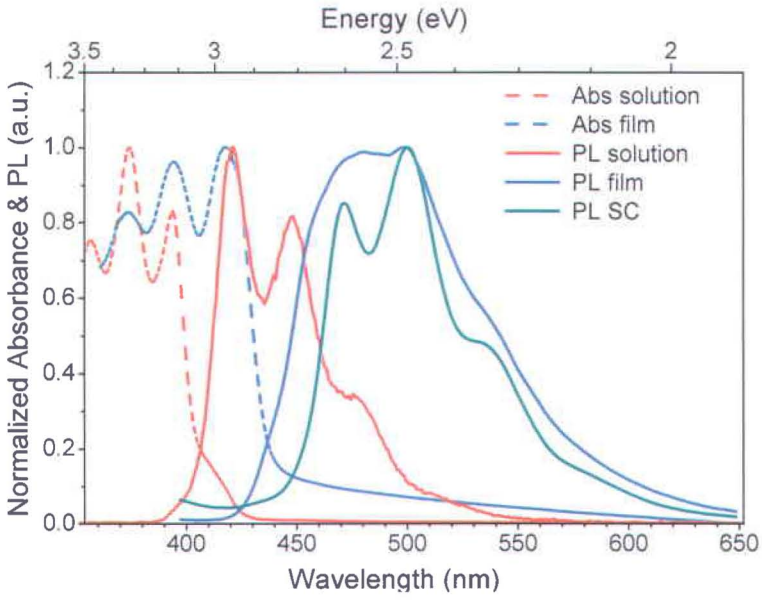

Figure 6.2: Absorption and PL spectra of HPVAnt in solution (2×10^{-5} M in PhCl), thin film (on quartz substrate) and single crystal. The shoulder at 410 nm in solution absorption spectrum is due to equilibrium with *s*-cis conformer.[20]

6.3 Device characteristics: The transistor properties of HPVAnt were studied in thin films (TF) and single crystals (SC), in top-contact configuration (Figure 6.3). Typical output and transfer characteristics of the TF-FET based on HPVAnt are shown in Figures 6.3c and 6.3d. Remarkably, without any device optimization, HPVAnt films grown on bare Si/SiO_2 at room temperature showed an average hole mobility μ^+ of 1.14±0.2 cm^2/Vs with a threshold voltage (V_T) of –20 to –24 V and on/off ratio 10^6–10^7. The highest hole μ measured in these devices was 1.5 cm^2/Vs. It should be noted that the mobility of HPVAnt slightly exceeded that of similar pentacene-based devices fabricated in our lab, despite the higher calculated reorganization energy of the former ($\lambda_{0/+}$ = 0.18 eV (SI) *vs.* 0.098 eV for pentacene[21]). The roughness of the dielectric plays an important role for film growth as somewhat lower mobilities were measured for TF-FETs fabricated on Si/SiO_2 modified with HMDS (0.8±0.1 cm^2/Vs) or PMMA (0.45±0.08 cm^2/Vs) layers.

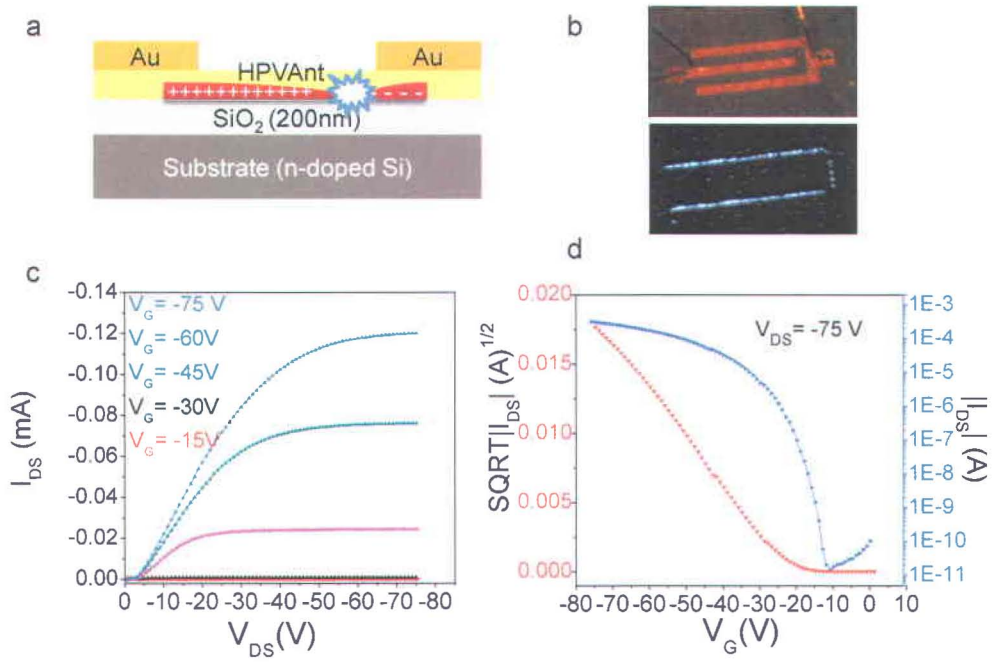

Figure 6.3: Top-contact TF-FET fabricated with HPVAnt: a) schematic; b) optical image and EL of the biased device; d) output and e) transfer characteristics thereof (μ = 1.33 cm^2/Vs, on/off =3×10^7, V_T = –24 V; W/L=1000μm/100μm).

6.4 Material and film morphology: The high observed mobility in TF-FET can be ascribed to the almost perfect layer-by-layer growth that leads to continuous OSC films at low nominal thickness at room temperature, as confirmed with Atomic Force Microscopy (AFM) (Figure 6.4a). The height profile suggests up-right orientation of molecules in the layers. The morphology of the film of HPVAnt grown on PMMA (Figure 6.4b) shows interruption in the smaller size of grains compared to films grown on SiO_2. This can be due to the higher surface energy of PMMA and also increased roughness of the PMMA surface (0.42 nm) compared to that of SiO_2 (0.18 nm). As a consequence, the high number of grain boundaries negatively affects the charge transport.

X-ray diffraction of the vacuum-deposited films corresponds well to that of bulk HPVAnt powder (Figure 6.4c). While the single crystal X-ray diffraction data is of insufficient quality (R=0.40) to deduce the exact inter-/intramolecular distances, the orientation of the molecules in the unit cell is clear (Figure 6.4d) and closely resembles that of the previously reported 2,6-bis[2-(4-pentylphenyl)vinyl]anthracene.[16] The molecules pack in a usual herringbone fashion. The anthracene groups of adjacent molecules align with one another forming two-dimensional sheets perpendicular to the long axis of the anthracene core. Such packing maximizes π-interactions

between the molecules, and it is slightly different from that of other long acenes, including pentacene, which show slippage along the long molecular axis.[22]

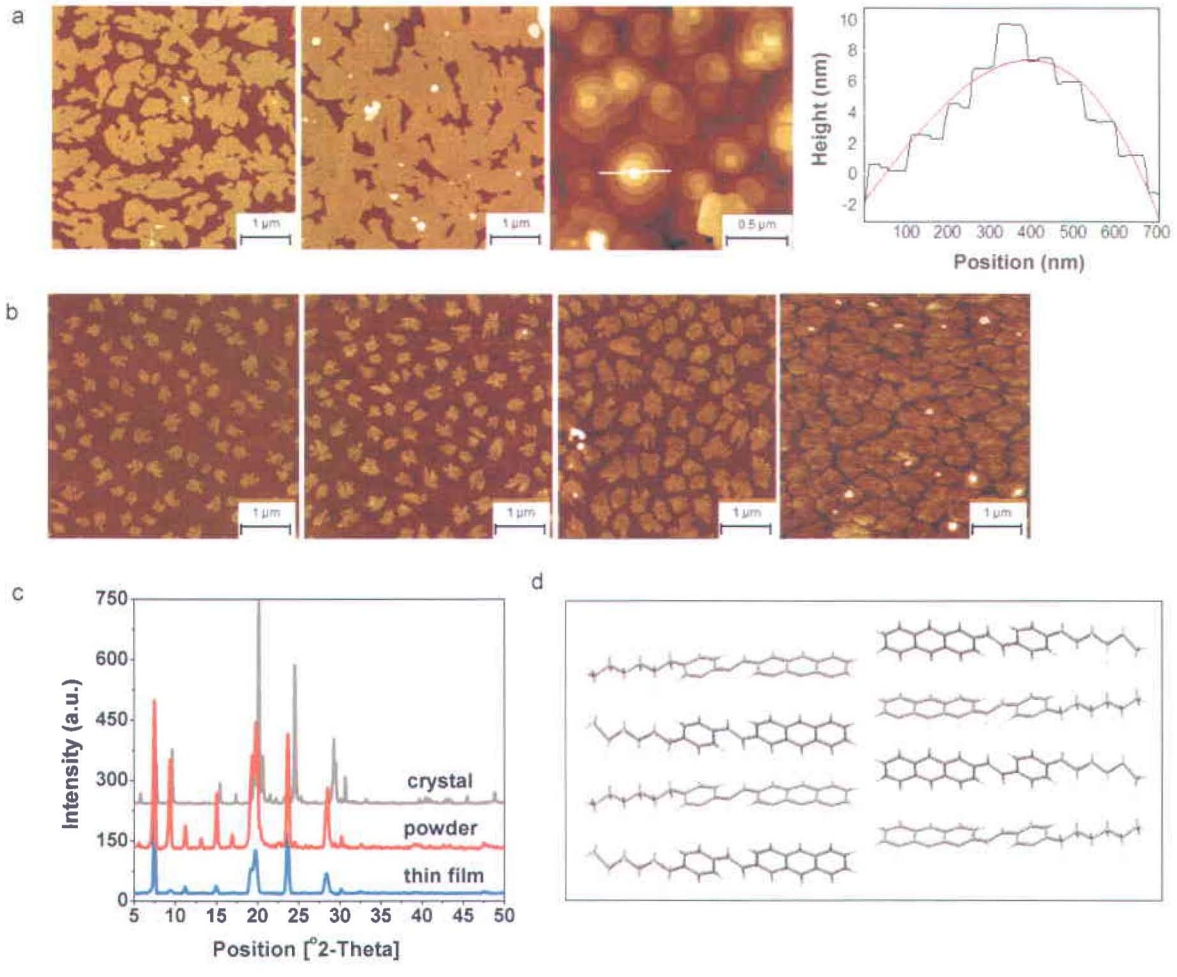

Figure 6.4: Morphological characterization of HPVAnt: a) AFM of films on Si/SiO_2 and b) on PMMA at different thickness ; c) diffraction pattern for thin film (blue), powder (red) and calculated from single crystal data (grey). Analysis reveals a monoclinic unit cell with a=5.92Å, b=7.56Å, c=47.14Å; β=91.4°; d) packing model deduced from diffraction data.

6.5 EL and stability of HPVAnt-based TF-FETs: The bias stress effects and device shelf stability are critical for the application of OSC.[23] HPVAnt-based TF-FETs made on bare SiO_2/Si showed excellent stability in >20,000 operating cycles (V_G=0...–70V) under vacuum (only small variation of the mobility and the threshold voltage: $\mu^+ = 1.01\pm0.09$ cm^2/Vs, $V_T = -24\pm1$ V, Figure 6.5). The on/off ratio was unchanged and no obvious hysteresis was observed. TF-FETs made on untreated Si/SiO_2 are less stable when operating in air. For testing in ambient conditions, HPVAnt films were grown on PMMA-coated Si/SiO_2 substrate. Such devices

demonstrated almost constant mobility of 0.5±0.05 cm^2/Vs and only a slight shift of the threshold voltage (from 20 to 23 V) for over 20,000 cycles (continuous 18h run). Storage of unencapsulated devices in ambient lab environment (exposed to air and light) shows excellent shelf-life stability for TF-FETs (a small drop of mobility from 1 cm^2/Vs to 0.9 cm^2/Vs over three months storage, exposed to laboratory light and atmosphere).

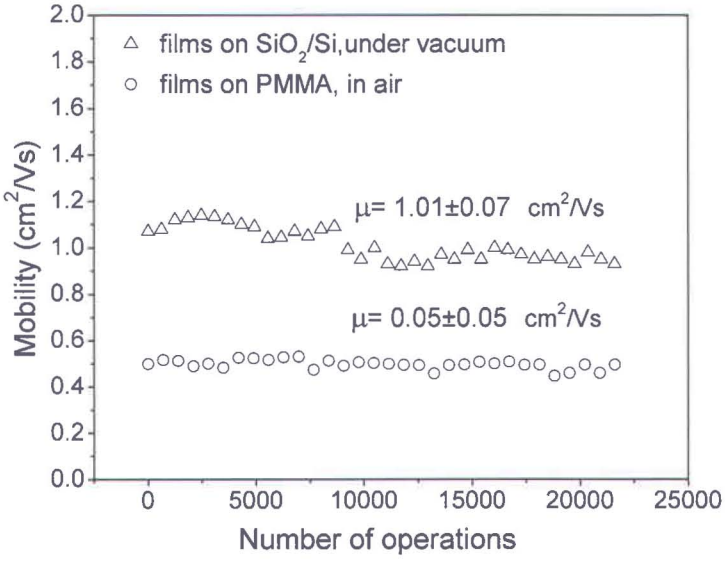

Figure 6.5: Bias stress measurements of TF-FETs in air and under vacuum (each operation presents a sweep of V_G from 0 to –75 V, keeping V_{DS} = –75 V)

Besides excellent transistor characteristics, almost all devices showed blue EL modulated by gate voltage V_G (Figure 6.3b). As in other OLET devices with a single carrier majority channel, the emission zone is concentrated in the vicinity of the drain electrode[3b] Because of the used top-contact configuration, most of the emitted light is thus buried under the drain. The intense blue emission is nevertheless clearly visible at the electrode edges. *Unlike* in other single layer OLETs, the emission of HPVAnt shows no "fatigue" effect, i.e. does not fade out during continuous operation. Figure 6.5 shows the modulated EL intensity of HPVAnt films grown on PMMA coated dielectric with applied V_G and V_{DS}. The emission on PMMA coated devices seems to be more intense compared to those of bare SiO_2/Si at a similar applied bias (Figure 6.6). This is due to the passivated surface from silanol groups in PMMA-coated devices.

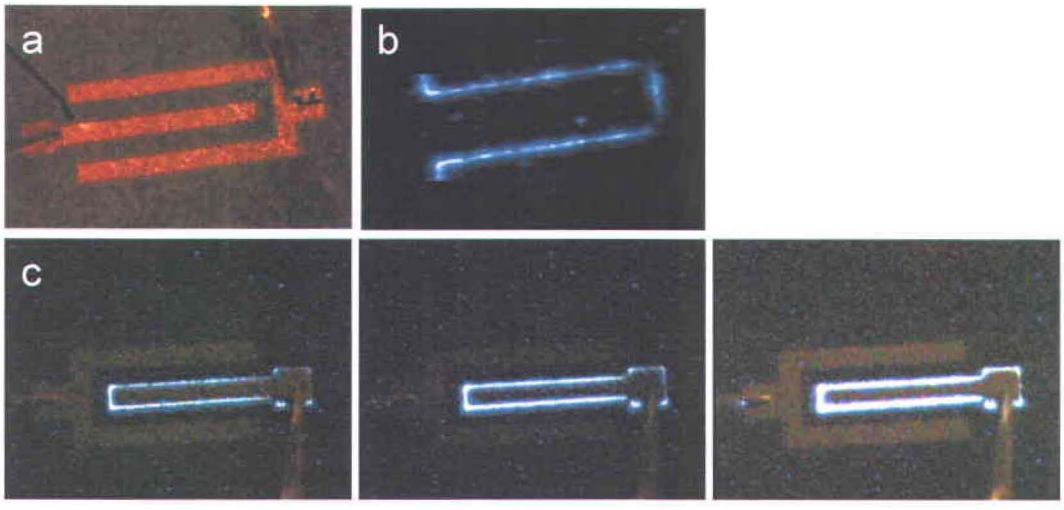

Figure 6.6: Optical images of (a) TF-FET device, (b) EL from TF-FET based on HPVAnt films grown on Si/SiO_2 substrate (c) modulated EL intensity with applied V_G and V_{DS}.

It is important to know that only a few blue-emitting OLET have been reported to date;[24] the highest field-effect mobility, measured for 4,4'-distyrylbiphenyl, was 0.01 cm^2/Vs (PLQY =20%).[24b]

6.6 HPVAnt-based SC-FETs: The performance of HPVAnt in single crystal OFET was also investigated. Single crystals of HPVAnt were grown from the vapor phase in a flow of argon.[25] SC-FET structures were prepared by laminating the crystals against PMMA-coated Si/SiO_2 substrate followed by patterning source and drain electrodes by shadow-mask evaporation (Figure 6.7a). Due to the relatively large thickness of the crystals (a few microns), the top metal contacts are located far from the charge accumulation zone (HPVAnt/PMMA interface), leading to a significant contact resistance.

Depending on crystal thickness, the buffer layer (MoO_3, CsF) and the electrode (Au or Ca), hole mobility was in the range 0.75–2.62 cm^2/Vs. Remarkably, the current density achieved in saturation regime (>40 kA/cm^2) exceeds that of the rubrene-based SC-FET devices[3c] (Figure 6.7d). Furthermore, an ambipolar behavior with electron mobility in the range of 0.04–0.13 cm^2/Vs was measured for SC-FET (Figure 6.7c).

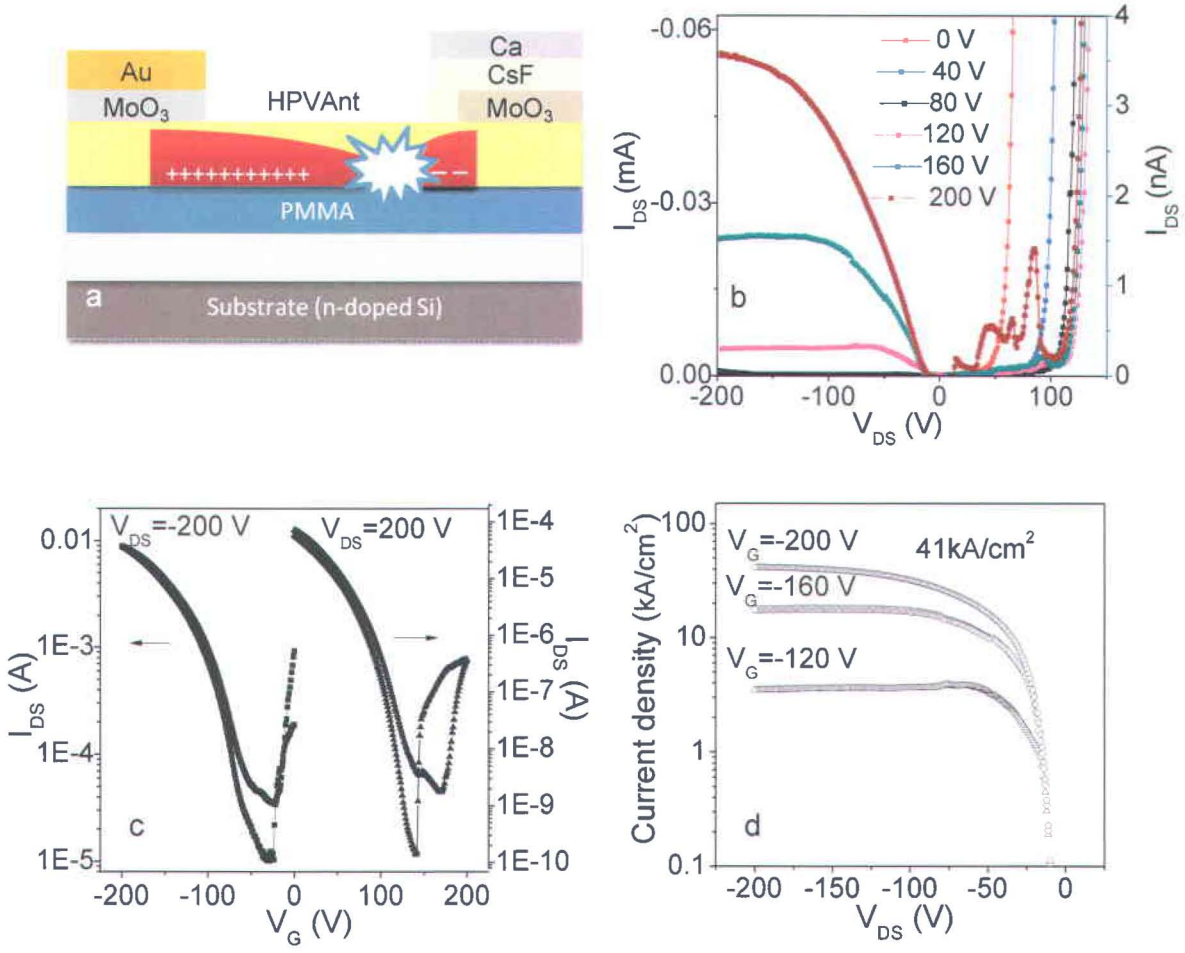

Figure 6.7: SC-FET fabricated with HPVAnt: a) schematic; b) output and c) transfer characteristics showing ambipolar behaviour (d) the current density was calculated assuming channel thickness of 1 nm, to make direct comparison to rubrene-based devices[3c].

The light-emitting properties of HPVAnt in SC-FETs configuration were also investigated. The optical image of the device and PL of the single crystal are displayed in Figures 6.8a and 6.8b. The EL spectrum closely resembles the PL; the emission band is broadened but the λ_{max} (490 nm) is not shifted (Figure 6.8c). Figure 6d shows optical images of EL taken from the surface of a device operating at fixed gate voltage (–200 V) while sweeping drain-source between 0 V and –200 V. At lower operating bias, EL is dominated by hole transport and the emission zone is close to the drain electrode. However, increasing the electron injection at higher V_{DS} progressively extends the light emission zone toward the source electrode, confirming the ambipolarity of HPVAnt SC-FET. The width of the charge recombination zone, W_z, (thus emission zone) is material dependent. The recent study on the recombination zone in ambipolar single crystal LETs suggests W_z ranging between 2 μm to 12 μm assuming that the

recombination zone size is equal to that of the emission zone.[26] Emission zone in HPVAnt SC-FET, however, extends over 100 μm. In order to verify this observation is not due to self-waveguide of the emission along the crystal plane, the EL of TF-FETs based on HPVAnt (~50 nm) and incorporating a thin layer (~5 nm) of Alq3 as buffer layer was investigated (Figure 6.9). Alq3 was employed to reduce the mismatch between workfunction of Au electrode and LUMO of HPVAnt, facilitating the electron injection and thus enhancing the exciton creation in heterostructure OLET.

The emission zone in this device also extended all across the OLET channel and completely covered the area between two electrodes. The blue emission of HPVAnt, however, was mixed with the green EL of Alq3. This experiment confirms the extension of the emission zone observed in SC-FETs which is promising for the potential application of this material and in EL displays.

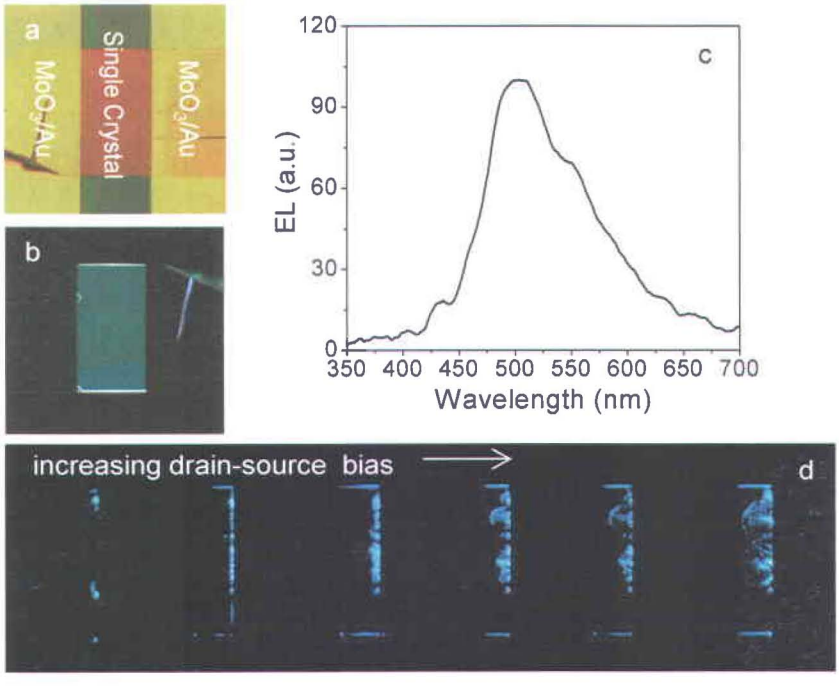

Figure 6.8: Light-emitting behavior of SC-FET: (a) optical image; (b) PL upon UV excitation; (c) EL spectrum of biased device; (d) shift of the EL zone upon increasing bias

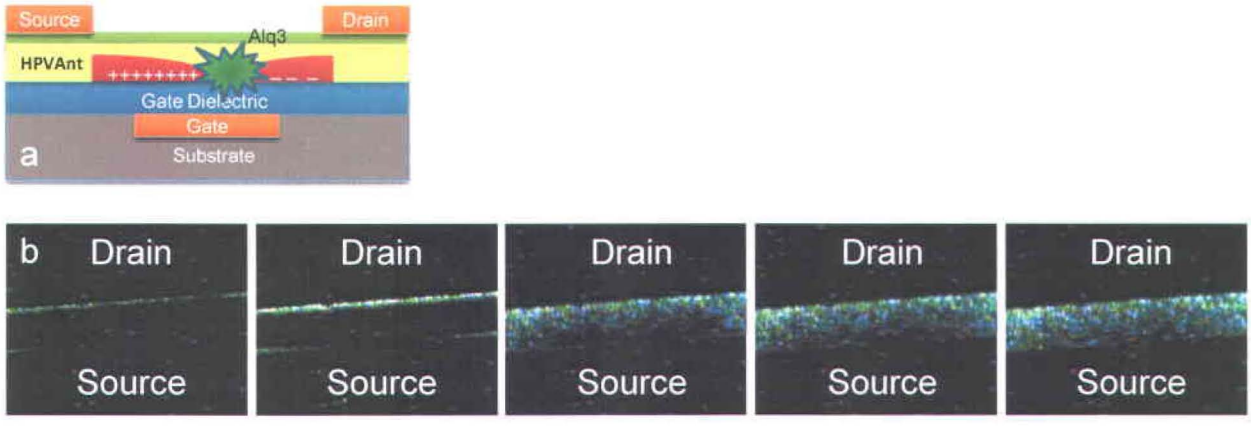

Figure 6.9: TF-FET based on HPVAnt and Alq3: (a) schematic; (b) shift of the EL zone upon increasing bias.

Conclusion: This work demonstrates a new structurally simple aromatic hydrocarbon HPVAnt which exhibits a unique combination of high field-effect mobility of up to 1.5 cm^2/Vs in thin films (2.6 cm^2/Vs in single crystals), strong solid state emission and exceptional operational stability in air with almost no degradation in $>10^4$ cycles. Both thin-film and single-crystal transistors showed bright blue EL stable under continuous operation; this accounts for the highest mobility OLET prepared to date. Importantly, high PLQY of 70% achieved for HPVAnt crystals disproves the common belief that the strong π-π interactions required for high charge mobility necessarily lead to quenching of the luminescence in the solid state. This could be attributed to high energy of the excited state T_1 relative to S_1 ($2T_1 > S_1$) which turns off emission quenching through singlet fission, thus suggesting a new design principle for achieving other highly emissive crystalline OSC.

Other designs of the styryl-substituted oligoacenes such as 2-(4-hexylstyryl)naphthalene were also tested for OLET application. However, they did not show efficient charge mobility likely due to the short conjugation length or the nature of their crystal packing in solid-state. Investigation on the optoelectronic properties of the studied styryl-substitute of oligoacenecs in this thesis suggest that HPVAnt is the optimum structure which combines the necessary requirements for application in OLETs configuration. For the perspective of this work, one can think of a modification of the chemical structure of HPVAnt in order to reduce the LUMO energy and facilitate the electron injection from the drain electrode for the efficient excite formation.

References

[1] Forrest, S. R., The path to ubiquitous and low-cost organic electronic appliances on plastic. *Nature* **2004,** *428* (6986), 911-918.

[2] Gather, M. C.; Kohnen, A.; Meerholz, K., White Organic Light-Emitting Diodes. *Adv Mater* **2011,** *23* (2), 233-248.

[3]a) Hepp, A.; Heil, H.; Weise, W.; Ahles, M.; Schmechel, R.; von Seggern, H., Light-emitting field-effect transistor based on a tetracene thin film. *Phys Rev Lett* **2003,** *91*, 157406. b) Cicoira, F.; Santato, C.; Dinelli, F.; Murgia, M.; Loi, M. A.; Biscarini, F.; Zamboni, R.; Heremans, P.; Muccini, M., Correlation between morphology and field-effect-transistor mobility in tetracene thin films. *Adv Funct Mater* **2005,** *15* (3), 375-380. c) Capelli, R.; Toffanin, S.; Generali, G.; Usta, H.; Facchetti, A.; Muccini, M., Organic light-emitting transistors with an efficiency that outperforms the equivalent light-emitting diodes. *Nat Mater* **2010,** *9* (6), 496-503. d) Santato, C.; Cicoira, F.; Martel, R., Organic Photonics Spotlight on organic transistors. *Nat Photonics* **2011,** *5* (7), 392-393. e) Bisri, S. Z.; Takenobu, T.; Sawabe, K.; Tsuda, S.; Yomogidao, Y.; Yamao, T.; Hotta, S.; Adachi, C.; Iwasa, Y., p-i-n Homojunction in Organic Light-Emitting Transistors. *Adv Mater* **2011,** *23* (24), 2753-2758. f) Takenobu, T.; Bisri, S. Z.; Takahashi, T.; Yahiro, M.; Adachi, C.; Iwasa, Y., High current density in light-emitting transistors of organic single crystals. *Phys Rev Lett* **2008,** *100*, 066601.

[4] a) Samuel, I. D. W.; Turnbull, G. A., Organic semiconductor lasers. *Chem Rev* **2007,** *107* (4), 1272-1295. b) Namdas, E. B.; Tong, M.; Ledochowitsch, P.; Mednick, S. R.; Yuen, J. D.; Moses, D.; Heeger, A. J., Low Thresholds in Polymer Lasers on Conductive Substrates by Distributed Feedback Nanoimprinting: Progress Toward Electrically Pumped Plastic Lasers. *Adv Mater* **2009,** *21* (7), 799-802.

[5] a) Perepichka, I. F.; Perepichka, D. F.; Meng, H.; Wudl, F., Light-emitting polythiophenes. *Adv Mater* **2005,** *17* (19), 2281-2305. b) Taranekar, P.; Qiao, Q.; Jiang, H.; Ghiviriga, I.; Schanze, K. S.; Reynolds, J. R., Hyperbranched conjugated polyelectrolyte bilayers for solar-cell applications. *J Am Chem Soc* **2007,** *129* (29), 8958-8959.

[6] a) Smith, M. B.; Michl, J., Singlet Fission. *Chem Rev* **2010,** *110* (11), 6891-6936. b) Najafov, H.; Lee, B.; Zhou, Q.; Feldman, L. C.; Podzorov, V., Observation of long-range exciton diffusion in highly ordered organic semiconductors. *Nat Mater* **2010,** *9* (11), 938-943.

[7] Wang, W. Z.; Lin, T. T.; Wang, M.; Liu, T. X.; Ren, L. L.; Chen, D.; Huang, S., Aggregation Emission Properties of Oligomers Based on Tetraphenylethylene. *J Phys Chem B* **2010,** *114* (18), 5983-5988.

[8] a) Deans, R.; Kim, J.; Machacek, M. R.; Swager, T. M., A poly (p-phenyleneethynylene) with a highly emissive aggregated phase. *J Am Chem Soc* **2000,** *122* (35), 8565-8566. b) Luo, J. D.; Xie, Z. L.; Lam, J. W. Y.; Cheng, L.; Chen, H. Y.; Qiu, C. F.; Kwok, H. S.; Zhan, X. W.; Liu, Y. Q.; Zhu, D. B.; Tang, B. Z., Aggregation-induced emission of 1-methyl-1,2,3,4,5-pentaphenylsilole. *Chem Commun* **2001,** (18), 1740-1741.

[9] Katoh, R.; Suzuki, K.; Furube, A.; Kotani, M.; Tokumaru, K., Fluorescence Quantum Yield of Aromatic Hydrocarbon Crystals. *J Phys Chem C* **2009,** *113* (7), 2961-2965.

[10] Gundlach, D. J.; Nichols, J. A.; Zhou, L.; Jackson, T. N., Thin-film transistors based on well-ordered thermally evaporated naphthacene films. *Appl Phys Lett* **2002,** *80* (16), 2925-2927.

[11] Lim, S. H.; Bjorklund, T. G.; Spano, F. C.; Bardeen, C. J., Exciton delocalization and superradiance in tetracene thin films and nanoaggregates. *Phys Rev Lett* **2004,** *92,* 107402.

[12]a) Menard, E.; Podzorov, V.; Hur, S. H.; Gaur, A.; Gershenson, M. E.; Rogers, J. A., High-performance n- and p-type single-crystal organic transistors with free-space gate dielectrics. *Adv Mater* **2004,** *16*, 2097-2101. b) Takeya, J.; Nishikawa, T.; Takenobu, T.; Kobayashi, S.; Iwasa, Y.; Mitani, T.; Goldmann, C.; Krellner, C.; Batlogg, B., Effects of polarized organosilane self-assembled monolayers on organic single-crystal field-effect transistors. *Appl Phys Lett* **2004,** *85* (21), 5078-5080.

[13] a) Wu, W. P.; Liu, Y. Q.; Zhu, D. B., pi-Conjugated molecules with fused rings for organic field-effect transistors: design, synthesis and applications. *Chem Soc Rev* **2010,** *39* (5), 1489-1502. b) Anthony, J. E.; Facchetti, A.; Heeney, M.; Marder, S. R.; Zhan, X. W., n-Type Organic Semiconductors in Organic Electronics. *Adv Mater* **2010,** *22* (34), 3876-3892. c) Allard, S.; Forster, M.; Souharce, B.; Thiem, H.; Scherf, U., Organic semiconductors for solution-processable field-effect transistors (OFETs). *Angew Chem Int Edit* **2008,** *47* (22), 4070-4098. d) Murphy, A. R.;

Frechet, J. M. J., Organic semiconducting oligomers for use in thin film transistors. *Chem Rev* **2007,** *107* (4), 1066-1096.

[14] Kang, M. J.; Doi, I.; Mori, H.; Miyazaki, E.; Takimiya, K.; Ikeda, M.; Kuwabara, H., Alkylated Dinaphtho[2,3-b:2 ',3 '-f]Thieno[3,2-b] Thiophenes (C(n)-DNTTs): Organic Semiconductors for High-Performance Thin-Film Transistors. *Adv Mater* **2011,** *23* (10), 1222-1225.

[15] Sokolov, A. N.; Atahan-Evrenk, S.; Mondal, R.; Akkerman, H. B.; Sanchez-Carrera, R. S.; Granados-Focil, S.; Schrier, J.; Mannsfeld, S. C. B.; Zoombelt, A. P.; Bao, Z. N.; Aspuru-Guzik, A., From computational discovery to experimental characterization of a high hole mobility organic crystal. *Nat Commun* **2011,** *2*, 437.

[16] a) H Meng, H.; Sun, F. P.; Goldfinger, M. B.; Gao, F.; Londono, D. J.; Marshal, W. J.; Blackman, G. S.; Dobbs, K. D.; Keys, D. E., 2,6-bis[2-(4-pentylphenyl)vinyl]anthracene: A stable and high charge mobility organic semiconductor with densely packed crystal structure. *J Am Chem Soc* **2006,** *128* (29), 9304-9305. b) Klauk, H.; Zschieschang, U.; Weitz, R. T.; Meng, H.; Sun, T.; Nunes, G.; Keys, D. E.; Fincher, C. R.; Xiang, Z., Organic transistors based on di(phenylvinyl)anthracene: Performance and stability. *Adv Mater* **2007,** *19* (22), 3882-3887. c) Cicoira, F.; Santato, C.; Dadvand, A.; Harnagea, C.; Pignolet, A.; Bellutti, P.; Xiang, Z.; Rosei, F.; Meng, H.; Perepichka, D. F., Environmentally stable light emitting field effect transistors based on 2-(4-pentylstyryl)tetracene. *J Mater Chem* **2008,** *18* (2), 158-161.

[17] S_1 state was determined as a cross-point of the absorption and emission spectra (406 nm).

[18] Shaw, J. R.; Webb, R. T.; Schmehl, R. H., Intersystem Crossing to Both Ligand-Localized and Charge-Transfer Excited-States in Mononuclear and Dinuclear Ruthenium(Ii) Diimine Complexes. *J Am Chem Soc* **1990,** *112* (3), 1117-1123.

[19] Higgins, R. W. T.; Monkman, A. P.; Nothofer, H. G.; Scherf, U., Effects of singlet and triplet energy transfer to molecular dopants in polymer light-emitting diodes and their usefulness in chromaticity tuning. *Appl Phys Lett* **2001,** *79* (6), 857-859.

[20] Fischer, G. & Fischer, E. Conformational equilibria in trans-1,2-diarylethylenes manifested in their emission-spectra. 4. 3-Anthryl and 3-pyrenyl derivatives. *J. Phys. Chem.* **85**, 2611-2613 (1981).

[21] Gruhn, N. E.; da Silva, D. A.; Bill, T. G.; Malagoli, M.; Coropceanu, V.; Kahn, A.; Bredas, J. L., The vibrational reorganization energy in pentacene: Molecular influences on charge transport. *J Am Chem Soc* **2002,** *124* (27), 7918-7919.

[22] Anthony, J. E., The larger acenes: Versatile organic semiconductors. *Angew Chem Int Edit* **2008,** *47* (3), 452-483.

[23] Sirringhaus, H., Reliability of Organic Field-Effect Transistors. *Adv Mater* **2009,** *21* (38-39), 3859-3873.

[24] a) Oyamada, T.; Chang, C. H.; Chao, T. C.; Fang, F. C.; Wu, C. C.; Wong, K. T.; Sasabe, H.; Adachi, C., Optical properties of oligo(9,9-diarylfluorene) derivatives in thin films and their application for organic light-emitting field-effect transistors. *J Phys Chem C* **2007,** *111* (1), 108-115. b) Sakanoue, T.; Yahiro, M.; Adachi, C.; Uchiuzou, H.; Takahashi, T.; Toshimitsu, A., Ambipolar light-emitting organic field-effect transistors using a wide-band-gap blue-emitting small molecule. *Appl Phys Lett* **2007,** *90*, 171118. c) Nakanotani, H.; Kabe, R.; Yahiro, M.; Takenobu, T.; Iwasa, Y.; Adachi, C., Blue-light-emitting ambipolar field-effect transistors using an organic single crystal of 1,4-Bis(4-methylstyryl)benzene. *Appl Phys Express* **2008,** *1*, 091801.

[25] Roberson, L. B.; Kowalik, J.; Tolbert, L. M.; Kloc, C.; Zeis, R.; Chi, X. L.; Fleming, R.; Wilkins, C., Pentacene disproportionation during sublimation for field-effect transistors. *J Am Chem Soc* **2005,** *127* (9), 3069-3075.

[26] Bisri, S. Z.; Takenobu, T.; Sawabe, K.; Tsuda, S.; Yomogidao, Y.; Yamao, T.; Hotta, S.; Adachi, C.; Iwasa, Y., p-i-n Homojunction in Organic Light-Emitting Transistors. *Adv Mater* **2011,** *23* (24), 2753-2758.

Résumé en Français

La découverte de la conductivité électrique des polymères organiques en 1977 par Heeger, MacDiarmid et Shirakawa[1,2] a eu un fort impact dans le vaste domaine de la microélectronique organique, offrant ainsi de nouvelles perspectives pour la fabrication des composants plastiques à bas prix. Durant ces dernières années, ce nouveau domaine de recherche, généralement appelé "électronique organique", a considérablement progressé. Cette nouvelle technologie commence à s'imposer de manière significative dans le monde commercial, et grâce à un progrès continu, devient même un pilier de la recherche technologique.[3] L'intérêt grandissant pour les matériaux Semi-conducteurs Organiques (SCOs) provient de leurs utilisations profitables au sein de dispositifs électroniques tels que les Transistors Organiques à Effet de Champ (TOEC), les Diodes Organiques Électroluminescentes (DOE), ou les Cellules Photovoltaïques (PV). Les matériaux organiques qui peuvent être employés comme semi-conducteurs actifs incluent de petites molécules et des polymères, utilisés pour préparer des films minces par sublimation sous-vide ou par traitement en solution, comme la tournette ou le dépôt par goutte. Le pentacène, les oligothiophènes, ou bien le polythiophène de phtalocyanine et d'hexadecafluoro-cuivre (molécules) sont quelques exemples de matériaux organiques utilisés en électronique.[4,5,6,7]

Le choix illimité de matériaux organiques permet de nombreuses possibilités pour développer des technologies de circuit intégré basées sur les TOECs, pour des applications peu coûteuses et sur de grandes surfaces.[8,9,10,11] La flexibilité mécanique des matériaux organiques les rend naturellement compatibles avec les substrats plastiques, permettant ainsi de concevoir des produits souples et légers. Les Étiquettes d'Identification par Fréquence Radio (EIFRs), les sondes portatives, le papier électronique et l'Affichage sur Écran Plat (AEPs) ne sont qu'une partie des applications des TOECs.[12,13] Les TOECs sont beaucoup plus intéressants car plus simples à fabriquer que leurs homologues à base de silicium qui requièrent des procédés de dépôt à haute température et sous vide poussé, ainsi que des méthodes de gravure photo-lithographique sophistiquées.[14] Cependant, la plupart des matériaux organiques possédant une conductivité faible, ils ne peuvent pas rivaliser avec les transistors à effet de champ à base de semi-conducteurs inorganiques monocristallins, en particulier dans les applications qui exigent un fort taux de commutation. De plus, une tension de travail supérieure à 30 V est souvent nécessaire

pour obtenir un courant suffisant au sein des TOECs. Il convient alors de diminuer la tension de travail afin de satisfaire aux conditions d'utilisation de nombreuses applications. La stabilité et la durée de vie de ces composants sont également des facteurs importants. La majorité des matériaux organiques réagissent avec l'air environnant. Ceci induit une évolution des paramètres et une réduction des performances. L'encapsulation des composants ou l'ingénierie moléculaire sont différentes manières de minimiser l'instabilité des matériaux. De nombreux efforts sont faits pour améliorer les performances de ces dispositifs : la structure de la molécule, du substrat diélectrique, et de l'interface du semi-conducteur organique avec le diélectrique de grille sont quelques uns des paramètres qui influencent directement le transport des porteurs de charge. Chaque paramètre joue un rôle important dans les performances des dispositifs. Par exemple, l'utilisation d'un diélectrique de grille de faible épaisseur ou avec une grande permittivité permet d'augmenter la capacité de l'isolant, et d'accumuler ainsi une densité plus élevée des charges pour une même tension de grille. Diminuer la longueur du canal peut également permettre de réduire la tension de travail et d'augmenter la vitesse d'opération.

La synthèse de nouvelles molécules organiques aux structures et aux propriétés élaborées, et le dépôt de ces molécules en couches minces sur divers substrats ouvrent un champ de recherche passionnant dans l'électronique organique.[15,16,17,18] Comme mentionné précédemment, les TOECs et les DOEs ont beaucoup d'applications dans l'éclairage, l'affichage, et au sein des circuits. La combinaison des propriétés d'émission des DOEs avec la propriété de commutation des TOECs ouvre la voie à une nouvelle classe de dispositifs électro-optiques à architecture innovante, en rapport avec la recombinaison des porteurs de charges et l'émission de lumière par des matériaux organiques.[19]

Les SCOs ont été dès le début décrits comme étant de type n ou p. Un semi-conducteur de type n correspond à un matériau transporteur d'électron, caractérisé par une haute affinité électronique, et beaucoup de molécules ont été envisagées relativement à cette caractéristique, comme le Naphtalène TétraCarboxylique Dianhydride (NTCDA), et une grande série de dérivés de pérylènes tels que le Pérylène Dianhydride Tétra-Carboxylique (PTCDA). Certains polymères conjugués comme le polyacétylène, peuvent délibérément être dopés n *via* l'implantation d'ions (Li^+), mais ces petits ions dopants sont mobiles en présence d'un champ électrique, ce qui n'est pas compatible avec le fonctionnement des dispositifs. Les dispositifs de type n ont une mobilité

de porteurs de charge inférieure et une grande sensibilité à l'oxygène et à l'humidité contenus dans l'air. Cependant, la majorité des TOECs sont fabriqués avec des matériaux organiques connus comme étant de type p. Les SCOs peut être monocristaux, poly-cristaux, ou amorphe. Les monocristaux montrent une meilleure mobilité tandis que dans le cas des matériaux polycristallins, les joints de grain peuvent limiter la conduction. Les petites molécules peuvent donner les films poly-cristaux ou de monocristaux. Les Tableaux suivants donnent la structure moléculaire et la caractérisation de transistor organique de différents matériaux: monocristaux, poly-cristaux, et des polymères.

Schème A. Structure moléculaire et Caractérisation de transistor organique basée sur 'heteroacenes'[1]

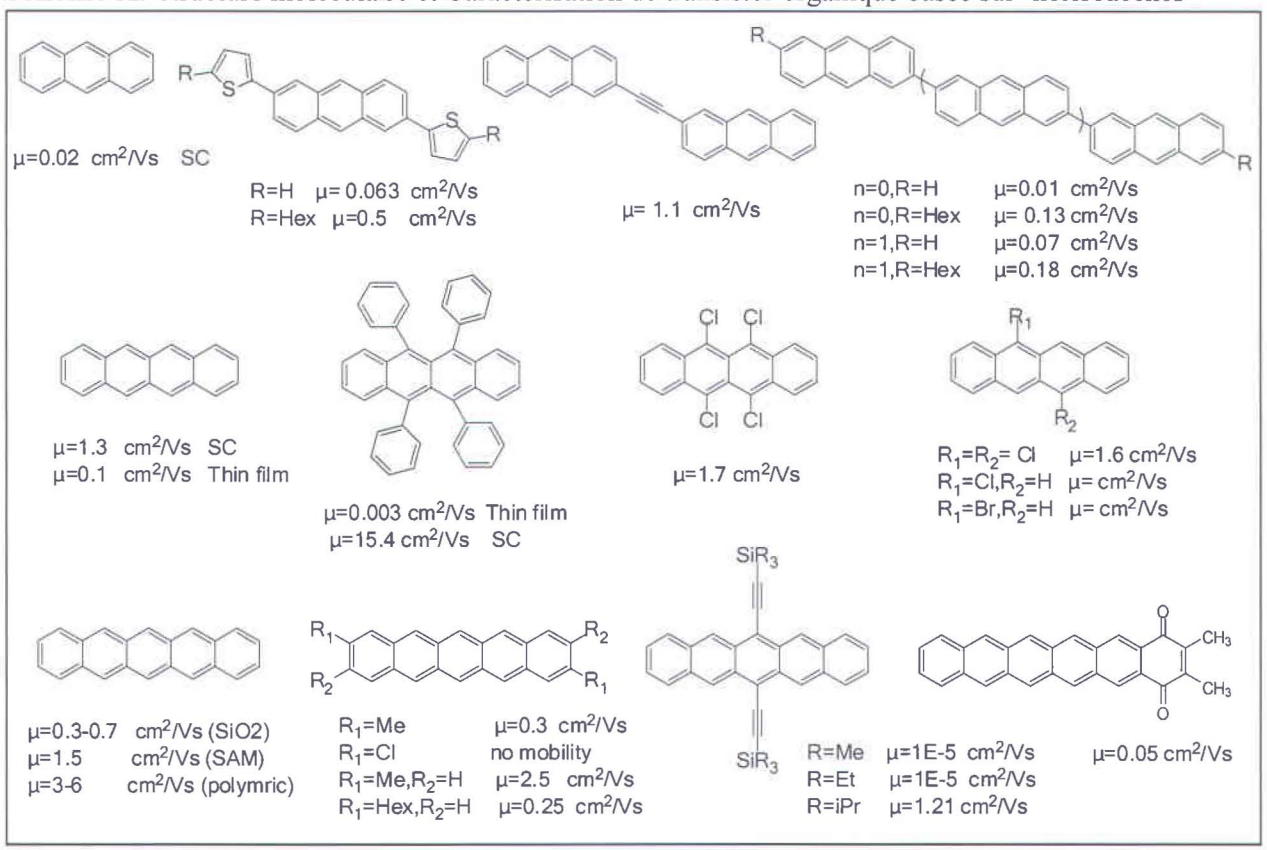

[1] "Organic Thin Film Transistors", Z. Bao and J.J. Locklin Eds, CRC Press, 2007.

Schème B. Structure moléculaire et Caractérisation de transistor organique basée sur 'thioacenes-oligomers'[2]

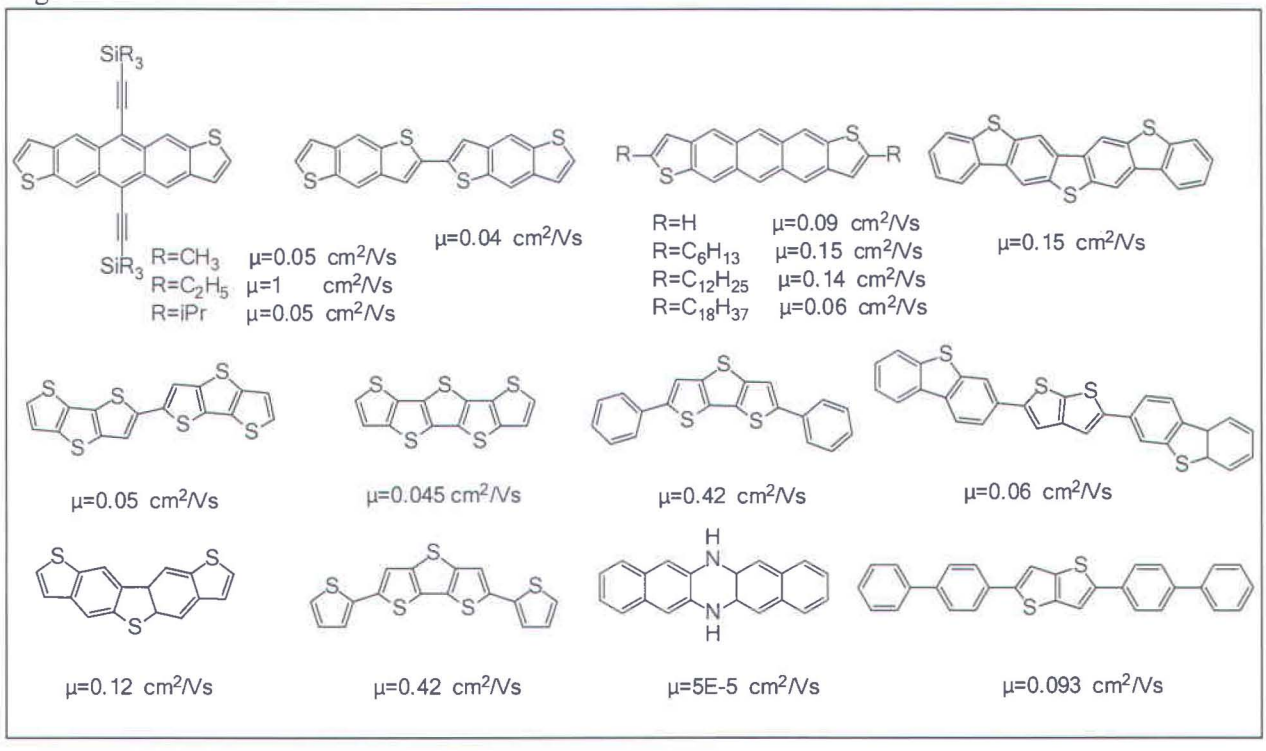

Schème C. Structure moléculaire et Caractérisation de transistor organique basée sur 'les dérivés de oligothiophène'[2]

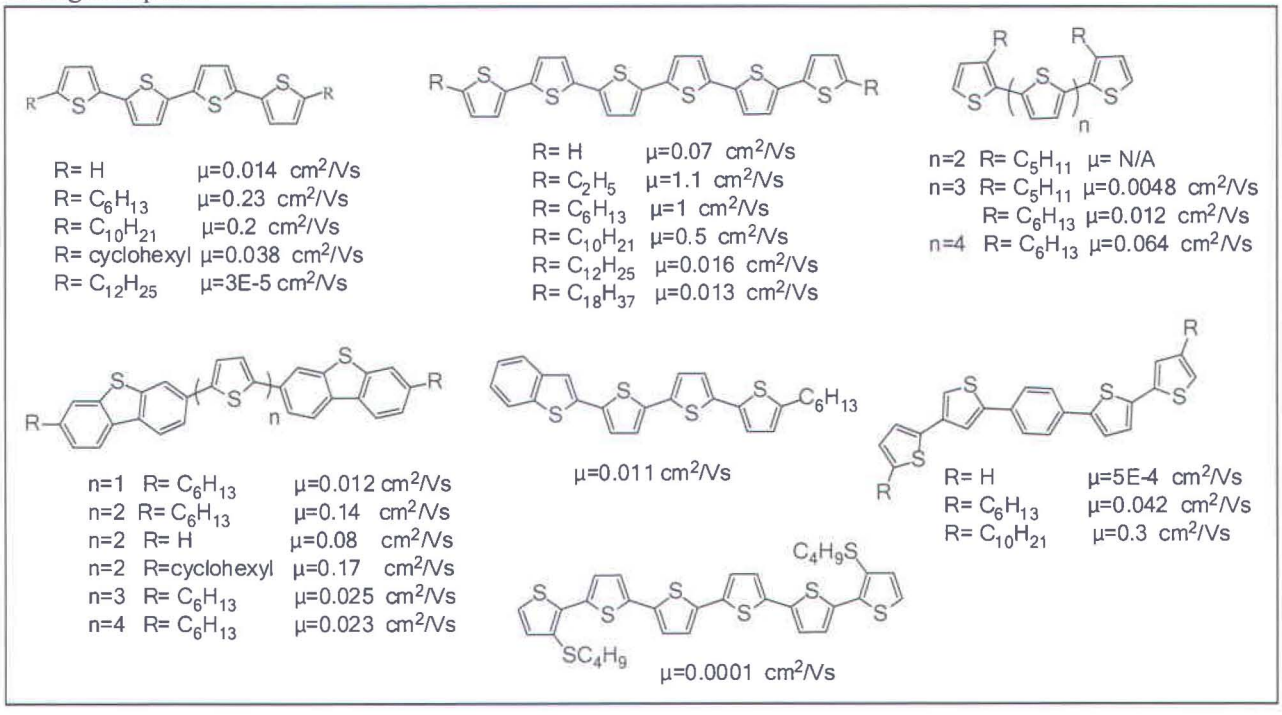

[2] "Organic Thin Film Transistors", Z. Bao and J.J. Locklin Eds, CRC Press, 2007.

Schème D. Structure moléculaire et Caractérisation de transistor organique basée sur 'les polymères conjugués'[2]

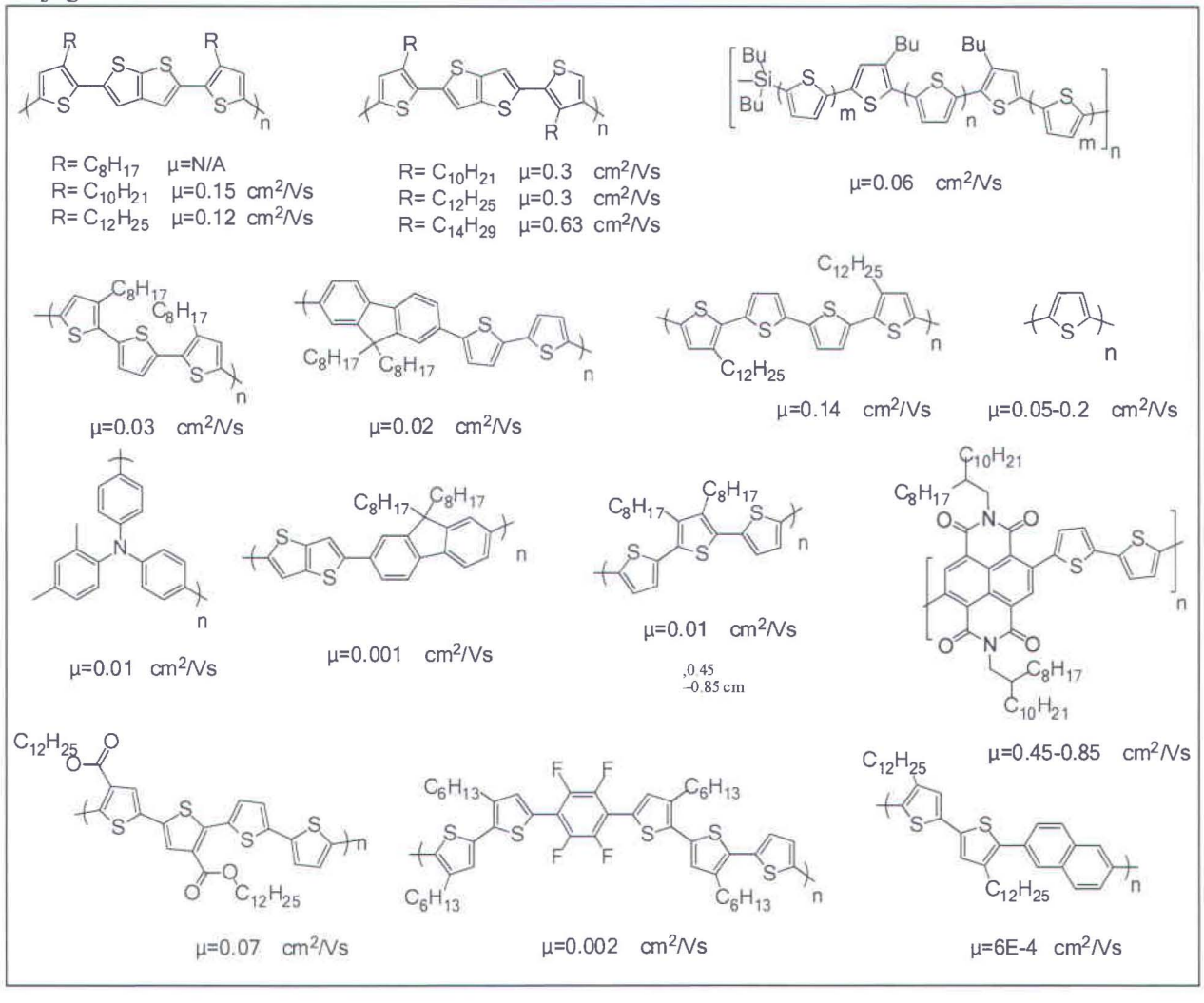

Les transistors à effet de champ sont composés de trois parties - un isolant, une couche mince de semi-conducteur, et trois électrodes. Deux des électrodes, la source et le drain, sont en contact direct avec le semi-conducteur; la troisième, la grille, est isolée du semi-conducteur par l'isolant. La structure du dispositif est régie non seulement par son mode de fonctionnement, mais également par les imperfections inhérentes à sa fabrication. Le schéma de fabrication de base consiste à empiler des couches minces de différents éléments. Puisque la plupart des semi-conducteurs organiques sont les matériaux fragiles, le dépôt des SCOs sur l'isolant est beaucoup plus facile que l'inverse. C'est pourquoi la grande majorité des TOECs actuels sont construits selon l'architecture bottom-gate « grille en bas », qui se décline alternativement en deux configurations, bottom-contact « contact en bas » et top-contact « contact en haut ».

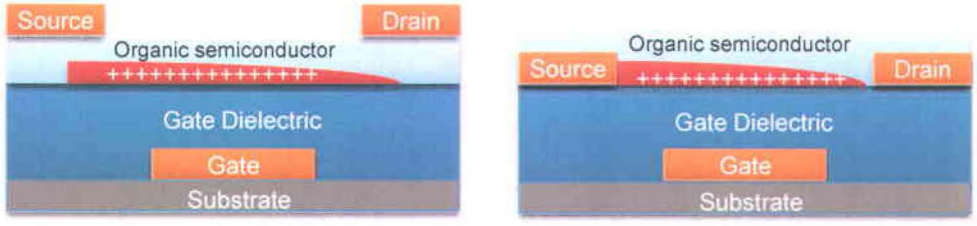

Figure R1: Structures schématiques de transistors organiques bottom-gate en géométrie bottom-contact et top-contact

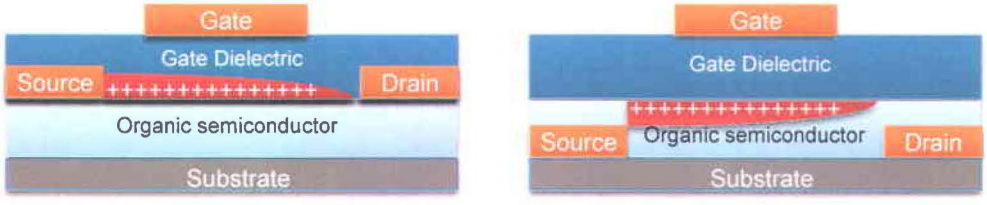

Figure R2: Structure schématique d'un transistor organique en géométrie top-gate

Divers facteurs induisent de meilleures performances (mobilité d'effet de champ élevée) pour les transistors « contact en haut », mais la principale cause d'une mobilité élevée est que le SCO grossisse sur une surface lisse.[20] Pour les dispositifs de « contact en bas », le transport de charge peut être influencé par la structure cristalline du SCO déposé à proximité des électrodes métalliques. En effet la structure microcristalline du SCO au milieu du canal est très différente de celle en bordure de canal, mais la fonctionnalisation des électrodes métalliques peut éliminer ou limiter cette perturbation de la croissance du SCO en modifiant l'énergie de surface des électrodes.[21] Il faut préciser que la réduction des quantités de matière utilisées pour les dispositifs « contact en bas » est limitée, car la photolithographie ou la lithographie e-faisceau ne peuvent pas être employées. En traçant les caractéristiques de transfert et de sortie du dispositif, divers paramètres tels que la tension de seuil V_{th} et rapport "on/off" peuvent être extraits. Les relations de base décrivant le courant de drain des TOECs aux régions linéaires et saturées sont :

$$I_{DS,\ lin} = \frac{WC_i\mu}{L}(V_G - V_{th} - \frac{V_{DS}}{2})V_{DS}$$

$$I_{DS,\ sat} = \frac{WC_i\mu}{2L}(V_G - V_{th})^2$$

où I_{DS} est le courant de drain, μ la mobilité d'effet de champ, W la largeur de canal, L la longueur de canal, C_i la capacité par unité de surface pour la couche d'isolant, V_{th} la tension de seuil, V_{DS} la tension de drain, et V_G la tension de grille.

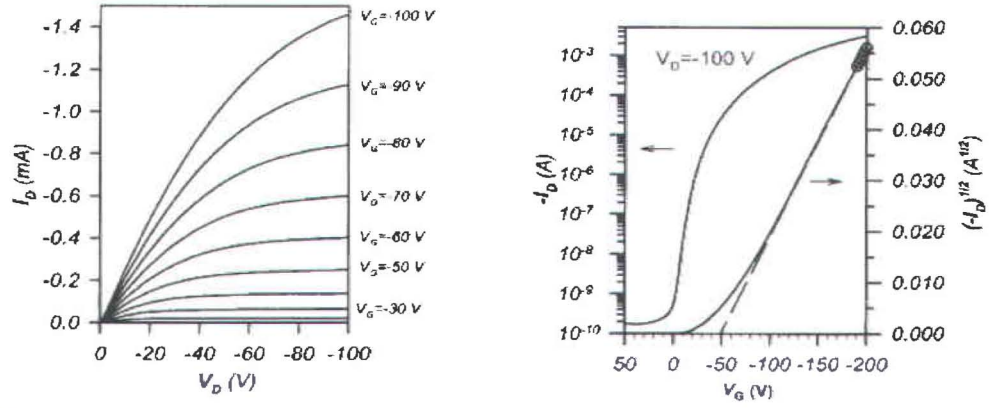

Figure R3: Caractéristiques de sortie et de transfert d'un transistor organique en pentacène avec du SiO_2.[3] À partir de ces courbes nous pouvons extraire V_{th} et la mobilité de charge (μ_{FET}). Sur l'échelle y gauche de caractéristiques de transfert, la racine de $|I_{DS}|$ $(A)^{1/2}$ en fonction de V_G est tracé et sur l'axe droite de y on trouve $|I_{DS}|$ contre V_G sur une échelle logarithmique, qui permet une évaluation de la tension de seuil et de rapport I_{on}/I_{off}

Il y a un grand intérêt à étudier les différentes techniques de dépôt pour comprendre la croissance des films et les propriétés des dispositifs. Pour une molécule organique qui présenterait une haute délocalisation électronique (mobilité de charge intramoléculaire élevée), il est nécessaire que les charges puissent se déplacer facilement entre les molécules. La mobilité intermoléculaire doit également être importante, nécessaire pour soutenir l'interaction des molécules entre elles. Les conditions de dépôt, le substrat et son interface avec le matériau organique jouent un rôle important dans la croissance du matériau organique. Le contrôle de cette interface est important car le transport a lieu dans les premières monocouches près du diélectrique. Des modifications chimiques de la surface du diélectrique de grille avec les monocouches auto-assemblées (SAMs) peuvent améliorer le transport du porteur de charge et permettre d'obtenir un rendement plus élevé. Les SAMs basées sur les alkyloctadécyltrichlorosilane (OTS), ou sur l'hexaméthyldisilazane (HMDS) peuvent modifier la surface du diélectrique.[22,23]

Les transistors luminescents organiques (TLOs) sont un nouveau type de dispositifs menant aux sources lumineuses du domaine du nanomètre et aux dispositifs optoélectroniques fortement intégrés. Cette structure est idéale pour améliorer l'efficacité quantique d'électroluminescence et la durée de vie des SCOs, dues aux différents modes de fonctionnement comparés aux DOEs.

---

[3] Dimitrakopoulos, C. D.; Malenfant, P. R. L., Organic thin film transistors for large area electronics. *Adv Mater* **2002,** *14* (2), 99-117.

Des structures chimiques et les caractéristiques des TLOs des matériaux moléculaires et celui de polymères utilisés en tant que couches actives dans TLOs sont présentés dans le Tableaux suivant.

Schème E. Structures chimiques et caractéristiques de TLO de différentes molécules[4]

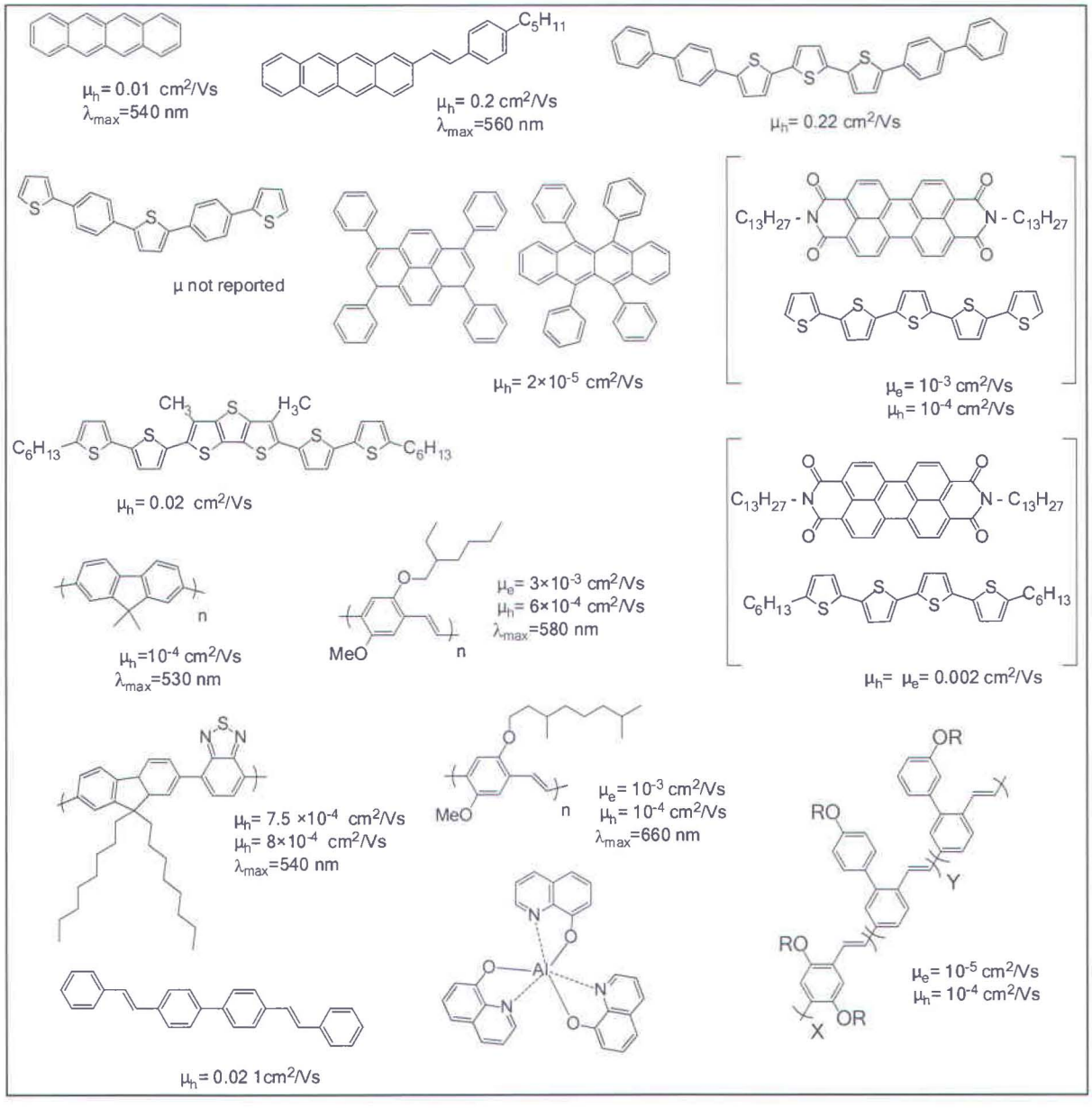

[4] "Organic Thin Film Transistors", Z. Bao and J.J. Locklin. Eds, CRC Press, 2007.

Cette thèse se déroule dans ce contexte. Elle se base sur la recherche autour des transistors organiques et présente une étude de l'évolution des performances des transistors organiques, en rapport avec la structure moléculaire du semi-conducteur organique, la configuration du transistor, et le diélectrique de grille. Cette thèse est divisée en six chapitres. En un premier temps nous présenterons quelques connaissances de base et les objectifs de recherche. Il est consacré à quelques rappels de base sur les transistors organiques et à l'état de l'art de ces composants. Le deuxième chapitre est une description des dispositifs utilisés pour le développement de nos structures. Nous décrirons la totalité des procédures expérimentales dans cette partie. Le chapitre trios à six traitera des résultats obtenus quant aux propriétés optoélectroniques et du mécanisme de croissance de film de différents types de semi-conducteurs organiques.

Dans ce projet nous avons utilisé différents outils et techniques pour nettoyer et fabriquer les dispositifs, mais également pour étudier le mécanisme de croissance des films et caractériser leurs propriétés optoélectroniques. Les transistors produits dans notre laboratoire sont principalement prévus pour la commutation et l'émission de lumière. Les transistors sont analysés par différentes techniques pour étudier leurs propriétés électriques et optiques. Une grande variété de SCOs et la modification de leur structure moléculaire et morphologique permettent de construire des transistors pour différents types d'applications. Nous essayons de fabriquer des transistors reproductibles et fiables à hautes performances (mobilité élevée et rapport "on/off", faible fuite de courant de grille,...) pouvant fonctionner à basse tension et ayant des propriétés de luminescence grâce aux SCOs bien connus, tels le pentacène et de nouveaux SCOs synthétisés. Dans ce travail, des propriétés optoélectroniques et le mécanisme de croissance de film de différents types de semi-conducteurs organiques ont été étudiés. Nous avons utilisé des SCOs bien connus tel que le pentacène pour créer une plateforme d'essai pour des semi-conducteurs bien connus et des SCOs nouvellement synthétisés. La structure chimique des molécules utilisées dans cette étude est décrite dans le Tableau suivant.

Figure R4: Structure moléculaire et caractérisation de TOEC avec les différents SCOs étudiés

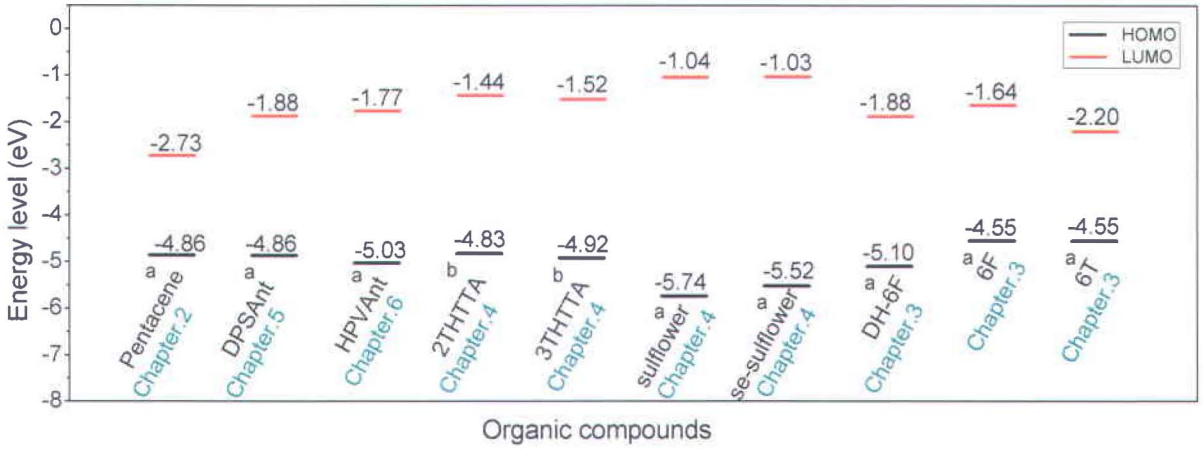

La diversité des techniques synthétiques organiques aussi bien que l'éventail de modules disponibles dans le commerce augmentent la flexibilité en accordant la structure moléculaire et ses propriétés optoélectroniques. Concevoir des SCOs avec des propriétés optoélectroniques spécifiques ouvre un champ de recherche passionnant dans l'électronique organique. En dépit de progrès impressionnants et rapides dans les transistors à effet de champ organiques, développer des dispositifs organiques fiables reste un défi.

Reference

[1] C. K. Chiang, C. R. Fincher, Y. W. Park, A. J. Heeger, H. Shirakawa, E. J. Louis, S. C. Gau, A. G. Macdiarmid, *Phys. Rev. Lett.*, **1997,** 39, 1098-1101.

[2] In 2000, A. J. Heeger, A. G. MacDiarmid, H. Shirakawa received the Nobel Prize in chemistry for the discovery and development of electrically conductive polymers.

[3] S. R. Forrest, *Nature*, **2004,** 429, 911-918.

[4] S. A. Ponomarenko, S. Kirchmeyer, A. Elchener, B. H. Huisman, D. Drechsler, *Adv. Func. Mat.*, **2003,** 13, 591-597.

[5] A. R. Murphy, J. Frechet, P. Chang, J. Lee, V. Subramanian, *J. Am. Chem. Soc.*, **2004,** 126, 1596-1597.

[6] B. S. Ong, Y. Wu, P. Liu, S. Gardner, *J. Am. Chem. Soc.*, **2004,** 126, 3378-3379.

[7] H. Klauk, M. Halik, U. Zschieschang, G. Schmid, W. Radlik, *J. Appl. Phys*, **2002,** 92, 5259-5263.

[8] J. A. Rogers, K. Bao, A. Baldwin, B. Dodabalapur, V. R. Raju, V. Kuck, H. E. Kats, K. Ammundson, J. Ewing, P. Drzaic, *PNAS*, **2001,** 98, 4835-4840.

[9] G. Horowitz, M. E. Hajlaoui, *Adv. Mater.*, **2000,** 12, 1046-1050.

[10] H. Klauk, T. N. Jackson, *Solid State Technology*, **2000,** 43, 63-77.

[11] C. D. Dimitrakopoulos, D. J. Mascaro, *IBM Journal of Research and Development*, **2001,** 45, 11-27.

[12] R. Wisnieff, *Nature,* **1998,** 394, 225-227.

[13] R. G. Nuzzo, *PNAS*, **2001,** 98, 4827-4829.

[14] S. A. Campbell, The Science and Engineering of Microelectronic Fabrication, Oxford University Press, New York, 2001

[15] S. Ando J. Nishida, E. Fujiwara, H. Tada, Y. Inoue, Sh. Tokito, Y. Yamashita, *Chem. Mater.*, **2005,** 17, 1261-1265.

[16] H. E. Katz, A. J. Lovinger, J. Johnson, C. Kloc, T. Siergist, W. Li, Y.Y. Lin, A. Dodabalapur, **2000,** *Nature*, 404, 478-481.

[17] A. Afzali, C. D. Dimitrakopoulos, T. L. Breen, *J. Am. Chem. Soc.*, **2001,** 123, 9482-9483.

[18] V. C. Sundar, J. Zaumseil, V. Podzorov, E. Menard, R. L. Willett, T. Someya, M. E. Gershenson, J. A. Rogers, *Science,* **2004,** 303, 1644-1646.

[19] J. Zaumseil, C. L. Donley, J. Kim, *Adv Mater* **2006,** 17, 1-6.

[20] P. V. Necliudov, M. S. Shur, D. J. Gundlacj, T. N. Jackson, *J. Appl. Phys.*, **2000,** 88, 6594-6597.

[21] I. Kymissis, C. D. Dimitrakopoulos, S. Purushothaman, *IEEE Trans. Electron Devices,* **2001**, 48, 1060-1064.

[22] Dimitrakopoulos, C. D.; Purushothaman, S.; Kymissis, J.; Callegari, A.; Shaw, J. M., Low-voltage organic transistors on plastic comprising high-dielectric constant gate insulators. *Science* **1999,** *283* (5403), 822-824.

[23] Kobayashi, S.; Nishikawa, T.; Takenobu, T.; Mori, S.; Shimoda, T.; Mitani, T.; Shimotani, H.; Yoshimoto, N.; Ogawa, S.; Iwasa, Y., Control of carrier density by self-assembled monolayers in organic field-effect transistors. *Nat. Mater.*, **2004,** *3* (5), 317-322.